MECHANICALLY- AND BIOCHEMICALLY-INDUCED DIFFERENTIATION OF BONE MARROW MESENCHYMAL STEM CELLS TO SMOOTH MUSCLE CELLS IN A THREE-DIMENSIONAL FIBRIN MATRIX

by

Jessica L. Lo Surdo

Bachelor of Science, Syracuse University, 2005

Submitted to the Graduate Faculty of

Swanson School of Engineering in partial fulfillment

of the requirements for the degree of

Master of Science

University of Pittsburgh

2008

UNIVERSITY OF PITTSBURGH

SWANSON SCHOOL OF ENGINEERING

This thesis was presented

by

Jessica L. Lo Surdo

It was defended on

August 5, 2008

and approved by

Dr. Bridget Deasy, Assistant Professor, Departments of Orthopaedic Surgery and Bioengineering

Dr. Kacey Marra, Assistant Professor, Departments of Surgery and Bioengineering

Dr. Kimimasa Tobita, Assistant Professor, Departments of Pediatrics and Bioengineering

Thesis Advisor: Dr. David A. Vorp, Associate Professor, Departments of Surgery and Bioengineering

Copyright © by Jessica L. Lo Surdo

2008

MECHANICALLY- AND BIOCHEMICALLY-INDUCED DIFFERENTIATION OF BONE MARROW MESENCHYMAL STEM CELLS TO SMOOTH MUSCLE CELLS IN A THREE-DIMENSIONAL FIBRIN MATRIX

Jessica L. Lo Surdo, M.S.

University of Pittsburgh, 2008

Bone marrow mesenchymal stem cells (BMMSCs) may serve as an alternative source to terminally differentiated cells for tissue engineering applications. Our group has demonstrated that BMMSCs subjected to a mechanical environment may differentiate toward a smooth muscle cell (SMC) phenotype. Growth factors in conjunction with mechanical stimulation have been shown in prior work to have a significant effect in regulating SMC phenotype in 2D. Simultaneous stimulation with mechanical strain and TGF-β has been shown to increase α-actin expression in SMCs when compared to mechanical strain alone. Taken together, this previous work suggests that mechanical and chemical factors may work together to promote differentiation of BMMSCs toward an SMC phenotype. Consequently, the hypothesis of the current work is that uniaxial cyclic strain and biochemical stimulation with TGF-β will differentiate BMMSCs towards an SMC-like lineage in a synergistic manner in 3D.

To evaluate this hypothesis, rat BMMSCs suspended in a fibrin gel were subjected to cyclic mechanical strains and frequencies physiologically consistent with the arterial system, in combination with chemical stimulation with TGF-β. Changes in morphology, proliferation, collagen production, and qualitative protein expression were assessed to determine if there were any synergistic effects between mechanical and chemical stimulation.

Results revealed that BMMSCs subjected to both mechanical and biochemical stimulation led to an increase in production of contractile machinery intrinsic to terminally-differentiated SMCs, an increase in expression of SMC marker proteins, and an increase in collagen production when compared to control groups. These results support our hypothesis and suggest that combined mechanical and biochemical stimulation may be important in stem cell-based regenerative medicine applications involving SMCs.

Future work will evaluate SMC gene expression and functionality to better define the role of mechanical and biochemical stimuli in differentiating BMMSCs toward a terminally differentiated SMC phenotype.

TABLE OF CONTENTS

LIST OF TABLES

LIST OF FIGURES

NOMENCLATURE

α-SMA, alpha smooth muscle actin

α-MEM, alpha Modified Eagle's Medium

ADSCs, adipose-derived stem cells

bFGF, basic fibroblast growth factor

BMMSCs, bone marrow-derived mesenchymal stem cells

CS, cyclic stretch

EC, endothelial cell

ECM, extracellular matrix

ESCs, embryonic stem cells

FF, free float

MCSCs, muscle-derived stem cells

MHC, Myosin heavy chain

MT, Masson's Trichrome

MSC, mesenchymal stem cell

PBS, phosphate buffered saline

PDGF, platelet-derived growth factor

PSR, picrosirius red

SMC, smooth muscle cell

SS, static stress

TEVG, tissue engineered vascular graft

TGF-β, transforming growth factor beta

VEGF, vascular endothelial growth factor

PREFACE

I first would like to acknowledge my thesis advisor, Dr. David Vorp. Thank for your support and wisdom through inconvenient times. I appreciate the opportunity to work for you and your lab.

To Drs. Deasy, Marra and Tobita; thank you for serving on my thesis committee. I appreciate your time and advice.

A special thank you to Doug Chew, whose enthusiasm for science has motivated me to seek new heights, and promote an interest in science to those where it has gone unnoticed.

To Burhan Gharaibeh, thank you for treating me as your 'adopted graduate student' and taking the time to share your knowledge. Your selflessness and passion for science are a true inspiration.

Thank you to my friends here at Pitt in BIOE, who have stood by my side through good times and bad. To Diana Gaitan, Laurie Meszaros, Christy Milburn, Melanie Ruffner, Priya Ramaswami, and Silvia Wognum, I am for forever grateful for your support and friendship.

I would like to acknowledge all members of the Vorp Lab, both past and present. To Tim Maul; thank you for teaching me most of what I've learned in graduate school. To Donna Haworth; thank you for your advice and support; and for being a great lab mate and friend. To

Deb Cleary, thank you for your assistance with the RNA isolations. To Lorenzo Soletti, thank you for your advice and friendship. It was a pleasure working with all of you.

To my loving parents and siblings; thank you for always believing in me. Your encouragement, wisdom and support are what got me through to this day, and I couldn't have done it without you.

Lastly, I would like to acknowledge the Biomechanics in Regenerative Medicine training grant that provided me with a scholarship during my graduate studies.

1.0 INTRODUCTION

1.1 POTENTIAL TARGETS FOR SMOOTH MUSCLE CELL-BASED REGENERATIVE MEDICINE

Smooth muscle cells (SMCs) are components of the excretory, respiratory, digestive, and vascular systems, all of which are susceptible to disease and dysfunction. Regenerative medicine and tissue engineering allows tissue and organ scientists to create biological substitutes for various diseases and conditions affecting the urethra, bladder, esophagus, trachea, colon and blood vessels, to name a few. When creating a biological substitute for these tissues and organs, there is an inherent need for SMCs. These organ systems in the body rely on a smooth muscle layer to functionally maintain the mechanical strength of the tissue. The limitations of using terminally differentiated cells in regenerative medicine may be inhibiting progress, as telomere shortening during cell replication may be associated with senescence of the cell [1, 2].

1.1.1 Urinary Tract Disorders

1.1.1.1 Urethra

Stress urinary incontinence is the involuntary loss of urine due to sudden increases in abdominal pressure. Acellular matrices, such as polyglycolic acid (PGA) and collagen-based substrates from the small intestine and bladder, have been utilized in animal models in an effort to

regenerate urethral tissue [3, 4]. These acellular matrices have been used clinically to treat patients with hypospadias and urethral stricture disease. The inherent off-the-shelf availability of the matrices is also ideal because of the decreased surgical time while eliminating the concern for donor site morbidity. Autologous cells have been utilized to create a cellular component using the same collagen matrices for urethral reconstruction [5]. As SMCs are an integral component to the native urethral architecture, there is a need to for this cell type in urethral tissue engineering applications. Researchers have shown that bladder cells seeded onto collagen matrices derived from bladder submucosa reveal differentiation toward an SMC phenotype via qualitative and quantitative protein analysis [5].

1.1.1.2 Bladder

Spina bifida, a common birth defect where the embryonic neural tube fails to close completely, leads to poor or absent bladder control later in life. Patients with this disease have been treated with catheterization and pharmacotherapy to promote urinary continence. Bladder augmentation is often achieved by replacing segments of the bladder using stomach or intestinal segments. While functionally this has been proven to be successful, there are several complications associated with this reconstruction, primarily involving the inability to void urine. A tissue engineered approach has therefore been sought out to alleviate the complications due to these augmentation procedures. Researchers have created tissue engineered bladder tissue using a combined PGA-collagen scaffold seeded with autologous urothelial and smooth muscle cells. This was evaluated clinically for the first time in 1999 [6]. Patients receiving the PGA-collagen scaffold for reconstruction showed increased compliance, increased capacity and longer dry periods [7]. However, the use of undifferentiated cells may prove to be more successful for

tissue engineered bladder applications, as mesenchymal stem cells have been shown to migrate to the bladder graft location and differentiate into SMCs [8].

1.1.2 Respiratory Disease

A clinically successful tracheal transplantation is still in the distant future, and efforts are still underway to create a tissue engineered trachea to treat congential defects such as stenosis, agenesis and atresia. While a rigid hyaline cartilage component is one the major requirements for a functional tissue-engineered trachea, SMCs are required to generate a muscular tube while promoting a vascular network [9]. Researchers have used bone marrow progenitor cells seeded onto decellularized small bowel submucosa. Under laminar flow perfusion, these cells were shown to differentiate to SMCs and were oriented longitudinally along matrix fibers [9]. For this application, functional SMCs are necessary to respond to mechanical stresses intrinsic to normal breathing to maintain normal contractile function, where loss of functionality may lead to ischemic injury. This work also demonstrates the possible role of mechanical forces in differentiating bone marrow-derived progenitor cells toward an SMC lineage.

1.1.3 Cardiovascular Disease

Cardiovascular disease is the leading cause of death in the United States, with an estimated one in three American adults having one or more types of cardiovascular disease (CVD). Care and treatment of those with CVD in the US will cost nearly 450 billion in 2008 [10]. Coronary artery disease is the most deadly form of CVD, where the blood supply to the heart is compromised due to an obstruction in the coronary arteries, often leading to myocardial infarction as a result of

oxygen deprivation. Coronary artery disease will often require surgery, with nearly 500,000 inpatient bypass procedures in 2005 [10]. Bypass surgery generally involves multiple vascular grafts, as the patient's internal mammary artery or saphenous vein is often utilized as an autologous vessel replacement. Although an autologous vessel is desired, there are many patients whose native vessels are unavailable for use either from being diseased themselves or due to being already used during a prior surgery. Moreover, these autologous grafts tend to fail within 10 years [11]. Synthetic grafting has also been prone to failure due to calcification, ingrowth of smooth muscle cells (SMCs) and thrombus formation [12, 13]. Clearly there is a need for an alternative small-diameter vessel substitute [14-16]. Tissue-engineered vascular grafts (TEVGs) usually involve the incorporation of cells within the scaffold or extracellular matrix. Several cell sources are available for use; however autologous cells are advantageous when considering immune rejection [17].

Due to the unique architecture and complicated mechanical properties of the vascular wall, the ideal tissue engineered vascular graft is still sought after. Because of this, the Holy Grail of vascular tissue engineering has been established; to create a small-diameter blood vessel substitute [18].

There are several key considerations in designing the ideal vascular substitute, primarily involving the mechanical and biological properties. From a mechanical perspective, a TEVG must be able to sustain the mechanical demand intrinsic to the vasculature, i.e. arterial blood pressure and flow [19]. Furthermore, the mechanical properties of a TEVG must match that of the host vessel, such that there is no compliance mismatch. A compliance mismatch may ultimately lead to intimal hyperplasia at the anastomosis, and in turn, lead to graft failure [20]. In the biological arena, several key factors come into play, namely the cell source, scaffold

material and growth factors. The primary goal when integrating biological components is to create an anti-thrombogenic conduit that exhibits long-term patency, while mimicking the complex architecture of a native blood vessel (see **Figure 1-1**).

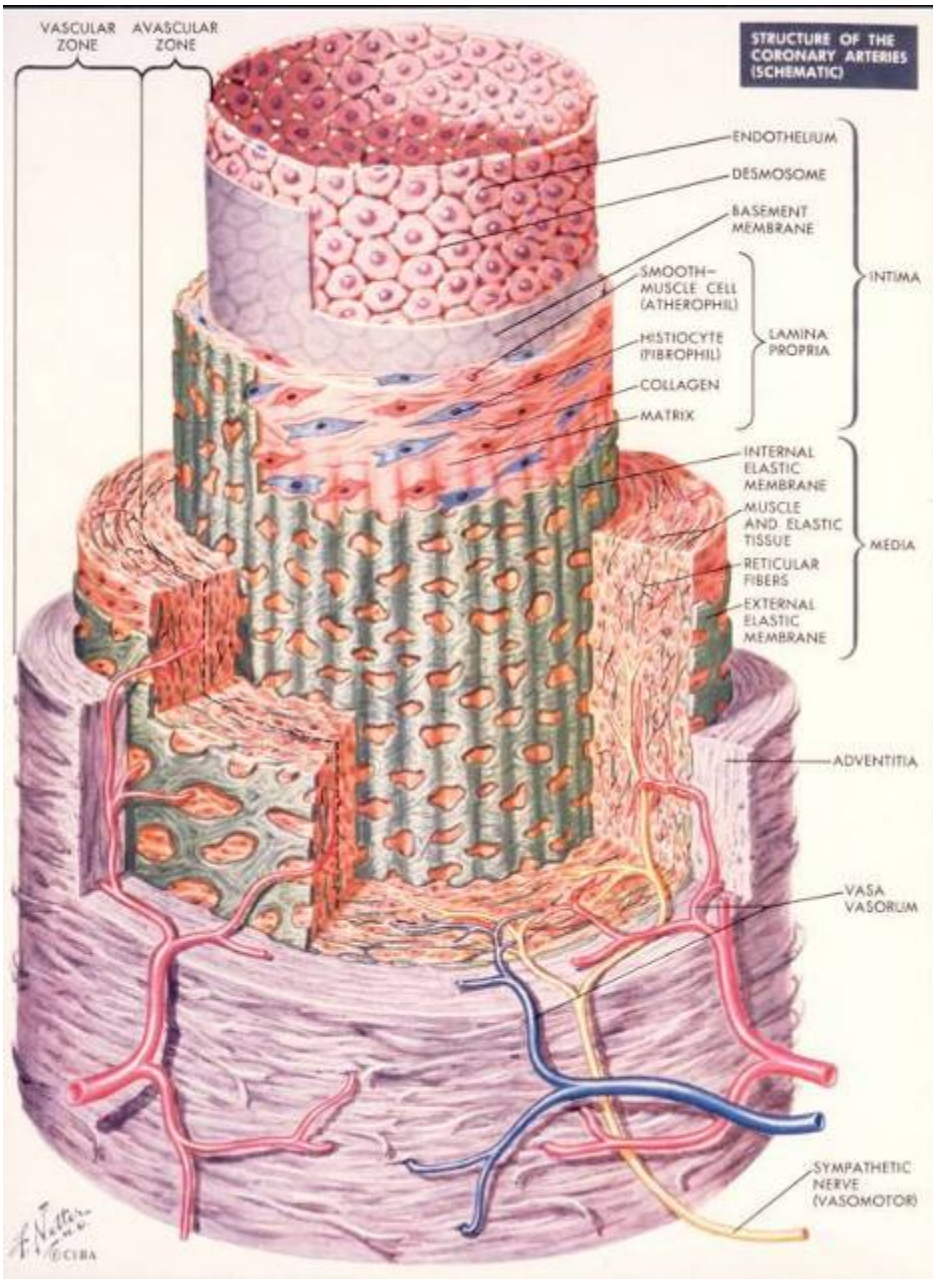

Figure 1-1: Anatomy of a blood vessel [21].

1.1.3.1 Cell sourcing

Cell sourcing is pivotal in creating a clinically viable TEVG. Complete functionality of a vascular graft may not be accomplished without an endothelialized lumen and contractile SMCs [22]. The use of non-autologous or allogenic cell lines may require immunosuppressive interventions to avoid host rejection. Therefore, an autologous cell line is advantageous by eliminating the concern for immunological rejection. Autologous cells may be either terminally differentiated cells or progenitor cells.

The use of terminally differentiated cells towards vascular graft applications, such as smooth muscle and endothelial cells, offers several advantages. The main benefit in using these cells is that they are of the desired phenotype, and better simulate the cellular constituency of a native blood vessel. However, the use of terminally differentiated cells comes with several limitations. Due to the high cell number required in creating a TEVG, meeting this demand is often difficult due to the limited expansion capabilities *in vitro.* Telomere shortening during DNA replication is the mechanism behind the restricted proliferation potential *in vitro.* Furthermore, terminally differentiated cells are often associated with the same disease pathology as the host tissue.

Progenitor cells have proven to be a valuable alternative to terminally differentiated cells in vascular graft applications [23]. Progenitor cells are easily obtainable and expandable, and there are several different types being utilized in tissue engineering applications. These different cell types may be found in skeletal muscle [24, 25], adipose tissue [26, 27], the placenta [28, 29], blood [30], blood vessels (i.e. pericytes) [31], and bone marrow [32].

1.1.3.2 Scaffolds

Scaffolds may be derived from a range of biomaterials, and can be either synthetic or naturally-derived/biologic. Polymeric biomaterials have been used as a synthetic scaffold to provide the required mechanical strength and support needed to withstand arterial blood pressure and flow. Synthetic biomaterials may be degradable or non-biodegradable. Non-biodegradable materials utilized for vascular graft applications include Dacron and ePTFE, while biodegradable materials consist of polylactic acid (PLA), polyglycolic acid (PGA) and poly (ester-urethane) urea (PEUU) [17]. The degradation properties of biodegradable materials may be manipulated such that the rate of degradation equals that of extracellular matrix production to ensure the mechanical stability of the TEVG. Natural biopolymers such as fibrin, collagen, elastin and glycosaminoglycans (GAGs) have been studied [17]. Other groups have avoided the use of synthetic and/or natural biomaterials and have opted for a more biological approach. L'Heureux *et al.* utilized cell sheet technology in creating a completely biological tubular scaffold [33, 34].

1.1.3.3 Cytokines and growth factors

Cytokines and growth factors drive many of the biochemical processes required for cellular proliferation and differentiation, and may be utilized to obtain the desired response of a particular cell type. Growth factors relevant to vascular tissue engineering applications, such as vascular endothelial growth factor (VEGF), platelet derived growth factor (PDGF), basic fibroblast growth factor (bFGF), and transforming growth factor beta (TGF-β), have been widely studied and are known to be involved in critical cellular functions. VEGF is widely studied because of its role in fetal development and angiogenesis, as CD34+ progenitor cells in the presence of VEGF has been shown to promote differentiation toward an endothelial cell lineage [35, 36]. PDGF-BB promotes proliferation while also decreasing expression of contractile

proteins, leading to a more synthetic, proliferative phenotype [37, 38]. bFGF plays a significant role in the wound healing response and angiogenesis via smooth muscle and endothelial cell proliferation [39, 40]. TGF-β is well known for its involvement in smooth muscle cell phenotype modulation and tissue remodeling via extracellular matrix production at varying concentrations [19].

1.2 STEM CELLS IN REGENERATIVE MEDICINE APPLICATIONS

Due to the continued organ donor shortage and the aging population, regenerative medicine and tissue engineering has emerged as a means of treating diseased and injured organs for patients suffering with various debilitations and diseases. The underlying goal behind all regenerative medicine applications is to repair, replace or regenerate tissues and/or organs. One of the most critical components in this field is determining the optimal cell source when utilizing cell-based therapies. Cells are often isolated from donor tissue, expanded *ex vivo*, seeded onto a matrix or scaffold, and then reimplanted into the host recipient. Cells can be either allogeneic or autologous. An autologous cell line is often desired to avoid any immunogenic effects. However, because autologous cells come from the diseased host, these cells may be abnormal and potentially difficult to expand in sufficient quantities. Because of this, stem cells have proven to be a viable alternative [41].

In 1963, Becker *et al.* was amongst the first to study stem cells, when they injected bone marrow cells in the spleens of irradiated mice. They found that size of the nodule formation on the mice spleen was proportional to the cell number they injected, and therefore came to the

conclusion that these nodules arose from an individual bone marrow cell [42]. What arose from this discovery was that stem cells are capable of self-renewal, a concept that is now intrinsic to stem cell behavior. Therefore, two distinguishing features of stem cells are self-renewal (giving rise to new stem cells) and the ability to differentiate in response to the appropriate environmental cues. Generally speaking, stem cells are either embryonic or adult. Embryonic stem cells (ESCs) exhibit pluripotency and therefore are capable of giving rise to the three germ layers (endoderm, mesoderm and ectoderm).

Adult stem cells (non-ESCs) are multipotent due to their ability to only differentiate into select cell and tissue types. These cells more lineage-committed that are lower in the stem cell ladder, and therefore do not retain the pluripotent characteristics of ESCs. Adult stem cells are multipotent due to their ability to differentiate toward prescribed lineages, depending on the environmental cues they receive. Non-ESCs can be derived from several tissues, including fat [43, 44], muscle [45], and bone marrow [23] to name a few, and may differentiate along different lineages when prompted with the appropriate milieu of cytokines, growth factors, and/or mechanical stimuli. They have also been shown to even exist in organs with slower turnover rates, such as the liver, brain and β-islets in the pancreas. While ESCs have been difficult to implement due to the ethical concerns, adult stem cells are an exciting and invaluable alternative to the regenerative medicine arena.

1.2.1 Adipose-Derived Stem Cells

Human fat has proven to be a good source of adipose-derived stem cells, or ADSCs, and been shown to have osteogenic capabilities *in vitro* [46]. ADSCs have been shown to be guided down several other lineages *in vitro,* including chondrogenic [47], hepatic [48], neurogenic [49], and

myogenic [50] cell lines. Researchers have demonstrated cardiomyocytic differentiation demonstrating functionality and phenotypic maintenance after 2 months of culture [51]. Upon characterization of ADSCs, studies have shown that this particular cell type is phenotypically similar to BMSCs [52], yet have varying differentiation potentials [53]. Most relevant to this work, however, is the ability of ASCs to differentiate toward a vascular SMC phenotype in response to mechanical and chemical stimulation with TGF-β in 2D [54].

1.2.2 Muscle-Derived Stem Cells

Muscle-derived stem cells (MDSCs) have been shown to self-renew and have multipotent capabilities. Several varieties of isolation techniques from muscle digests have yielded cells capable of giving rise to myogenic, osteogenic, chondrogenic, and adipogenic cell lineages as reviewed by Deasy and Huard [24]. These differentiation modalities may be harnessed to treat diseases such as muscular dystrophy, while they also may be used as a delivery vehicles and therapeutic agents to promote bone remodeling, cardiac tissue repair and stress urinary incontinence. Toward vascular graft applications, these cells have been integrated with polymeric scaffolds and implanted *in vivo*, and have demonstrated the potential to differentiate into SMCs upon implantation [55].

1.2.3 Bone Marrow-Derived Mesenchymal Stem Cells

Bone marrow-derived mesenchymal stem cells, or BMMSCs, are thought to be an ideal cell source for tissue engineering and regenerative medicine applications, as they may be readily harvested from a patient, while avoiding the ensuing debate over ethical concerns associated with the use of ESCs. It has been known for a significant amount of time that stem cells exist in the bone marrow, as they are the most widely studied sources of adult stem cells. BMMSCs were first isolated from bone marrow in the 1960s by Friedenstein [56]. More recently, it was determined that these stem cells derive from hematopoietic and mesenchymal lineages, and they have been characterized as progenitors based on their use to treat leukemia. Multipotency can be maintained in an undifferentiated state *in vitro*, while this cell type has the potential to differentiate down osteogenic, chondrogenic, neurogenic, and adipogenic lineages [44, 57-60]. Based on evidence suggesting that these BMMSCs are capable of differentiating into SMCs, ECs, and cardiomyocytes, the vascular tissue engineering field has successfully moved forward [61-65]. Furthermore, progenitor cells from the bone marrow have been found in circulation and have been shown to be involved in neovascular formation [35, 66, 67]. Autologous BMMSCs were also utilized in a recent clinical trial where progenitor cells were aspirated from the bone marrow, seeded onto the polymer scaffold of a TEVG, and implanted all within the same surgery [68]. The clinical relevance of this work underscores the need to understand cardiovascular differentiation of BMMSCs. More interesting and relevant to this work, however, is their ability to differentiate toward a smooth muscle cell phenotype in response to mechanical and/or chemical stimuli *in vitro* [37, 69-80]. This will be discussed in more detail in a later section.

1.3 SMOOTH MUSCLE CELLS (SMCS)

Smooth muscle cells (SMCs) are derived from the mesodermal layer during embryonic development. Two processes contribute to vessel formation during embryonic development. Vasculogenesis, the *de novo* formation of blood vessels, allow vascular precursor cells to differentiate into endothelial cells, which come together to form a hollow tube or blood vessel. From these preexisting blood vessels, budding or sprouting of new vessels may occur; a process called angiogenesis. During the development of larger vessels, SMC precursors are recruited to the site of new vessel formation and give rise to vascular SMCs [81].

SMCs have long been described as having either a contractile or synthetic phenotype, depending on the local mechanical and biochemical stimuli. However, it is now more widely recognized that SMC phenotypes exist in a spectrum rather than a two-state model (**Figure 1-2**) [81]. As such, SMCs express different contractile proteins during various states of differentiation, as they are plastic due to their dependence on local environmental cues and stimuli.

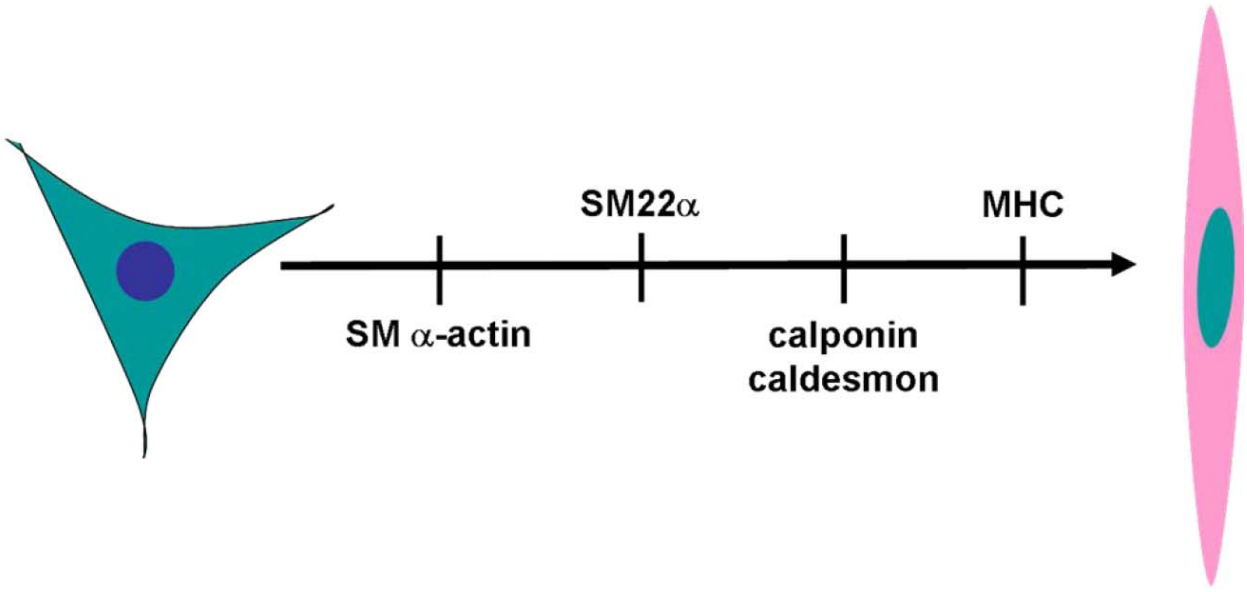

Figure 1-2: Expression of SMC differentiation markers during development. The cell on the left indicates a synthetic SMC. Expression of various markers exists as a hierarchy, as the cell on the right indicates a fully differentiated contractile SMC. Contractile SMCs express all of the differentiation markers. Figure adapted from [81].

1.3.1 SMC Markers

The primary function of vascular SMCs is contraction. SMCs exist in a plastic state where they may lose their contractile phenotype and become more synthetic. These different phenotypic states are associated with different marker proteins. For example, contractile phenotypes are less proliferative and more quiescent, and express alpha-smooth muscle actin (α-SMA), calponin, myosin heavy chain (MHC) SMC markers. Synthetic phenotypes are associated with

proliferation and lack of expression of the above-mentioned SMC markers. Details about these SMC protein markers will be described in the subsequent sections.

1.3.1.1 α-smooth muscle actin

Smooth muscle alpha-actin or α-SMA is the most abundant isoform of actin in mature, fully differentiated SMCs, comprising 40% of the total cell protein and more than 70% of the total actin within an SMC [82]. A high α-SMA protein is necessary for a SMC's force generating capacity, and intrinsic to the SMC contractile machinery [83]. Because of this, α-SMA can be evaluated quantitatively to determine the extent of differentiation and maturation of an SMC. α-SMA is not exclusively present in SMCs but rather a variety of mesoderm-derived cells that are seen in development and wound repair. Expression of α-SMA may also be induced exogenously with the addition of growth factors such as transforming growth factor-beta (TGF-β), as can be seen with microvascular endothelial cells and myfibroblasts. α–SMA is the first protein expressed in during vasculogenesis, while also increasing its level of expression during vascular development [81].

1.3.1.2 Calponin

Calponin is involved with the interaction between f-actin and tropomyosin in a calcium-independent fashion. Two isoforms of calponin are known to exist, namely h1-calponin and l-calponin, for high and low molecular weight respectively. h2-calponin is a novel variant, and is expressed in both SMCs and some non-SMCs, such as lung alveolar cells [84], macrophages [85], epidermal keratinocytes and fibroblasts [86]. Unlike h2-caplonin, h1-calponin is exclusive

to SMCs, where it is expressed early in aortic development and continues to be expressed in mature SMCs [81].

1.3.1.3 Myosin heavy chain

Myosin is critical to the contractility of all muscle and non-muscle cells. Myosin heavy chain (MHC) is a subunit of myosin and exists in multiple isoforms, where expression of these isoforms is regulated in tissue-specific and developmental stage-related mechanisms. However, the SM-1 and SM-2 isoforms are thought to be exclusive to SMC expression. SMemb is a third isoform of MHC that is found in cultured SMCs as well as human atherosclerotic lesions. Because SM-2 expression was only first detectable 10 days postnatally in vascular SMCs followed by gradual increases in expression, this confirms that SM-2 MHC is the latest differentiation marker of mature SMCs [81].

1.3.2 Determinants of an SMC Phenotype

1.3.2.1 Mechanical stimulation of SMCs

Terminally differentiated vascular SMCs are intrinsically subjected to mechanical forces that arise from the pulsatile nature of blood flow. These mechanical forces primarily consist of cyclic strain and pressure, whereby these forces are transmitted through the walls of a blood vessel. These forces are crucial in maintaining the functionality, viability, proliferation and protein expression of vascular cells, as changes in the mechanical environment may play a role in

vascular disease. An understanding of the role of mechanical stimulation in maintaining the contractile vascular SMC phenotype is important in both healthy and disease states.

As seen in **Figure 1-2**, SMC phenotype exists as a spectrum, whereby these cells may differentiate and dedifferentiate while expressing different contractile proteins. In atherosclerosis, SMCs are of a more synthetic or proliferative phenotype, where they lose expression of late differentiation markers such as calponin and MHC. Conversely, increased expression of these late differentiation markers leads to a more contractile phenotype, which are necessary to carry out the contractile functions of SMCs in the vasculature [81]. Because blood vessels are consistently subjected to mechanical forces in the vessel wall, there is much evidence to suggest that these forces are necessary to regulate and maintain the vascular smooth muscle phenotype.

Depending on the location, different mechanical forces are sensed in the vessel wall. For instance, the lumen or endothelial layer is highly subjected to shear stress due to blood flow. The focus of this work, however, will highlight the effect of mechanical strain as sensed by the medial layer of blood vessels.

Mechanical strain has been studied extensively in 2D formulations [87-90] where cells are typically cultured on deformable substrates so as to apply various strains and frequencies to the substrate, which may in turn be sensed by the cells. Equibiaxial and uniaxial cyclic mechanical strains have been traditionally used to better understand the effects of these strains *in vitro.*

1.3.2.1.1 Equibiaxial strain

The effect of equibiaxial strain, where stain is imposed equally in two directions (**Figure 1-3A**), has been studied to elucidate the response of SMCs to mechanical stimulation. Beginning attempts at creating a device to subject cells to biaxial stretch was initiated by Banes *et al* [91], by creating a negative vacuum pressure beneath the deformable substrate, as seen in **Figure 1-3B**. However, this approach creates a non-uniform strain at the edges of the deformable substrate, thereby creating inhomogeneous strain distribution. More recent attempts have solved this issue by deforming the substrate over a post, and therefore creating a more uniform strain distribution. The Flexcell® strain unit (Hillsborough, NC) was born by coupling the idea of an applied vacuum over a post (**Figure 1-3C**). Other devices have been created by fabricating a moveable circular post that imposes cyclic equibiaxial strain without the use of a vacuum pressure [92] (**Figure 1-3D**).

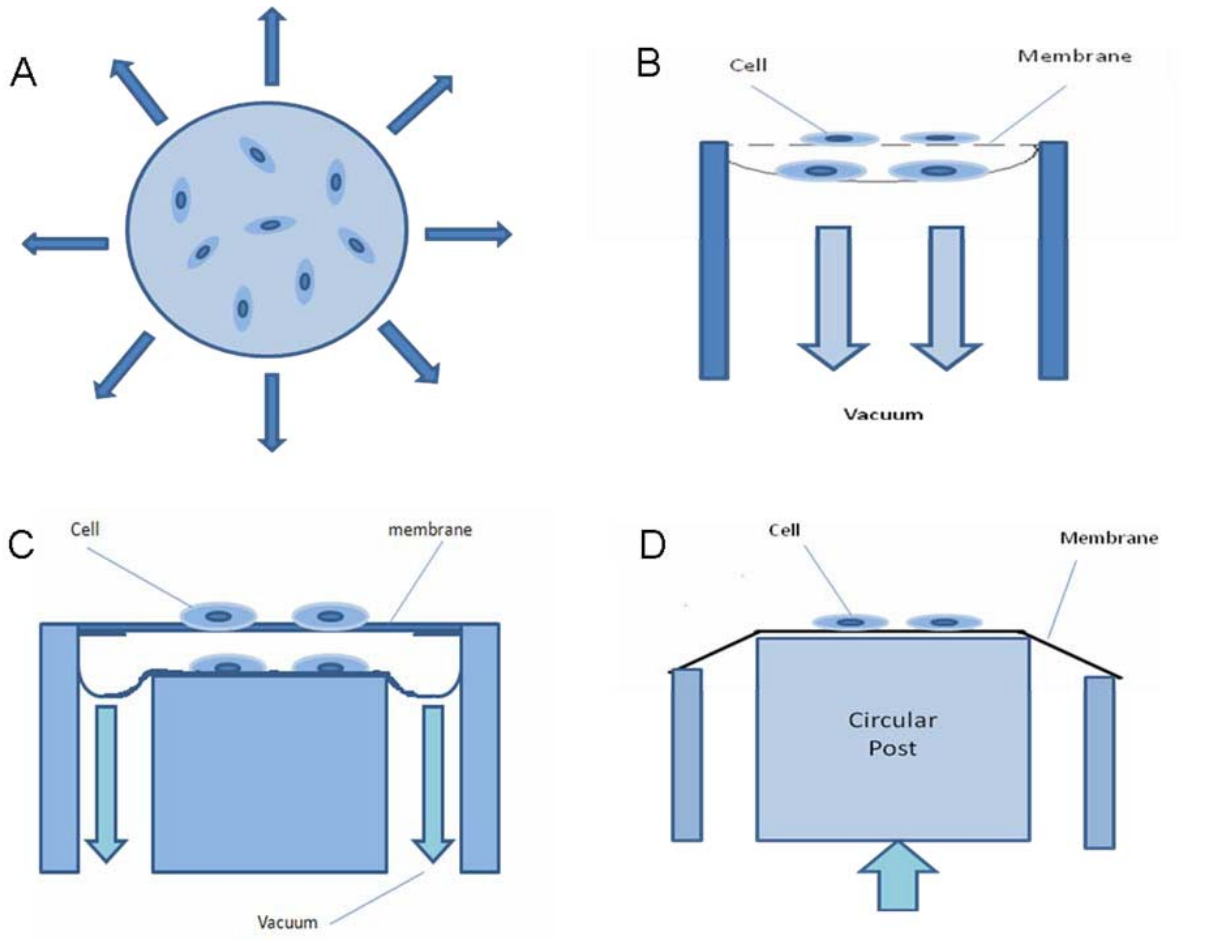

Figure 1-3: Mechanical devices used to induce equibiaxial strain. (A) Schematic of application of equibaxial strain. (B) Apparatus used to apply equibiaxial strain with the application of a vacuum directly under a deformable substrate. (C) Apparatus used to apply equibiaxial strain with the application of a vacuum over a circular post. (D) Application of equibiaxial stretch utilizing a moveable post (as opposed to a vacuum). Figure adapted from [93].

The goal behind a mechanical straining regimen is to replicate the forces seen *in vivo*. Earlier work by Birukov *et al* has shown that equibiaxial strain can influence SMC phenotype, where they demonstrated that equibiaxial strain led to an increase in h-caldesmon expression [94]. Other studies have reported matrix-dependent effects, where laminin or collagen type-I-coated substrates led to increases in SM-1 expression, while SMCs cultured on fibronectin led to

no upregulation of SM-1 [95]. This work suggests that cell-matrix interactions, when coupled with mechanical stimulation, may play a role in the maintenance of an SMC phenotype.

While much of this work suggests that equibiaxial mechanical strain plays a substantial role regulating a contractile SMC phenotype, as evidenced by upregulation of late differentiation markers, others have demonstrated a more proliferative and synthetic response to cyclic equiabiaxial stretch. Sudhir *et al.* and Yang *et al.* have reported SMC proliferation [39, 96]. Others have again underscored the cell-matrix interdependence and have noted increased proliferation of SMCs on fibronectin- and vitronectin-coated membranes, with no change in SMC proliferation on laminin- and collagen type I-coated membranes [97].

1.3.2.1.2 Uniaxial strain

Because SMCs in a native blood vessel align in the circumferential direction and have an elongated morphology which is necessary for contraction of the vessel wall, uniaxial strain has been utilized to study strain effects on SMCs, as it better mimics physiologic strain than equiaxial strain. Uniaxial strain is the application of strain along one axis. Several devices have been created to apply unaxial strain to cells in 2D. Park *et al.* [98] created a device where the substrate is fixed at one end and stretched uniaxially by pulling on the non-fixed end (see **Figure 1-4**). However, this again creates a non-uniform strain distribution at the fixed edge. The versatility of Flexcell® allows for the aforementioned circular posts to be replaced by arctangle posts. As such, a uniaxial strain may be imposed on a flexible substrate, based on the geometry of the post (see **Figure 1-4**).

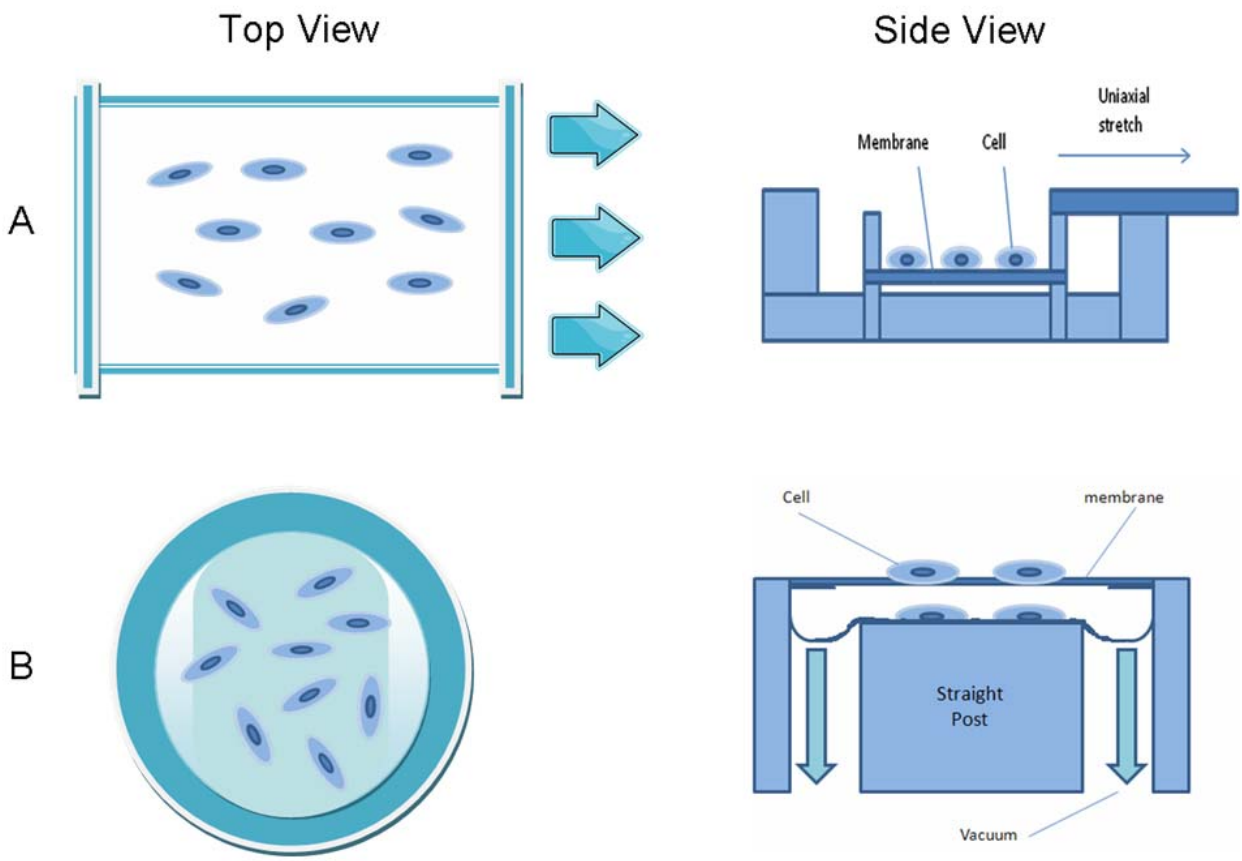

Figure 1-4: Mechanical devices used to induce uniaxial strain. (A) Application of uniaxial stretch of a deformable membrane. (B) Application of uniaxial strain using an applied vacuum over an artangle post. Figure adapted from [93].

In vivo, vascular SMCs are subjected to 5-15% cyclic circumferential strain, depending on the location in the vasculature [99]. Once explanted and cultured *in vitro* in a static environment, SMCs begin to downregulate their expression of SMC proteins such as MHC and calponin, and thereby exhibiting a shift from a contractile phenotype to a more synthetic phenotype [19, 100]. This underscores the dynamic nature of the vasculature and its importance in maintaining a functional SMC phenotype. SMCs are highly responsive to magnitude and

frequency of stretch, where lower stretch magnitudes lead to more proliferation [19]. Physiologic magnitudes of stretch are required to maintain a contractile and quiescent phenotype, where higher magnitude of strain has been shown to increase proliferation, apoptosis, and ECM production, and therefore shifting toward a more synthetic phenotype [19].

1.3.2.1.3 Need for 3D stimulation

While these experiments have provided much insight on the response of SMCs to 2D culture, the application of strain in 3D better mimics the vascular environment *in vivo*. SMCs behave differently in 3D as compared to 2D. *In vitro* culture of cells in 2D looking into the effect of uniaxial strain on vascular cells demonstrated perpendicular alignment relative to the direction of strain [101]. This preferential alignment may be due to an effort to minimize the stress applied to the cells, and cell orientation may lead to different cellular responses to mechanical stimulation. In contrast, SMCs in a 3D dynamic environment align in the direction of stretch and have a more elongated, spindle-shaped morphology [78].

The mechanical and extracellular matrix environment surrounding SMCs *in vivo* is important in maintaining cell function and phenotype. SMCs *in vivo* are inherently subjected to mechanical forces, including cyclic mechanical strain. When removed from this mechanically-vigorous environment to an *in vitro* culture environment, SMCs begin to downregulate SMC-specific proteins necessary for the maintenance of a contractile phenotype. However, once SMCs are subjected to mechanical forces *in vitro*, SMCs are capable of retaining a differentiated phenotype. Several researchers have successfully demonstrated the maintenance of an SMC phenotype *ex vivo* in a 3D environment coupled with mechanical strain [37, 72, 93].

1.3.2.2 Chemical stimulation of SMCs

Growth factors are essential in promoting proliferation and differentiation of stem cells towards a desired phenotype. There are several growth factors that are known to stimulate smooth muscle and progenitor cells, specifically basic fibroblast growth factor (bFGF), platelet derived growth factor (PDGF), and transforming growth factor beta (TGF-β) [17].

1.3.2.2.1 bFGF

bFGF plays a role in the wound healing response and angiogenesis via the proliferation of SMCs and ECs at the site of injured tissue. bFGF coupled with other biochemicals, such as ascorbic acid, has been shown to act synergistically in the production of ECM and proliferation of SMCs [40].

1.3.2.2.2 PDGF

PDGF causes proliferation of SMCs by allowing cells pass from G_0 to the G_1 phase of the cell cycle. Furthermore, several researchers have reported that the PDGF suppresses the expression of SMC markers [81, 102]. Others have also demonstrated synergy between mechanical stimulation and PDGF supplementation in 3D. Mechanical stimulation of SMCs and PDGF stimulation has been shown to decrease expression of contractile proteins [37].

1.3.2.2.3 TGF-β

When considering all of the biochemical factors that may play a role in vascular development, TGF-β is of particular interest as several researchers have demonstrated its role in maintaining terminally differentiated SMCs, where it has been shown to up-regulate SMC markers,

including α-SMA, h1-calponin, and MHC [103, 104]. Furthermore, it has also been shown that 50% of TGF-β knockout mice die *in utero* at days 10.5 – 11.5 with vascular defects and compromised vessel wall integrity [105]. This work suggests that TGF-β is necessary for SMC maturation during vasculogenesis and angiogenesis during maturation.

SMCs respond to TGF-β in a concentration-dependent manner. Lower concentrations of TGF-β (1-2 fg/ml) leads to SMC proliferation through the activation of PDGF receptors [106, 107]. Conversely, higher concentrations of TGF-β (10 pg/ml – 10 ng/ml) has been shown to inhibit proliferation by downregulating PDGF receptors [107, 108].

Lastly, TGF-β has been shown to increase ECM production by both increasing the expression of type I collagen while also decreasing matrix metalloproteinase (MMP) activity [106, 109].

1.3.2.3 Combined mechanical and chemical stimulation of SMCs

The most physiologically significant approach in studying maintenance of an SMC phenotype is combining the mechanical and chemical factors to create a more complex milieu in which to study differentiation. Stegemann and Nerem used SMCs embedded in a 3D collagen type I matrix, and subjected these constructs to cyclic mechanical strain with biochemical stimulation. Biochemical stimulation was added exogenously to the media using PDGF and TGF-β. Mechanical stimulation was applied using a bioreactor, and gel compaction, cell proliferation and α-SMA expression were subsequently assessed. Mechanical strain was shown to cause an increase in compaction and proliferation as compared to statically cultured controls [37]. While PDGF increased cell proliferation and decreased α-SMA expression, TGF-β supplementation led

to decreased cell proliferation and an increase in α-SMA expression. These results indicate that mechanical and various chemical stimuli may work together in regulating SMC phenotype [37].

1.4 ADULT STEM CELLS

Adult stem cells provide an exciting alternative to ESCs toward regenerative medicine applications. Several sources of adult stem cells have been expanded upon briefly in Chapter 1. The focus of this chapter will now be on mesenchymal stem cells derived from bone marrow, or bone marrow mesenchymal stem cells (BMMSCs), and how researchers have guided their differentiation toward a desired phenotype.

1.4.1 Determinants of Differentiation of MSCs

1.4.1.1 Mechanical stimulation of MSCs

It has been discussed in section 1.3 that mechanical stimulation is required to maintain the terminally differentiated phenotype of SMCs. However, it is necessary to elucidate role of mechanical strain on the differentiation of BMMSCs. While several research groups have utilized mechanical stimulation to differentiate BMMSCs toward several different cell lineages, the following sections will be focused on differentiation toward a vascular SMC phenotype Mechanical strain has been shown have effects in both 2D and 3D culture, and will be discussed further in the following sections.

1.4.1.1.1 2D mechanical strain

Our group was among the pioneering efforts assessing the ability of BMMSCs to differentiate using mechanical stimulation in 2D. Hamilton *et al.* have demonstrated that BMMSCs differentiate toward a vascular SMC phenotype while decreasing proliferation in response to mechanical stimuli [74]. Other groups have corroborated these findings. Park *et al.* revealed that uniaxial cyclic stretch is required for SMC gene transcription and subsequent SMC protein production [98]. As previously mentioned, mechanical stimulation in 2D leads to cellular realignment perpendicular to the direction of strain. The findings of Park *et al.* were based on gene expression from these reoriented cells. Because SMCs *in vivo* are aligned in the direction of strain, Kurpinski *et al.* sought to force the alignment of BMMSCs via channel fabrication, while still maintaining two-dimensionality. Mechanical stimulation of BMMSCs that were forced to align parallel to the direction of stretch with the use of channels led to a greater increase in SMC markers as compared to BMMSCs stretched without forced alignment [76].

1.4.1.1.2 3D mechanical strain

As noted previously, mechanical strain in 3D better simulates the mechanical environment *in vivo,* and thus it is advantageous to study stem cell differentiation in this manner. Altman *et al.* used 3D collagen gels and rotational strains to induce MSC differentiation, while also showing an increase in collagen I and III expression [69]. Cummings *et al.* have performed studies on 3D collagen/fibrin gel mixtures using BMMSCs, and have demonstrated a stronger ultimate tensile stress with upregulation in SMC gene expression when compared to statically cultured gels [72]. Most recently, our group published data on the effect of mechanical stimulation on bone marrow stem cells, and it was shown that mechanical stimulation in 3D promotes differentiation toward

an SMC phenotype, promotes cellular alignment in the direction of strain, and an increase in collagen production when compared to static controls [78].

1.4.1.2 Chemical stimulation of MSCs

Differentiation of BMMSCs may be induced by several different biological factors, similar to those described in Section 1.3.2.2. While more work has been done to the demonstrate maintenance of a terminally differentiated SMC phenotype, others have looked towards differentiation of mesenchymal stem cells toward an SMC phenotype. Several groups have demonstrated the ability to regulate BMMSC differentiation toward an SMC phenotype utilizing PDGF-BB [80, 110], TGF-β [75, 111], ascorbic acid (AA) [70]; and retinoic acid [71, 112]. A recent paper published by Narita *et al.* focused on the role of TGF-β and AA on differentiation of human MSCs into SMCs [77].

1.4.1.2.1 PDGF

While PDGF has been shown to decrease SMC protein expression in smooth muscle cells, several researchers have demonstrated its role in promoting an SMC-like phenotype in bone marrow-derived mesenchymal stem cells. Yoon *et al.* induced differentiation of human bone marrow-derived multipotent stem cells (hBMSCs) *in vitro* with culture media supplemented with PDGF-BB. Following 14 days of culture, hBMSCs stained positive for α-SMA and calponin. De novo expression of SMC genes, including α-SMA, SM22α and SM1 was confirmed via RT-PCR [113]. Others have demonstrated the role of PDGF in differentiating circulating smooth muscle progenitor cells (originating from the bone marrow) via SMC protein expression [80].

1.4.1.2.2 Retinoic Acid

Retinoids have been shown to play a role in vasculogenesis in many species [112]. In an effort to better understand the mechanism behind SMC differentiation, researchers have cultured P19 embryonal carcinoma cells with high concentrations retinoic acid, and have demonstrated SM1-positive (an isoform of MHC) cells [114]. Others have confirmed these findings by demonstrating treatment of this same cell line with PDGF leads to differentiation toward an SMC phenotype via expression of SMC-specific proteins, while also exhibiting functionality via the response to various contractile agents [71].

1.4.1.2.3 Ascorbic Acid

Arakawa *et al.* have demonstrated the response of a bone marrow stromal cell line to ascorbic acid via inducible expression of SMC-specific genes, namely α-SMA, SM22α, h-caldesmon and h-calponin when cultured in differentiation medium [70]. Others have confirmed these findings. Narita *et al.* demonstrated a significant increase in SM22α expression in response to ascorbic acid supplementation. In the same publication, this group also examined additive effects of AA and TGF-β supplementation on BMMSCs, and has demonstrated upregulation of SMC genes when compared to TGF-β or AA stimulation alone [77].

1.4.1.2.4 TGF-β

TGF-β has been shown to play a role mesenchymal in stem cell differentiation toward an SMC phenotype both *in vitro* and *in vivo.* Kinner *et al.* examined the effects of TGF-β on α-SMA expression, and results from their work concluded that TGF-β significantly upregulated expression of α-SMA [75]. As mentioned previously, Narita *et al.* looked in the role of both

TGF-β and ascorbic acid supplementation on BMMSCs, while also examining the role of TGF-β alone. BMMSCs cultured with TGF-β revealed an upregulation of SMC-specific genes in a dose-dependent manner [77]. Work by Gong and Niklason has corroborated these findings using human BMMSCs. Qualitative protein expression of α-SMA and calponin were demonstrated in cells supplemented with TGF-β growth media [73].

1.4.1.3 Combined mechanical and chemical stimulation of MSCs

Growth factors in conjunction with mechanical stimulation in 2D have been shown to have a significant effect in regulating the cell phenotype. Several researchers have explored the possible synergism between chemical and mechanical stimulation, and the subsequent regulation of SMC markers. TGF-β together with mechanical strain increased α-SMA when compared to mechanical strain alone [37]. More recent work shows that embryonic mesenchymal stem cells cultured under cyclic strain with TGF-β supplementation revealed an increase in mRNA levels of α-SMA and MHC by 10- and 2-fold respectively, when compared to statically cultured cells [79]. These findings suggest that chemical and mechanical factors may work together to modulate the cell phenotype, when compared to each stimulus alone. This work has led to the formulation of our specific hypothesis and will be discussed in Chapter 2.

Most recent work by Gong and Niklason utilized human bone marrow-derived mesenchymal stem cells embedded in a biodegradable scaffold, and studied their ability to differentiate into SMCs. Using a biomimetic perfusion system, cyclic strain was combined with exogenous growth factors to investigate the effects on SMC proliferation and differentiation. Qualitative and quantitative protein expression was demonstrated for early and midstage SMC differentiation markers. This work demonstrates the ability of BMMSCs to be successfully

integrated into scaffolds for vascular graft applications, while underscoring their ability to differentiate into SMCs in response to the appropriate mechanical and chemical environment [73].

2.0 SPECIFIC AIMS

Multi-potential progenitor cells may serve as an alternative source of terminally differentiated cells for tissue engineering applications. The bone marrow has been shown to contain these multi-potent progenitor cells, and they have been shown to differentiate toward several hematopoietic and mesenchymal lineages [60, 115-118]. Bone marrow mesenchymal stem cells (BMMSCs) may alleviate issues associated with cell sourcing [22], as they are easily obtained and are an autologous cell source. Despite this, the use of BMMSCs towards vascular applications is still preliminary. Biochemical differentiation has been traditionally used to provide the appropriate environmental cues to direct BMMSC differentiation [57, 60, 63]. However, chemical stimuli used *in vitro* is required to be maintained *in vivo* to retain the desired differential effects. Without the appropriate chemical stimulation, the differentiated phenotype may not be retained *in vivo.* This further emphasized the need to study the effects of the mechanical environment on BMMSCs, as it is well known that the mechanical environment plays a pivotal role in maintaining the phenotype of terminally differentiated cells [119-124]. Recent data suggests that BMMSCs subjected to a mechanical environment may differentiate towards a SMC phenotype [74]. Growth factors in conjunction with mechanical stimulation have been shown to have a significant effect in regulating the cell phenotype. Simultaneous stimulation with mechanical strain and TGF-β has been shown to increase α-actin expression when compared to mechanical strain alone [37, 79]. This work suggests that mechanical and

chemical factors may work together to promote differentiation towards a SMC phenotype [37]. Consequently, the purpose of this research was to further investigate the effects of both mechanical and chemical stimulation.

Hypothesis: Uniaxial cyclic tension and chemical stimulation with TGF-β will differentiate BMMSCs towards an SMC-like lineage in a synergistic manner.

2.1 SPECIFIC AIM 1

To determine the effect of cyclic tension and frequency on BMMSCs in a 3D fibrin matrix.

2.2 SPECIFIC AIM 2

To determine the synergistic effects of mechanical and chemical stimulation with TGF-β at various strains and frequencies as in Specific Aim 1.

Mechanical stimulation has been demonstrated to play a role in both the maintenance of an SMC phenotype and differentiation toward an SMC phenotype of cells derived from mesenchymal lineages. Similarly, chemical stimulation has proven to both maintain and promote an SMC phenotype. Other groups have then begun to question whether there are any syngeristic effects between mechanical and chemical stimulation, and the role in which simultaneous stimulation

may play in promoting an SMC phenotype in BMMSCs. In the first specific aim, BMMSCs will be subjected to uniaxial mechanical stimulation alone. In the second specific aim, BMMSCs will be subjected to uniaxial mechanical stimulation with simultaneous TGF-β supplementation. The effects of mechanical stimulation alone and the combined effects of mechanical and chemical stimulation will be assessed to determine SMC differentiation of BMMSCs. Chapter 3 will discuss the experimental design and the methods utilized for this thesis. Chapter 4 will show the results obtained from this work, and Chapter 5 will discuss these results in greater detail. Chapter 6 will relay final thoughts and conclusions, and Chapter 7 will discuss potential future work for this project.

3.0 METHODS

3.1 CELL CULTURE AND SOURCE

Rat bone marrow mesenchymal stem cells (BMMSCs) were obtained from the Tulane Center for Gene Therapy as an established cell source [125]. According to their protocol, BMMSCs were harvested from the femurs of adolescent Lewis rats and have been characterized as $CD90^+$ and $CD59^+$ [125]. BMMSCs were plated at a density of 200 cells/cm^2 and cultured at 37ºC and 5% CO_2 in α-Modified Eagle's Medium (α-MEM, Invitrogen) supplemented with 20% fetal bovine serum (FBS, Atlanta Biologicals, Atlanta, GA) 1% antibiotic/antimicotic (Invitrogen) and 10mM L-Glutamine (Invitrogen). The lot of FBS was selected for optimal growth based on the growth kinetics [126]. BMMSCs were expanded until confluent, and used up to passage 10. Media changes were preformed every 48 hours with complete media.

Once cells reached confluence, BMMSCs were rinsed in Dulbecco's phosphate buffered saline (PBS) and trypsinized using 0.1% tryspin (Invitrogen) at 5% CO_2 and 37ºC for 5 minutes until cells were detached. Media was then added to stop the effects of trypsin, and the cell suspension was transferred to a conical tube for centrifugation at 1200 rpm for 5 minutes. Following centrifugation, the cell pellet was resuspended in an appropriate volume of complete media to achieve a desired concentration to create 3D constructs, as described in the next section.

3.2 FABRICATION OF 3D TISSUE TRAIN CONSTRUCTS

To create a 3D construct that was capable of withstanding cyclic stretch, a fibrin gel was utilized, as it is capable of being molded into the Flexcell^{TM} Tissue-Train^{TM} (Flexcell, Hillsborough, NC) troughs utilized in our experimental model. Fibrin gels were created via an enzymatic reaction with fibrinogen and thrombin, allowing cells to be easily integrated homogeneously into the constructs. A cell/fibrinogen solution was created by suspending $1x10^6$ cells/ml in a solution of fibrinogen (5 mg/mL, Sigma Aldrich, St. Louis, MO) supplemented with 6-aminohexanoic acid (1 mg/mL, Sigma-Aldrich, St. Louis, MO). A thrombin solution (2.5 units/ml, Sigma-Aldrich, St. Louis, MO) created with α-MEM was made separately and kept aside on ice. TGF-β was supplemented to the thrombin solution at a concentration of 10 ng/mL for experimental groups with TGF-β supplementation. To form a fibrin gel, the thrombin solution was added to the fibrinogen/cell suspension, mixed via conical tube inversion, then 180 µl of the fibrinogen/thrombin mixture was added to each well (see **Figure 3-1**).

Constructs were allowed to gelate at 37ºC and 5% CO_2 for 30 minutes, then complete media was added to each well. For constructs made with TGF-β, complete media supplemented with 10 ng/mL of TGF-β was added following gelation. Samples were incubated for 48 hours to allow for compaction before beginning mechanical straining regimens. See Appendix A for more details on tissue train construct fabrication.

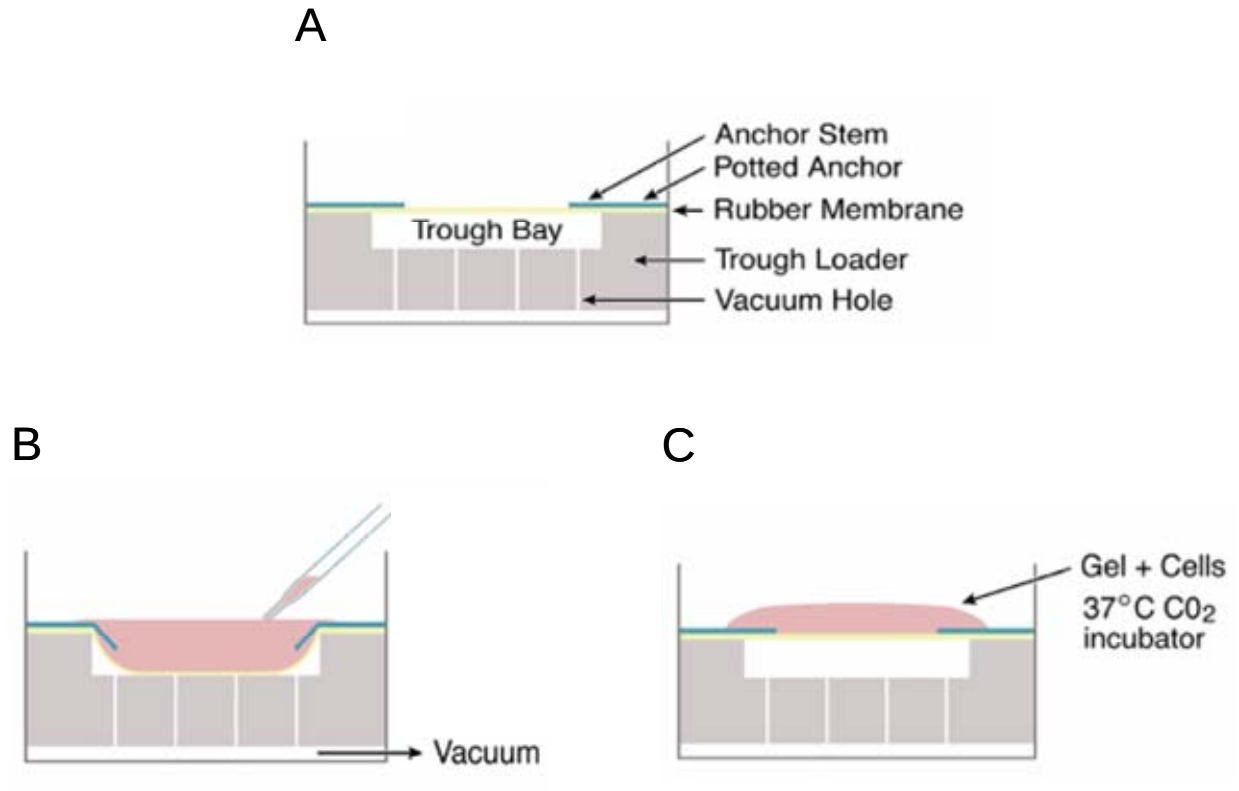

Figure 3-1: Creation of a fibrin gel using tissue train. (A) Side view of tissue train posts with no applied vacuum. (B) Application of a vacuum through vacuum holes in tissue train troughs. Deformable membrane is pulled into the trough via a vacuum, allowing for the addition a gel solution into the trough. (C) Anchor stems allow for gels to attach completely at ends, and the compacted gel may be released from the vacuum following compaction. Figure adapted from www.flexcellint.com.

3.3 DETERMINATION OF OPTIMAL LOCATION FOR TGF-β IN THE EXPERIMENTAL MODEL

Based on a literature search, it was determined that a concentration of 10 ng/ml of TGF-β would be appropriate for this application, as a concentration any higher than 10 ng/ml was shown to have no additional effects. Because growth factors are expensive, it was important to determine where the addition of TGF-β would be made for the desired effects: either added with the construct, supplemented to the media, both, or neither (see **Figure 3-2** and **Figure 3-3** for schematic). In the event that TGF-β appeared to have no effect, this would not have been pursued further. Therefore, for this purpose, constructs were fabricated with TGF-β in the construct, in the media, or in both the construct and media. The control group had no additional TGF-β in either location. To conclude where TGF-β exerted the greatest effects, constructs were fabricated as described previously, and subjected to the same experimental conditions (i.e. CS, SS or FF) with the noted locations of TGF-β. Samples were then processed as described in Section 3.6.2 and assessed under phalloidin staining. Constructs were wet mounted in PBS and viewed under a confocal microscope as described in Section 3.6.4. Z-stacks created during microscopy were subsequently analyzed and f-actin was quantified.

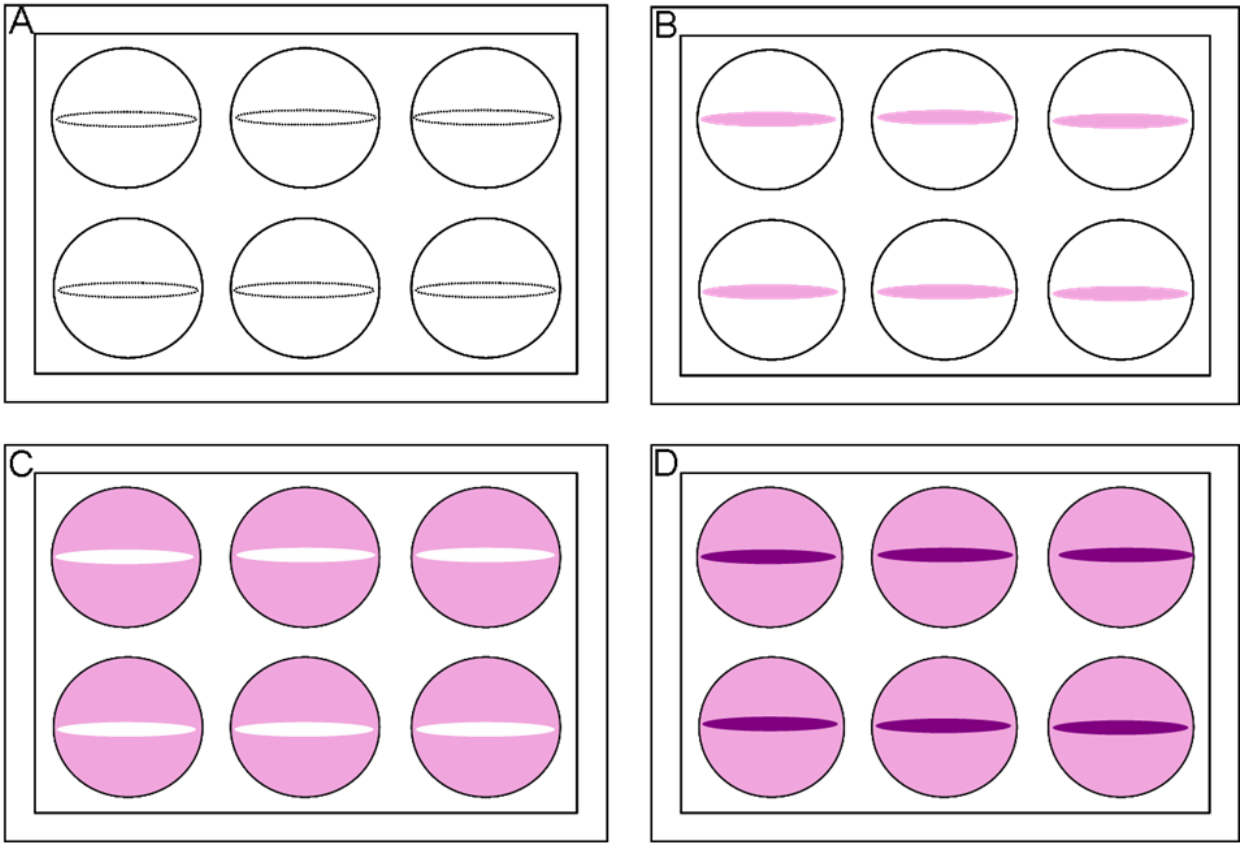

Figure 3-2: Schematic of location of TGF-beta in experimental model for CS and SS groups. (A) No TGF-beta. (B) TGF-beta in the construct. (C) TGF-beta supplemented to the media. (D) TGF-beta added to both the construct and media.

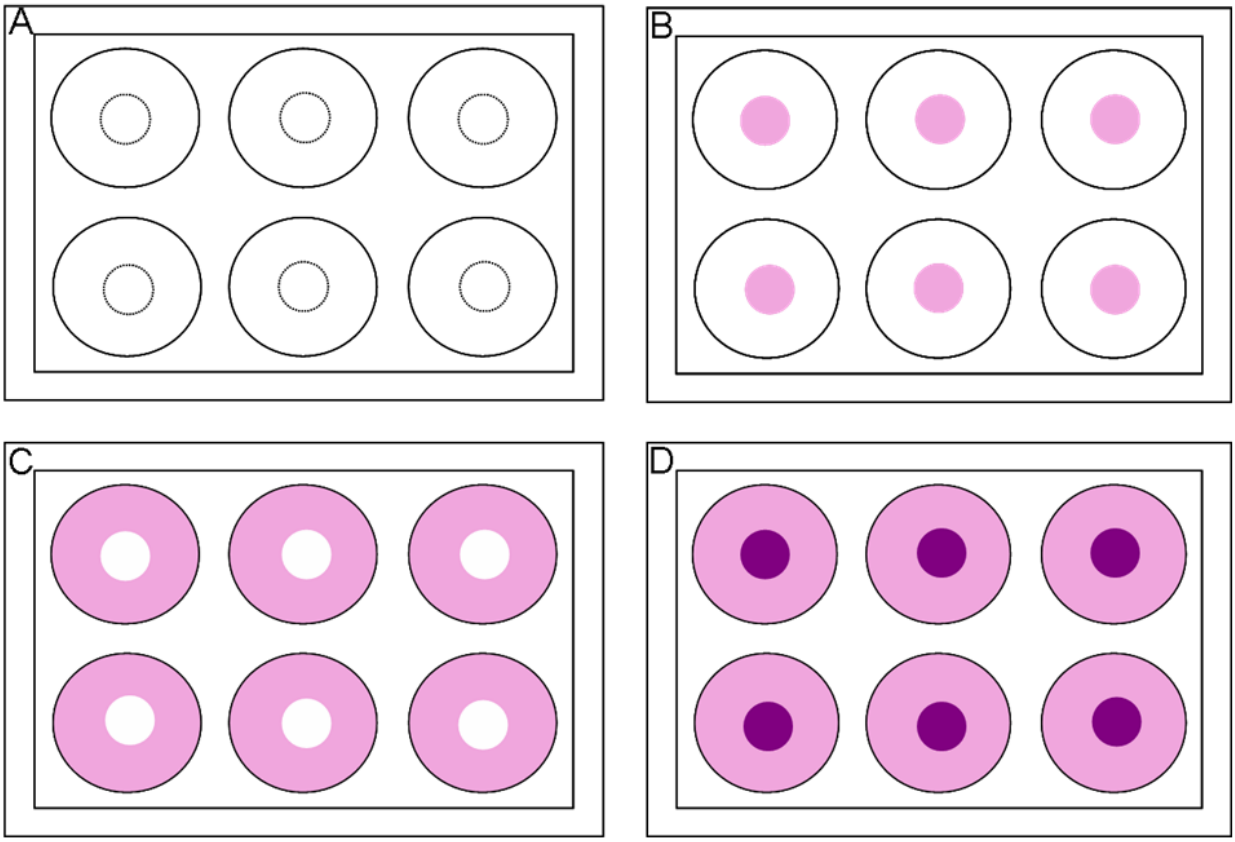

Figure 3-3: Schematic of location of TGF-beta in experimental model for FF groups. (A) No TGF-beta. (B) TGF-beta in the construct. (C) TGF-beta supplemented to the media. (D) TGF-beta added to both the construct and media.

3.4 EXPERIMENTAL DESIGN

3.4.1 Flexcell

For experimental conditions requiring a cyclic straining regimen, the Flexercell FX4000T^{TM} Tissue Train^{TM} unit was utilized to create cyclic stretch imposed in fibrin gel constructs. This system works via a vacuum applied underneath culture plates with deformable membranes. The flexible membrane surfaces are stretched over rigid posts under the applied vacuum, allowing for a prescribed direction of stretch. In these particular experiments, we utilized an arctangle post to

impose a uniaxial cyclic strain on the fibrin constructs. The vacuum can be regulated via a computer-controlled system, allowing for control over various strain magnitudes and frequencies desired for a particular cyclic straining regimen. The baseplates allow for up to four 6-well tissue train plates to be stretched at once (see **Figure 3-4**).

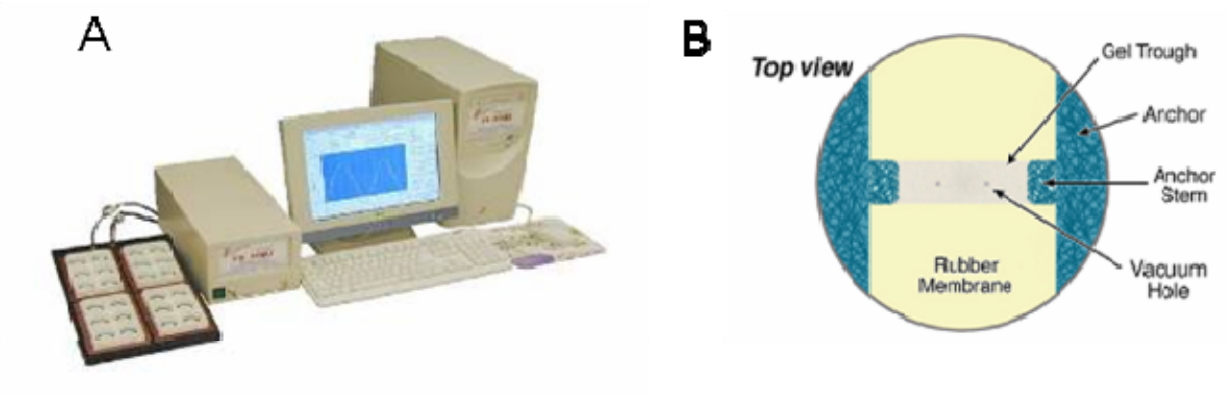

Figure 3-4: (A) Flexcell device and (B) top view of tissue train plate. Figure adapted from www.flexcellint.com.

3.4.2 Experimental Groups

The constructs were divided into 6 experimental groups: cyclic stretch (CS), static stress (SS), and free float (FF) control (stress- and strain-free), and each group was studied with (+) and without (-) TGF-β. Once CS and SS samples were compacted after the 48 hour period, tissue train constructs were released from the bottom of the plates in between the anchors using a cell scraper. This was to allow for a homogeneous strain distribution along the longitudinal direction of the constructs. The CS constructs were subjected to 10% strain at a frequency of 1 Hz for 6

days. A human-physiologic strain and frequency was chosen so as to best mimic the mechanical environment in the human arterial system *in vivo.* Parameters related to rat-physiologic strains and frequencies may have been relevant, however these strains and frequencies would not be achievable in the Flexercell^{TM} system. The SS groups were created in the same manner, however these constructs remained in static conditions for the duration of the experiment. Lastly, FF groups were created in 12-well plates (i.e. not placed in tissue train troughs within the tissue train plates) to allow for gels to freely compact in all directions. Briefly, the fibrin/cell suspension was pipetted into a 12-well plate, and gels remained attached to the bottom surface of the plates for 48 hours. Following the 48 hour compaction period, fibrin gels were released from the bottom using a cell scraper, allowing them to be 'free floating', or stress- and strain-free, for the duration of the experimental period. These experimental groups are visualized and summarized in **Figure 3-5**.

All experiments were completed in parallel with groups containing TGF-β under the same conditions. Therefore, each experiment consisted of 6 experimental groups: cyclic stretch (CS), static stress (SS), and free float (FF), with (+) and without (-) TGF-β. For the remainder of this thesis, groups will be denoted as CS+, SS+, FF+, CS-, SS- and FF- to designate with or without the addition of TGF-β, respectively.

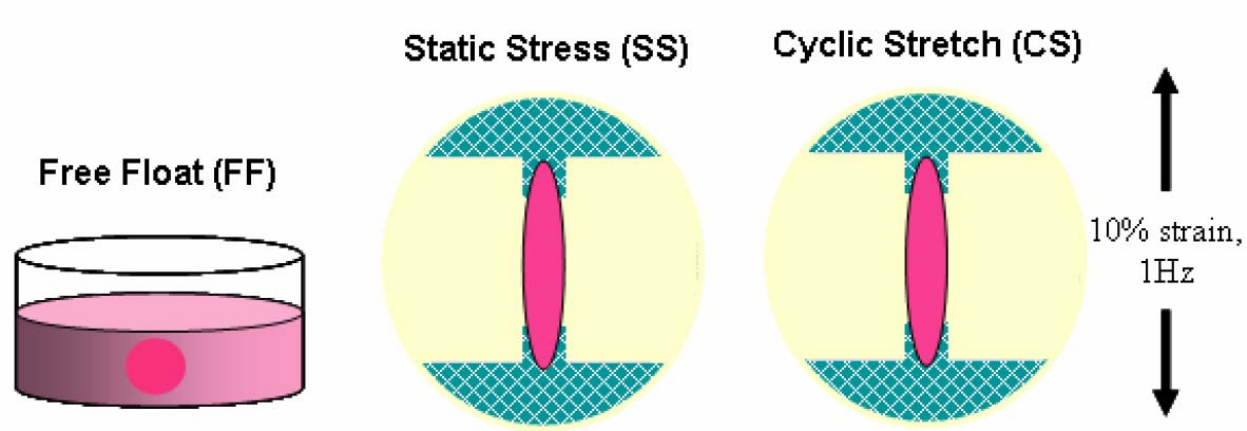

Figure 3-5: Schematic of experimental groups. CS groups are fabricated in tissue train troughs and are subjected to 10% strain and 1Hz. SS samples are created in a similar manner, however are not subjected to any external mechanical forces. FF groups are created in 12-well plates and are allowed to compact freely in all directions upon releasing the gels from the bottom of the wells following the compaction period.

3.5 APPLICATION OF CYCLIC STRETCH

Tissue train plates were mounted on the FX4000T baseplates and connected to the strain unit following the 48 hour compaction period. Cyclic stretch was applied via membrane deformation from the applied vacuum across an arctangle post, thereby creating uniaxial cyclic strain across the tissue train constructs. SS and FF groups required no additional manipulation.

3.6 ENDPOINT ANALYSIS

3.6.1 Viability

To measure viability and quantify BMMSC proliferation, samples were evaluated using an MTT assay. Briefly, constructs were added to a 96-well plate with 200 µl of α-MEM and 20 µl of Thyazolyl Blue Tetrazolium Bromide (MTT solution, Sigma-Aldrich, St. Louis, MO), and incubated at 37ºC and 5% CO_2 for 4 hours to allow for crystal formation. Following the incubation step, 220 µl of the α-MEM + MTT solution was removed, then 200 µl 0.04N HCl in 2-propanol were added to dissolve the crystals and kept at 4ºC in the dark for 24 hours. Using a microplate reader (Bio Rad, Hercules, CA), absorbance readings for 100 µl of each sample were taken, and a final fold increase in cell number was calculated using a standard curve based on known cell concentrations.

3.6.2 Morphology

Following the termination of an experiment, samples were rinsed in PBS, fixed with 4% paraformaldehyde, rinsed 5 times with PBS, and then incubated in 0.1% Triton-X 100 to permeabilize the cell membranes. Samples were then incubated with Alexa 488-conjugated phalloidin (Sigma-Aldrich, St. Louis, MO) for 60 minutes. Samples were then washed with PBS 5 times to remove any unbound phalloidin, and then counter-stained with DAPI. All samples were wet-mounted with PBS and viewed under an inverted confocal microscope (Olympus F1000). Details of the image acquisition process will be described in greater detail in a

subsequent section. Images were analyzed by calculating the stress filament area for each image in the z-stack. Filaments were evaluated using gray-scale thresholding, and the area of stress filaments per cell was measured using MetatMorph Image analysis software (v 6.3, Molecular Devices, USA). Thresholded filaments were measured in pixels and normalized to the cell number for each image in the z-stack.

3.6.3 Immunohistochemistry

To evaluate SMC phenotype via immunofluorescence, samples were fixed in 4% paraformaldehyde, washed 5 times in PBS, and then incubated in 0.1% Triton-X 100 to permeabilize the cell membranes. Samples were blocked with 5% normal donkey serum in PBS plus 0.5% bovine serum albumin (BSA, Equitech-bio, Kerrville, TX) and 0.15% glycine (Sigma-Aldrich, St. Louis, MO) for 45 minutes to prevent nonspecific binding of primary antibody. Samples were then rinsed again with PBS, and incubated with primary antibodies, namely α-smooth muscle actin (α-SMA), h1-calponin, and myosin heavy chain (MHC). See **Table 3-1** below for details on the antibodies used. Primary delete samples were not incubated with primary antibody, and served to set the threshold for imaging all other samples. After washing with PBS to remove unbound primary antibody, samples were incubated with DAM 488-conjugated secondary antibody, counterstained with DAPI, and then wet-mounted and viewed under an inverted confocal microscope (Olympus F1000). Details of the image acquisition process will be described in greater detail in Section 3.5.4. Images were evaluated qualitatively by inspection to determine differentiation.

Table 3-1: Antibodies used for qualitative SMC phenotype characterization.

Classification	Antibody	Dilution	Catalog Number	Manufacturer
SMC	α-SMA	1:500	MAB1522	Chemicon, Temecula, CA
SMC	α-SMA	1:500	A5228	Sigma-Aldrich, St. Louis, MO
SMC	h1-calponin	1:400	M3556	Dako, Capinteria, CA
SMC	MHC	1:400	M3558	Dako, Capinteria, CA

3.6.4 Confocal Microscopy

As noted previously, all samples requiring immunofluorescent imaging were wet mounted in PBS and viewed under an inverted confocal microscope. Fluorescent microscopy was preformed at 40X for all samples. Primary delete samples were viewed under the FITC filter and then used to set the threshold intensity. All samples were viewed at this intensity or less to ensure there was no non-specific binding of secondary antibody and to eliminate any background signal. Because samples were not sectioned, but rather mounted in 3D, z-stacks were created for all samples, and later reconfigured in MetaMorph (version 7.0, Downingtown, PA) Image analysis software as one, combined image.

3.6.5 Histology

Following the termination of an experiment, samples were fixed in 4% paraformaldehyde and rinsed in PBS. Samples were then fixed in 10% neutral buffered formalin for 1 hour and subsequently embedded in paraffin blocks and sectioned using a Shandon Finesse microtome (Thermo Shandon, Pittsburgh, PA) and mounted to slides. To evaluate collagen production, samples were stained with Masson's Trichrome (MT) and picrosirius red (PSR). To evaluate cell morphology within the constructs, constructs were stained with H&E. Samples were viewed under brightfield (Olympus Provis), and images were qualitatively assessed for collagen production and overall morphology. All images were taken at identical exposure times for a given experiment. For PSR-stained samples, a light polarizer was necessary to measure the birefringence.

3.7 STATISTICAL ANALYSES

All experiments and endpoints were completed 5 times unless otherwise noted in the results section. All data is reported as mean ± standard error of the mean (SEM). Statistical analyses were performed using Microsoft Excel. A paired t-test was utilized to compare groups with and without TGF-β. A $p\text{-value} < 0.05$ was considered significant.

4.0 RESULTS

4.1 DETERMINATION OF OPTIMAL LOCATION FOR TGF-β IN THE EXPERIMENTAL MODEL

Experimental groups receiving TGF-β in both the construct and media in SS and FF conditions led to greatest the stress filament area per cell. In the CS group, constructs fabricated with TGF-β in the construct only led to the greatest increase in pixel density of f-actin filaments per cell. This was considered an anomaly as this data is a result of one experiment. Therefore, because the addition of TGF-β would not cause any detrimental effects, it was concluded that TGF-β will be added to both the construct and media for the subsequent experiments. See **Figures 4-1** and **4-2**.

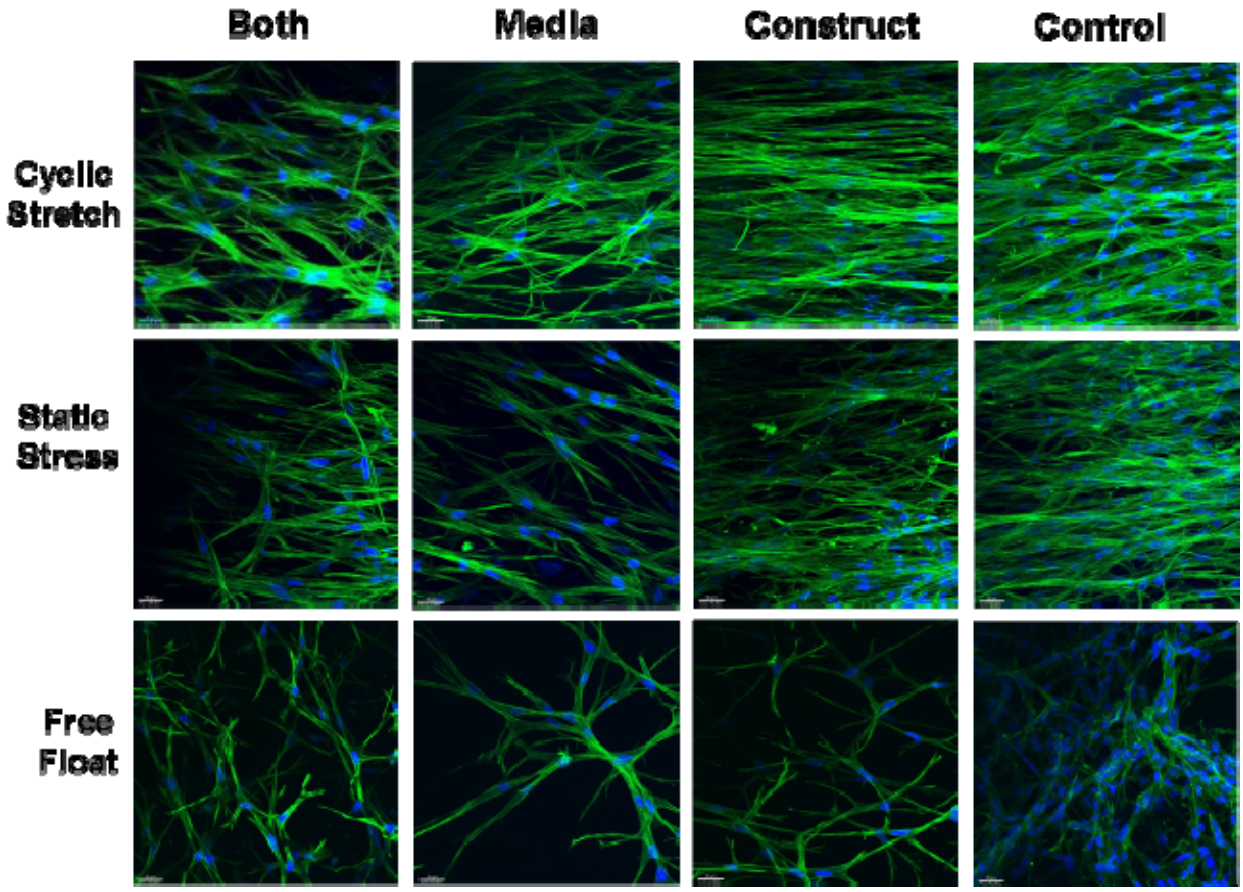

Figure 4-1: F-actin images to determine location optimal location of TGF-beta in the experimental design. Images based on a single experiment. F-actin fibers are in green; nuclei are seen in blue. All images taken at 40x.

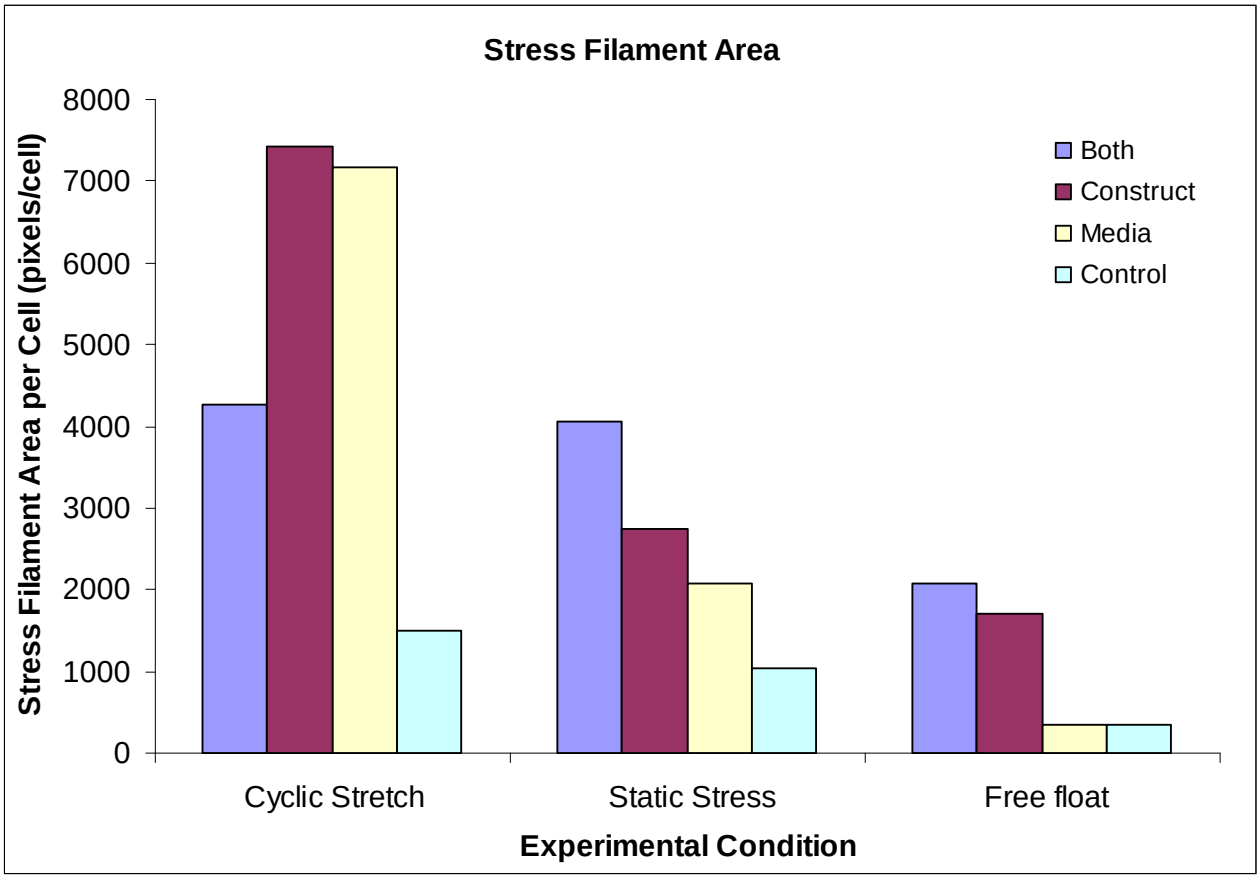

Figure 4-2: Calculated stress filament area/cell in determination of optimal location of TGF-β. Data shown is a result of one experiment.

4.2 VIABILITY

BMMSCs effectively integrated into fibrin gel constructs, and cells remained viable throughout the experimental period, as evidenced by the MTT assay (**Figure 4-3**). The CS+ group yielded the greatest fold increase in cell number when compared to all other experimental conditions. When comparing within the experimental groups, both static stress and free float groups

demonstrated a greater fold-increase over day 0 when there was no TGF-β supplementation. However, in the presence of cyclic strain, TGF-β supplementation led to a greater fold-increase in cell number as compared to control. Statistical analysis revealed a significant fold-increase in cell number when comparing CS+ to FF+ and SS+ ($p < 0.001$ and $p < 0.01$, respectively). CS- and SS- groups also demonstrated a significant fold-increase in cell number when compared to FF- ($p < 0.01$ and $p = 0.03$ respectively).

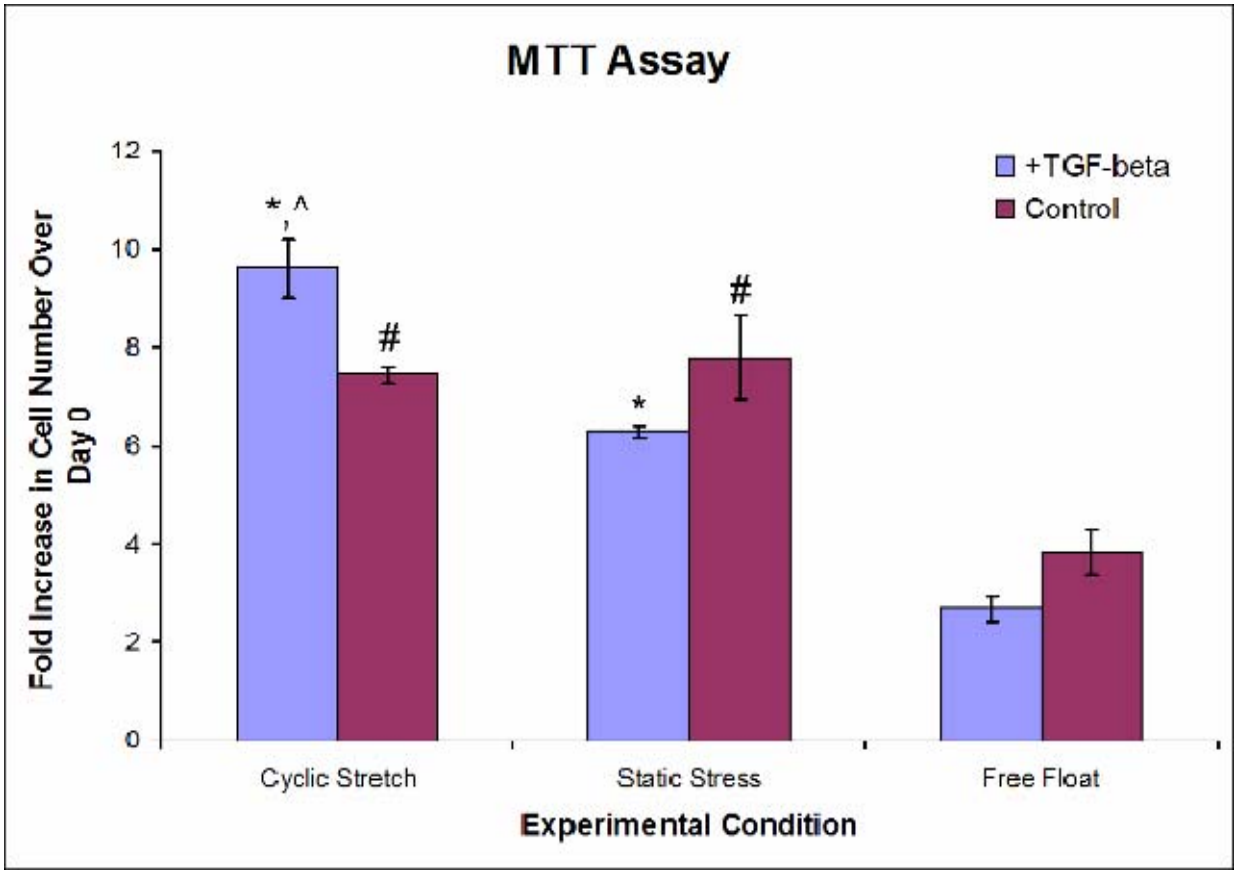

Figure 4-3: MTT Assay. Data represented as mean ± SEM, and based on n = 4. Blue bars indicate groups with TGF-β; purple bars indicate samples without TGF-β. *, #, and ^ indicates a significant difference ($p<0.05$) when compared to the FF+, FF- and SS+ groups, respectively.

4.3 MORPHOLOGY

4.3.1 F-actin

The presence of either cyclic strain or static stress had a profound impact on the cell alignment in these fibrin gel constructs. A qualitative assessment demonstrates that CS+/- and SS+/- groups align parallel to the direction of strain or static stress (see **Figure 4-4** for representative images, and Appendix D for all images from all experiments). Unlike CS+/- and SS+/- groups, FF+/- groups exhibited random cellular orientation. The presence of TGF-β vs. no TGF-β had no effect on cell alignment within the constructs.

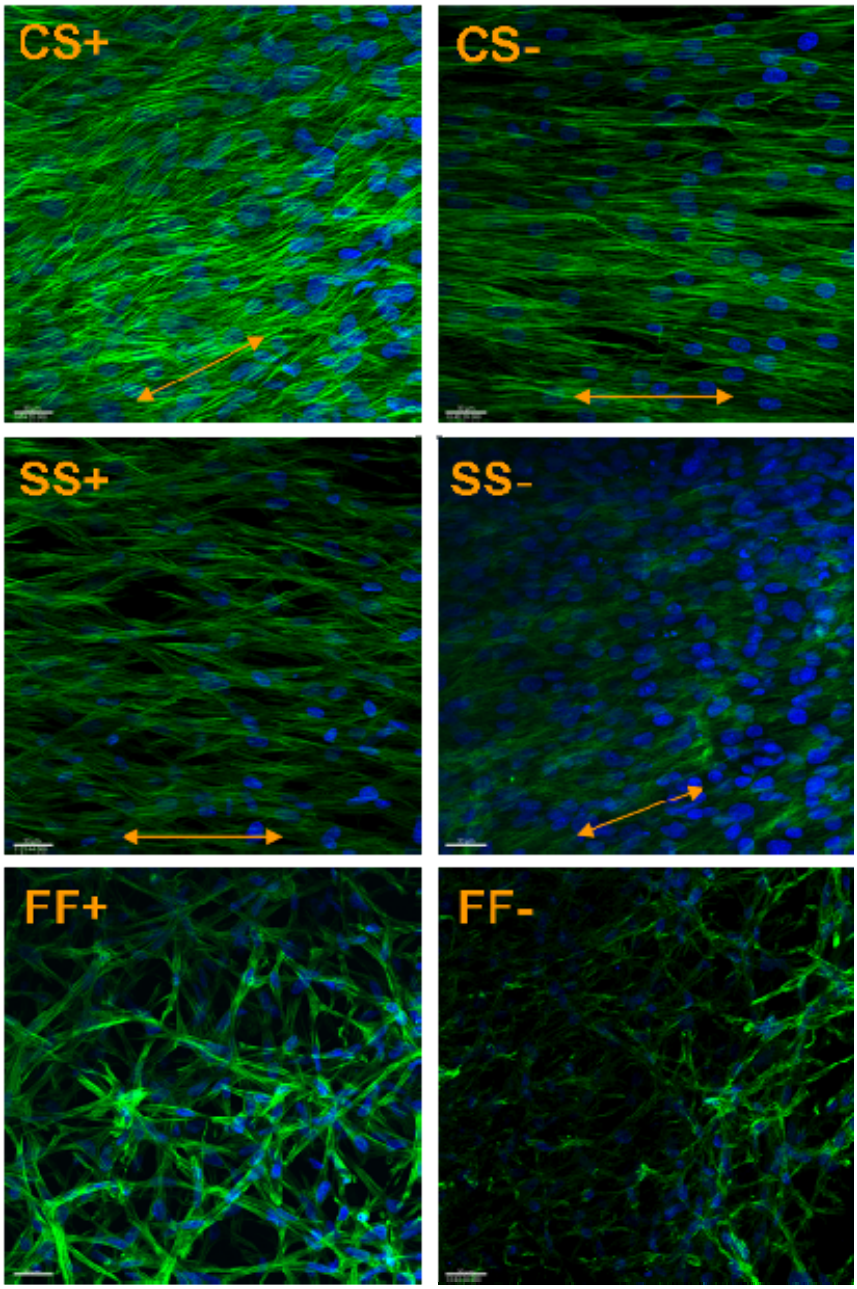

Figure 4-4: Phalloidin staining of CS, SS and FF groups with (+) and without (-) TGF-beta. Arrows indicate the direction of stretch. F-actin fibers are in green; nuclei are seen in blue. Data shown is representative of all experiments. See Appendix D for images from all experiments. All images taken at 40x.

Quantification of the f-actin fibers allows for a better understanding of the relative differences between experimental groups. F-actin images (such as those in **Figure 4-4**) were quantified as

described in Section 3.6.2 and data is represented as pixels per cell. Regarding groups with TGF-β supplementation, there is a trend toward increasing f-actin fiber density upon the addition of an external mechanical force. FF+ samples yielded 1759.4 ± 319 pixels per cell, while the CS+ group led to the greatest f-actin fiber density of 3582.2 ± 832 pixels per cell (**Figure 4-5**). The data below reveals that the CS+ group was statistically significant when compared to CS- ($p = 0.039$) and its free float control, FF+ ($p = 0.012$).

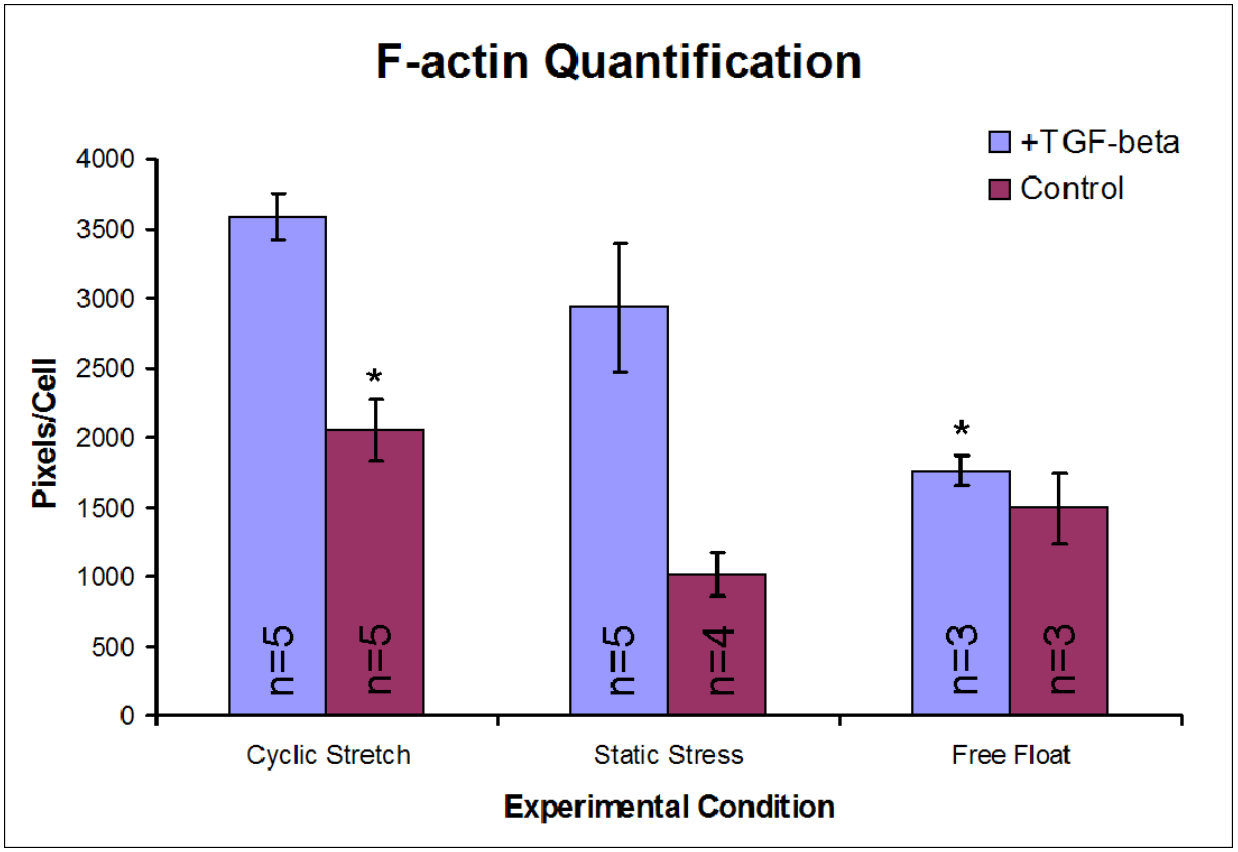

Figure 4-5: F-actin quantification. Data represented as mean ± SEM. Blue bars indicate groups with TGF-β; purple bars indicate samples without TGF-β. *Indicates a significant difference ($p<0.05$) when compared to the CS+ group.

4.3.2 Hematoxylin & Eosin

While f-actin staining demonstrates cell alignment within the fibrin constructs, H&E allows the visualization of how compacted the cells are, as well as the location within the construct. In these images, the nuclei are stained in purple and the fibrin gel is stained in pink. As shown with f-actin statining, H&E confirms the alignment of cells in the direction of stretch. Several samples also revealed that cells tend to reside at the edges of the constructs, as seen in the CS-panel in **Figure 4-6**. Furthermore, cells in both FF groups demonstrated cell localization toward the center (marked 'c' in **Figures 4-6** and **4-7**) of the constructs.

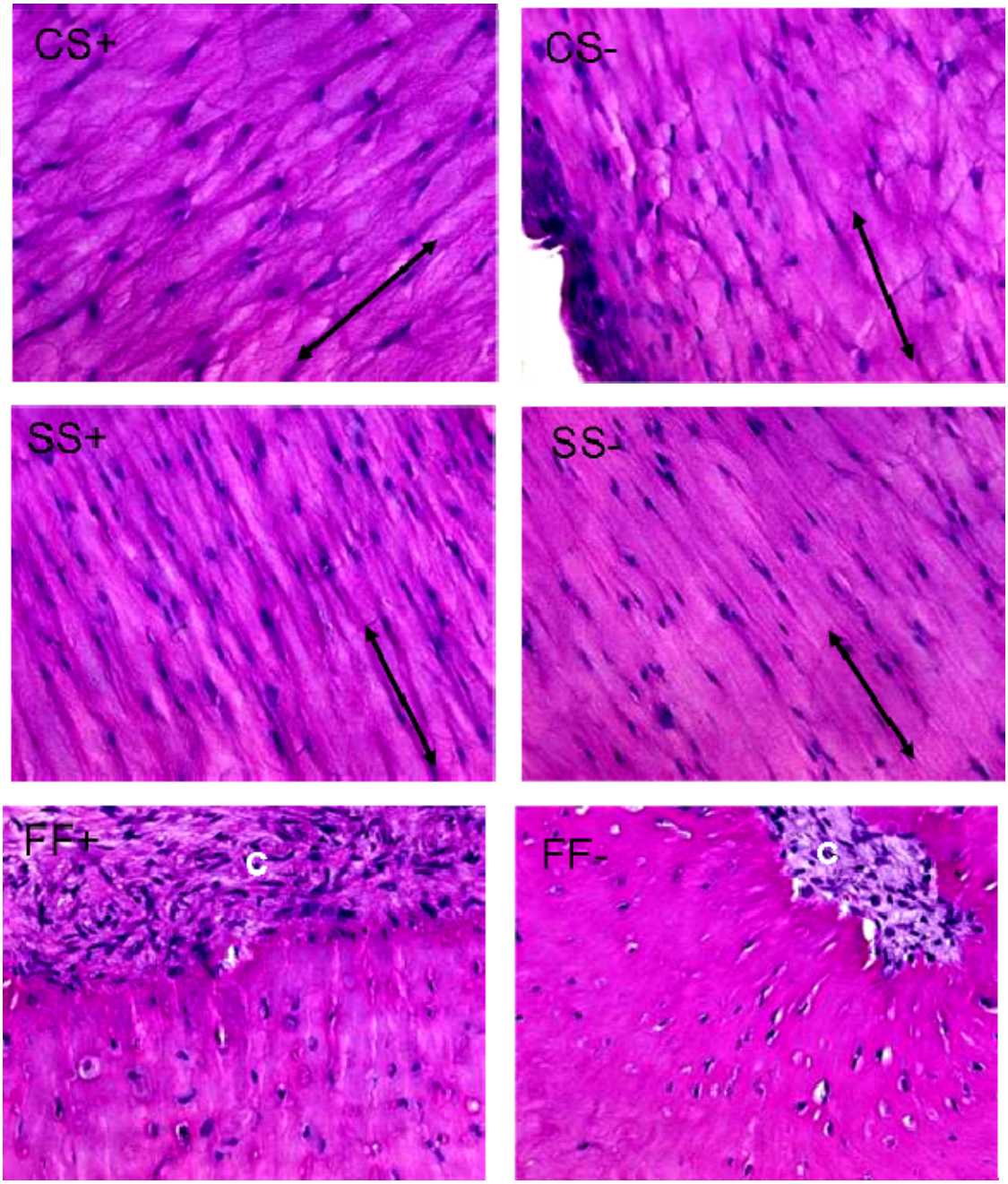

Figure 4-6: H&E staining of CS, SS and FF groups with (+) and without (-) TGF-beta. Data shown is representative of all experiments. Nuclei = purple; Fibrin = pink. See Appendix C for images from all experiments. Arrows indicate the direction of stretch. C indicates the center of the construct. All images taken at 40x.

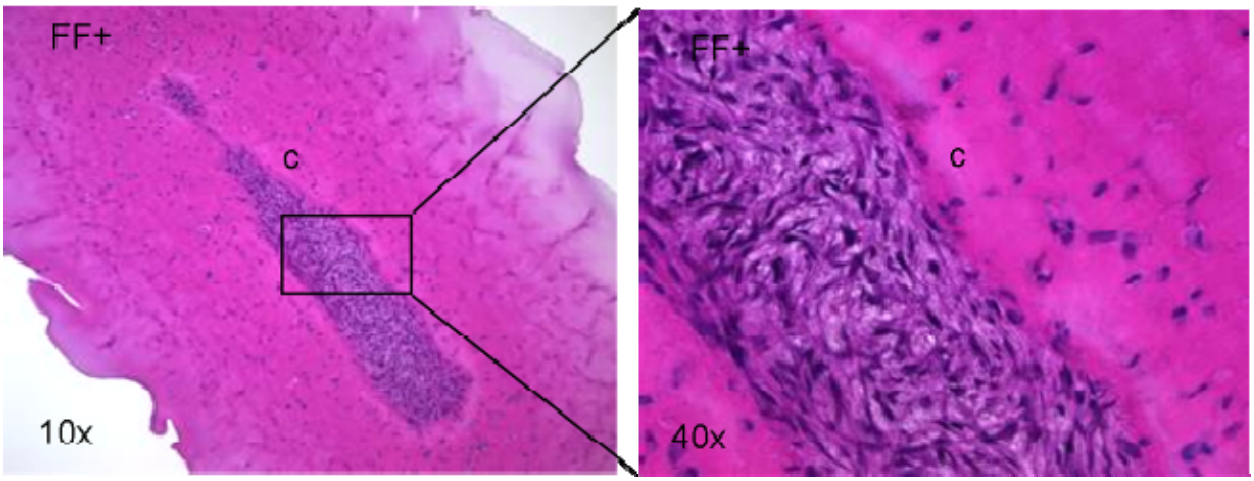

Figure 4-7: H&E staining of FF+ group revealing cell localization in FF constructs. Nuclei = purple; Fibrin = pink. Left panel image taken at 10x. Right panel image taken at 40x.

4.4 QUALITATIVE PROTEIN EXPRESSION VIA IMMUNOHISTOCHEMISTRY

4.4.1 α-SMA

α-SMA is the earliest differentiation marker of SMCs. CS+ and CS- groups both show abundant expression of this marker protein, while SS+/- groups reveal more sparse expression (see **Figure 4-8**). Neither of the FF+/- groups showed any positive staining for α-SMA. It must be noted, however, that this data is a result of a single experiment (n = 1), as immunostaining for this particular antibody in remaining experiments proved to be difficult due to reasons that will be discussed in Chapter 5.

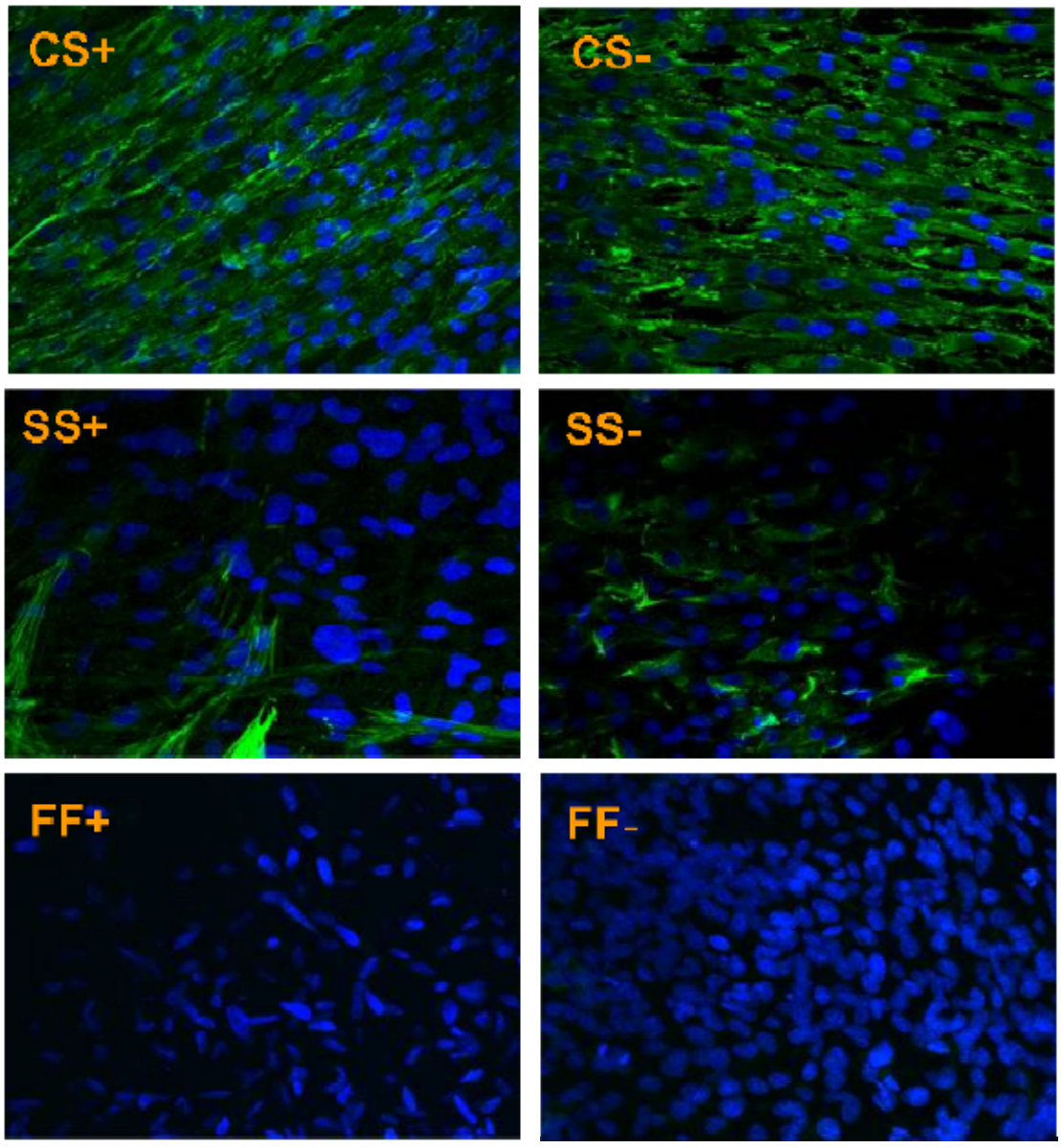

Figure 4-8: Immunostaining with α-SMA for CS, SS and FF groups with (+) and without (-) TGF-beta. Green indicates positive α-SMA staining; nuclei are seen in blue. See Appendix E for images from all experiments. Data shown is representative of a single experiment. All images taken at 40x.

4.4.2 Calponin

Calponin is a mid-stage differentiation marker of SMCs. As seen in **Figure 4-9**, both CS+ and CS- groups, as well as SS+, show some degree of positive staining for this antibody. SS-, FF+ and FF- groups show no positive staining for calponin. Green indicates positive calponin staining and nuclei are seen in blue. Data seen in **Figure 4-9** are representative images of n = 3.

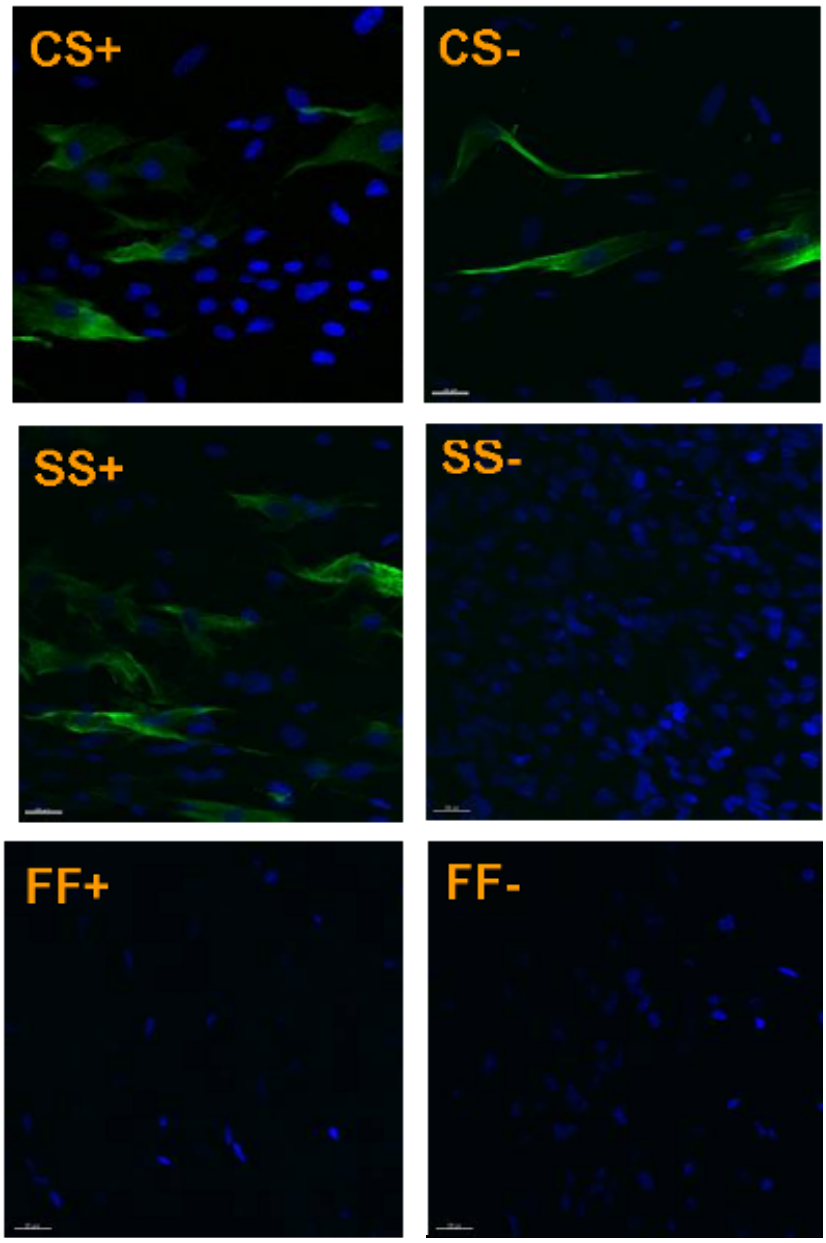

Figure 4-9: Immunostaining with calponin for CS, SS and FF groups with (+) and without (-) TGF-beta. Green indicates positive calponin staining; nuclei are seen in blue. Data shown is representative of all experiments. See Appendix F for images from all experiments. All images taken at 40x.

4.4.3 MHC

MHC is a marker of terminally differentiated SMCs. As seen in **Figure 4-10**, none of the experimental groups showed positive staining for MHC. The images in **Figure 4-10** are representative images for all experiments.

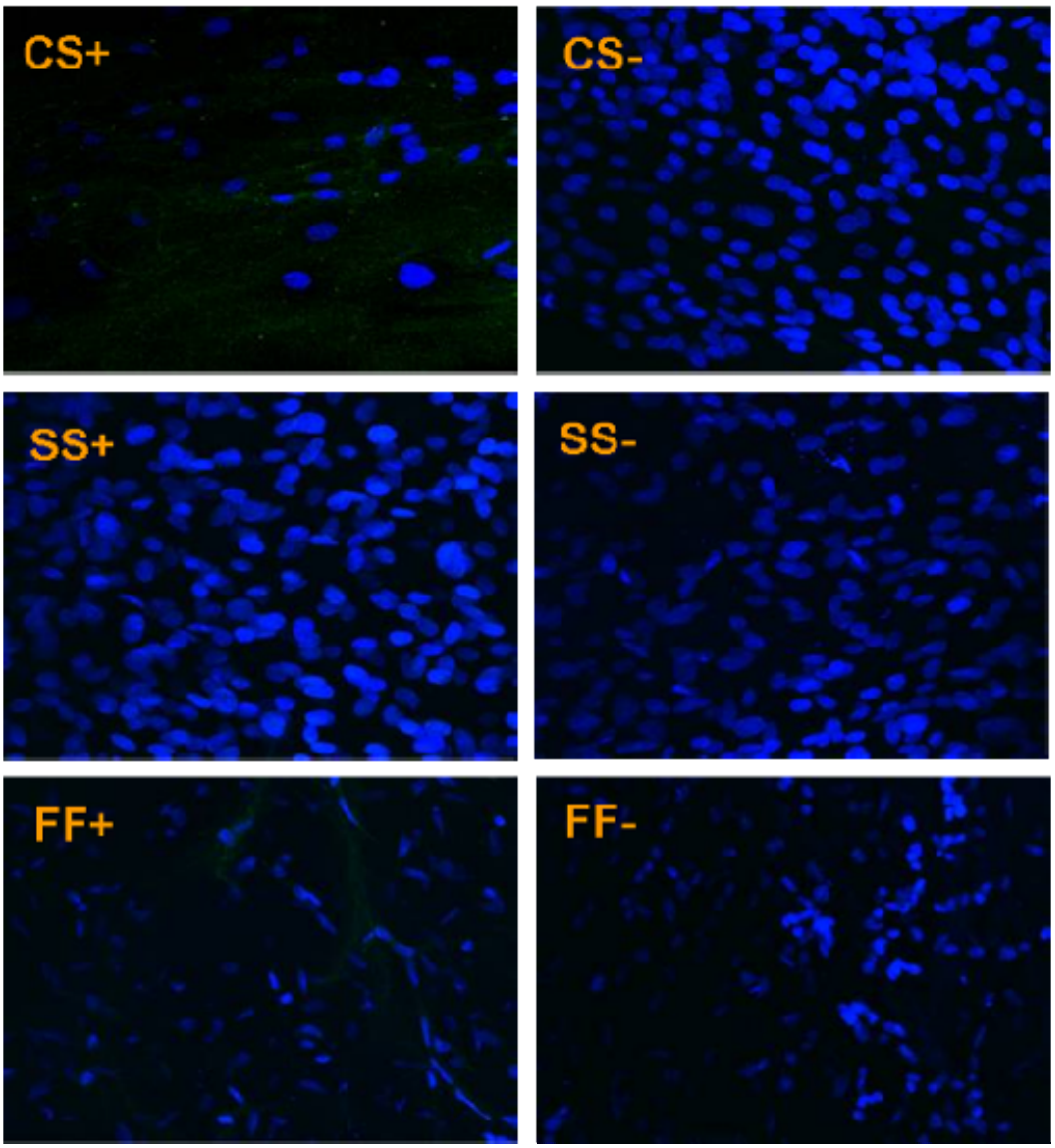

Figure 4-10: Immunostaining with MHC for CS, SS and FF groups with (+) and without (-) TGF-beta. Nuclei are seen in blue. Data shown is representative of all experiments. See Appendix G for images from all experiments. All images taken at 40x.

4.5 COLLAGEN PRODUCTION

4.5.1 Masson's Trichrome

Masson's trichrome staining allows for visualization of collagen production. Collagen staining (seen in blue in (**Figure 4-11**) indicates some degree of collagen production in most samples. In CS+/- samples, collagen is predominantly located on the outer edges of the construct. FF+/- samples, however, demonstrates a high degree of collagen production toward the center of the constructs. This seems to draw a parallel with the cell localization described in Section 4.2.2, where cells were shown to be localized toward the center of FF+/- constructs. Based on a qualitative assessment, both CS groups seem to have a higher degree of collagen present when compared to SS groups.

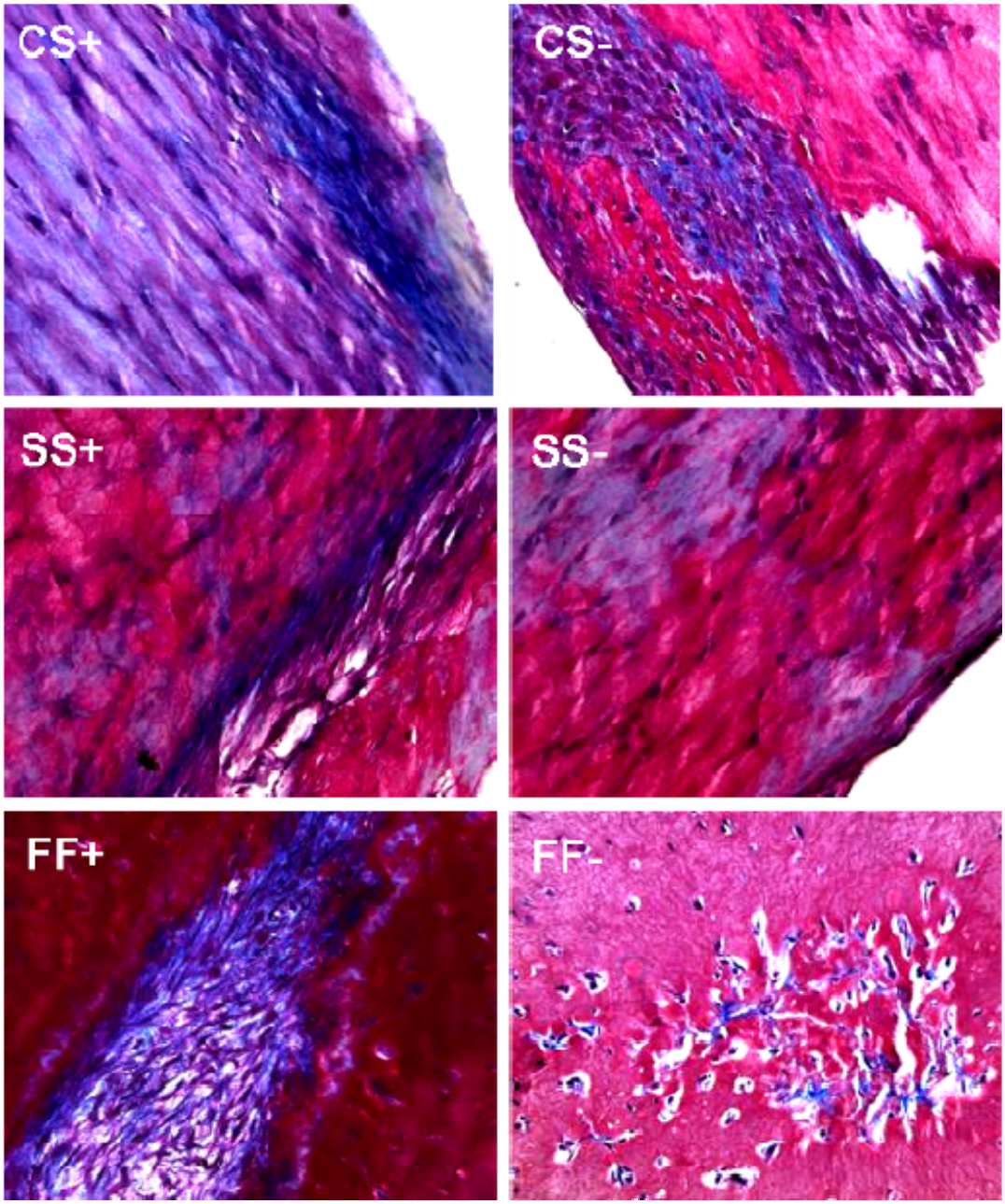

Figure 4-11: Masson's trichrome staining for CS, SS and FF groups with (+) and without (-) TGF-beta. Data shown is representative of all experiments. Blue = collagen; pink/red = fibrin; purple/black = nuclei. See Appendix H for images from all experiments. All images taken at 40x.

4.5.2 Picrosirius Red

Picrosirius red staining gives more detailed insight into the maturity of collagen fibers when compared to Masson's trichrome staining. Utilizing birefringence properties and polarized light microscopy, mature fibers (red and orange) may be distinguished from more immature collagen fibers (yellow and green).

Figure 4-12 confirms the presence of collagen (to some degree) in all experimental groups. The CS+ group appears to have the greatest amount of collagen, as seen in yellow in the CS+ panel. The yellow fibers seen in the CS+ and CS- groups indicate the presence of immature collagen fibers. The SS+ group indicates less mature collagen fibers when compared to CS+/- groups, as indicated by green fibers. As with cell localization, PSR seems to reveal the presence of collagen at the outer edge of CS+/- and SS+/- groups (as indicated by 'e' in the panels in **Figure 4-12**), while FF+/- groups demonstrate more collagen production toward the center (as indicated by 'c').

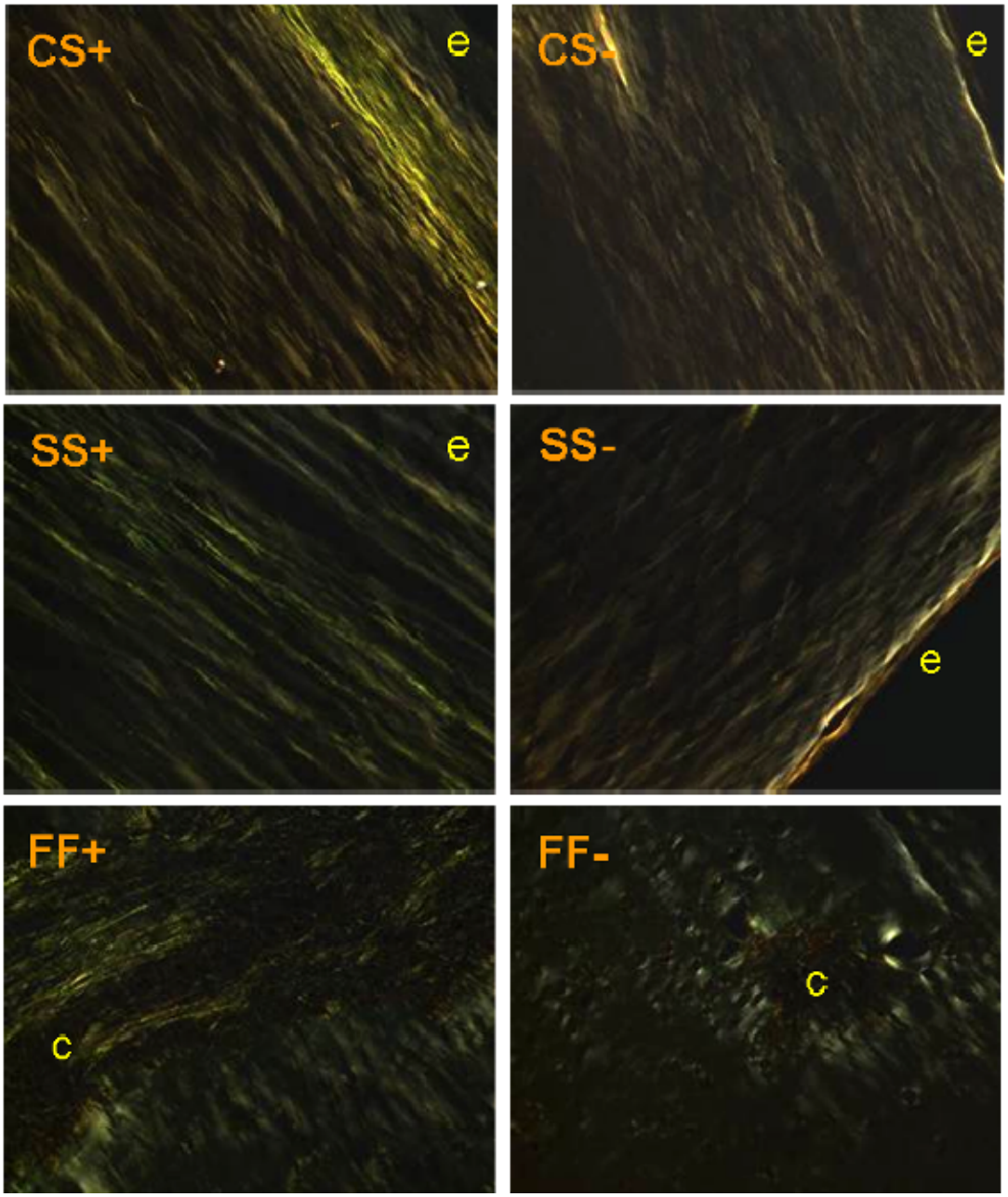

Figure 4-12: Picrosirius red staining for CS, SS and FF groups with (+) and without (-) TGF- beta. Data shown is representative of all experiments. See Appendix I for images from all experiments. The edge of the construct is denoted by an 'e'; the center of the construct is denoted by a 'c'. Green and yellow fibers indicate more immature collagen while orange and red is denotes mature collagen fibers. All images taken at 40x.

5.0 DISCUSSION

Mechanical stimulation has been shown to regulate SMC differentiation in both smooth muscle cells and mesenchymal stem cells [93], suggesting that it may promote differentiation of BMMSCs toward a vascular smooth muscle cell phenotype. Combined mechanical plus chemical stimulation has also proven to be potent regulators of SMC phenotype in *in vitro* bioreactor and culture systems [34, 37, 79]. To our knowledge, this is the first study that investigated the effects of combined mechanical and chemical stimulation of BMMSCs in a 3D fibrin matrix in an *in vitro* culture system. Straining regimens consisted of 10% strain and 1 Hz, consistent with physiologic values as pertaining to the arterial system. Biochemical supplementation with TGF-β was combined with mechanical stretching to elucidate any synergistic effects on cell viability, morphology, qualitative protein expression and collagen production.

5.1 PROLIFERATION, VIABILITY AND MORPHOLOGY

An MTT assay served as the most feasible cell viability assay for this work, as 3D models are notably difficult in regards to working with various assays and kits, which tend to be designed for 2D work or sections (see Section 5.4 on limitations). Despite this, some trends still arise

from the data on viability that parallel the findings of Nieponice *et al* [78]. When comparing no TGF-β groups (i.e. CS-, SS- and FF-) the SS- group yielded the greatest fold increase in cell number over day 0 (see **Figure 4-3**), which is consistent with the findings of Nieponice *et al.* When TGF-β is combined with mechanical stretch (the CS+ group), there is almost a 10-fold increase in cell number over day 0, yielding the greatest fold increase in cell number of all experimental groups. This is suggestive of a synergistic effect, as TGF-β supplementation in SS and FF groups led to a decrease in cell proliferation. However, because MTT is based on mitochondrial activity, measurement of cell proliferation may be an inaccurate portrayal, as mitochondrial activity may be different from cell to cell. Therefore, this data may be viewed in the perspective of metabolic activity. Because much of this work is relying on SMC protein production and expression, it may be valuable to consider metabolic activity as it relates to the production of 'contractile machinery'. As such, one may note that the CS+ group demonstrates the greatest amount of metabolic activity to produce the contractile machinery necessary for a fully differentiated SMC phenotype (see **Figure 4-3**). This parallels the presence of SMC markers as seen via immunohistochemistry. On the contrary, both FF groups yielded the lowest levels of metabolic activity, while both were also negative for SMC contractile markers.

All groups of constructs compacted over the 6-day experimental period. Morphology of BMMSCs in a 3D fibrin matrix was best-assessed using phalloidin staining for f-actin. The presence of static stress or cyclic stretch altered the morphology of the BMMSCs when compared to stress- and strain-free controls (see **Figure 4-4**). Both CS and SS groups align in the direction of strain, while FF groups exhibit random orientation. This is contrary to related work done in 2D, where mechanical stimulation in 2D leads to perpendicular alignment relative to the direction of strain [74]. However, alignment of BMMSCs in the direction of strain in a 3D

environment *in vitro* parallels what is seen *in vivo,* further supporting the use of a 3D culture model for this work.

Following qualitative analysis, f-actin was subsequently quantified using gray-scale thresholding in image analysis software and then normalized to numbers of cell nuclei. Statistical analysis revealed a significant difference between CS+ and CS-, suggesting a possible synergistic effect with mechanical and chemical stimulation. When comparing all groups with TGF-β supplementation (i.e. FF+, SS+ and CS+), there is a trend toward increasing pixel density with increasing external mechanical stimuli (in other words, from FF+ to SS+ to CS+); see **Figure 4-4**. Within cyclic stretch, static stress or free float groups, those with TGF-β supplementation led to greatest pixel density per cell when compared to counterpart groups with no TGF-β stimulation.

Overall, there seems to be some subtle consistencies in trends with the MTT assay and f-actin quantification. Both of these endpoints demonstrate a trend toward increasing either proliferation or pixel density (MTT and f-actin quantification respectively) with increasing external mechanical stimulation, where CS+ groups demonstrate the greatest values for both endpoints. This serves to confirm the idea that MTT can be represented in terms of contractile machinery production via metabolic activity, as there seems to be a correlation between f-actin and the MTT values.

It is also worth mentioning the location of cells in the constructs following the 6-day experimental period, as it is assumed that BMMSCs are homogeneously suspended in the fibrin matrix at day 1 of the compaction period. H&E staining allowed for better visualization of BMMSCs in sections when compared to phalloidin staining. Cells seem to migrate toward the outer edges of the constructs in all CS+/- and SS+/- groups (see, e.g., **Figure 4-7**). This may be

due to the ease of nutrient diffusion at the outer edge of the construct compared to the center line. On the other hand, the majority of the cells in FF+/- groups seem to migrate toward the center of the constructs. It is speculated that this cell mobility toward the center of the construct may be a requirement for cell-mediated contraction of these fibrin gels. It is perhaps interesting to question why cells in FF groups aren't migrating toward the edge for better nutrient diffusion, but rather toward the center. This may be due the density of the fibrin in the free float conformation during compaction, and therefore the inability of cells to migrate toward the edges for better nutrient and O_2 diffusion. Compaction of the gels may also be forcing the cells toward the center of the constructs. More work needs to be done to better understand these migratory mechanisms in the free float conformation during compaction. These cells could likely be dead at the end of the experimental period, perhaps also accounting for the low values seen in the MTT assay for the FF+/- groups (see **Figure 4-1**). The location of cells in all groups also seems to correlate well with the location of collagen, and this will be the focus of Section 5.2.

5.2 COLLAGEN PRODUCTION

TGF-β and mechanical strain alone have been shown to play a role in collagen production in various applications [106, 115]. This suggests that TGF-β with mechanical stimulation may also promote collagen production in BMMSC-laden constructs used in the 3D model. As such, Masson's Trichrome and picrsosirius red staining were completed as an assessment of qualitative collagen production in the fibrin gel constructs.

The CS+ group appears to have the greatest amounts of collagen when compared to the remaining groups, as seen by Masson's Trichrome staining for collagen. Other experimental

groups, namely CS-, SS+ and SS-, also show some degree of collagen production. The collagen seems to be localized at the edges of the constructs in both CS+/- and SS+/- groups, which is consistent with the localization of cells (see Section 5.1). Because the cells are producing and laying down the ECM, it seems logical that the location of collagen matches that of the cells in the fibrin matrix.

Unlike the CS+/- and SS+/- groups, the FF+/- groups show collagen production toward the center of the constructs, which is also consistent with the cell localization (see **Figures 4-6** and **4-11**). Perhaps surprising is that there is some collagen production in these experimental groups, which are not subjected to any external mechanical strain. TGF-β seems to play a role in producing ECM in FF+ groups when compared to FF- (see **Figure 4-11**).

Picrosirius red staining corroborates the findings seen with collagen production via Masson's Trichrome staining, while giving more detailed information on the maturity of the collagen that is present. The CS+ group reveals the most mature collagen fibers present (as seen in yellow in **Figure 4-12**). The localization of collagen toward the center of the constructs in the FF+/- groups is also apparent here.

Overall, collagen production seems to be regulated by both mechanical and chemical stimulation, and when combined it seems to enhance collagen production by BMMSCs in a 3D fibrin matrix.

5.3 QUALITATIVE PROTEIN EXPRESSION

Since the main objective of this work is to explore factors in the differentiation of BMMSCs toward an SMC phenotype via exogenous mechanical and chemical stimuli,

immunohistochemistry was used to determine the degree of differentiation of SMCs. As noted earlier, SMCs are plastic cells whose phenotype exists as a spectrum between a synthetic and contractile phenotype. As such, experimental groups were evaluated for qualitative protein production and phenotype via immunostaining. Experimental groups were stained for α-SMA, calponin, and MHC as early, mid-stage, and terminally-differentiated SMC markers respectively.

Immunostaining for α-SMA gave highly variable results. The data shown in **Figure 4-6** is most consistent with the findings from both prior work [78] as well as the immunostaining for calponin (see **Figure 4-7**). However, this finding was for only one out of five experiments. There are several potential reasons for this variability. Because fibrin constructs are extremely small (180 μl when originally fabricated) they cannot be cryosectioned nor paraffin-embedded for immunostaining purposes. This was the volume limit to utilize the tissue train system. Therefore, the permeabilization period during immunostaining had to be adjusted to account for this. It is speculated that α-SMA antibody may not have been small enough to reach the cells and bind to the α-SMA proteins within the cell. However, because there is positive calponin expression for CS+/- and SS+ groups (**Figure 4-9**), it was expected that α-SMA expression would also be evident for these groups, due to the hierarchical nature of protein expression for mature SMCs. It was therefore concluded that there may have been an issue with the α-SMA antibody, the permeabilization time, or both. A suitable positive control is necessary to determine these parameters.

As indicated above, some positive calponin expression was evident in CS+/- and SS+ groups (**Figure 4-9**). This indicates that some of BMMSCs are differentiating toward an SMC phenotype in response to TGF-β, mechanical stimuli, or both. None of the groups showed any positive staining for the terminally-differentiated SMC marker, MHC (**Figure 4-10**). This may

be due to the short experimental period. A longer experimental time-frame may have allowed for MHC protein synthesis. Future work including SMC gene expression may determine if MHC is being upregulated during this experimental timeframe.

5.4 LIMITATIONS

There are several limitations to this work that will be discussed in this section. While the chosen model allows for the understanding of the effects mechanical and chemical stimulation in 3D, it is difficult to process for various quantitative endpoints due to the small size of each construct, and therefore the lower cell number and, consequently, low SMC protein and ECM production.

Despite the ability to better mimic physiologic conditions using a 3D model, it is often more tedious and difficult to work with than 2D models. As mentioned previously, samples could not be cryosectioned for immunostaining, and therefore the permeabilization time in whole-mounted samples had to be tailored such that the antibodies could diffuse into the cell without compromising the cell membrane. This proved to be difficult as seen with the α-SMA staining.

The quality antibodies used in this work may have been evaluated using an appropriate positive control. There were several possibilities in choosing a positive control. One option was a cryosection of a rat aorta. However, because this would not mimic the density or thickness of the fibrin gel, this was not considered to be appropriate. Permeabilization of rat aorta would not be consistent with that of cells embedded in fibrin. Fibrin incorporated with SMCs was also considered as a positive control. This was also inappropriate because SMCs dedifferentiate once

removed from a mechanical environment. Also, the density of fibrin embedded with BMMSCs increased through the duration of the experiment, making a positive control with SMCs at t_0 also inappropriate.

An appropriate cell counting assay was difficult to employ with our model. Several attempts have been made at digesting the constructs to utilize 2D cell counting kits, such as CyQUANT^{TM}. However, because several of these assays rely on flurochromes binding to DNA and measuring the absorbance, fragments of fibrin following digestion often interfered with the absorbance readings, likely giving inaccurate values.

As it was noted that there was collagen production in samples being made of only fibrin gel and BMMSCs at day 0 of the experimental period, it may have been more interesting to make quantitative measures on collagen production to determine more concrete differences between experimental groups. Attempts have been made to do this via a hydroxyproline assay. However, because the 3D constructs are extremely small (each with a volume of 180 µl) the amount of detectable collagen was at the low end of the detectable region of the standard curve and therefore could not be accurately measured.

Lastly, confirmatory work including gene expression and western blotting would be ideal to confirm the qualitative protein expression via immunohistochemistry. However, the size of the constructs again proves to be a limitation, as the fewer number of cells leads to lower expression of mRNA and lesser protein production for these purposes, respectively. Increasing the concentration of cells in the fibrin gel was attempted to overcome this limitation. However, this did not yield an adequate number of cells per group for RNA analysis purposes. Pooling samples together from all experiments may have been a solution to this limitation, however this would create a sample size of one.

6.0 FUTURE WORK

This work has several elements that may be interesting to explore further in future work. BMMSCs are ideal for the reasons described in Section 1.2.3, however other cell types are also capable of responding to mechanical and/or chemical stimulation. As cell sourcing is one the major components in creating the ideal TEVG, the perfect cellular component for this application is still a missing puzzle piece. The experimental time frame may also be manipulated to determine the optimal time in which SMC differentiation is the greatest. A longer experimental period may have yielded greater protein expression and ECM production, and further work may investigate the time required to produce SMC contractile proteins that are necessary for a fully differentiated SMC phenotype.

In regards to chemical stimulation, TGF-β is not the only growth factor known to promote SMC differentiation. It would be therefore interesting to look at a cadre of various growth factors to determine any synergistic effects with other growth factors, either individually or in combination, along with mechanical stimulation.

SMA and calponin expression may have been semi-quantified just as f-actin was using gray-scale thresholding. This would allow for a more direct comparison between groups. This may be done in future work to generate more quantitative data and allow for a statistical analysis between experimental groups.

Fibrin is not the only scaffold material that could be used for this 3D model application. Others have used collagen, collagen/fibrin mixtures, and polymers to act as an appropriate scaffold to induce mechanical stimulation in 3D [22].

A major component of this work that was unfortunately beyond the scope of this current project was an evaluation of gene expression. An assessment of gene expression would allow for detection of more subtle differences between experimental groups, while gaining insight as to how BMMSCs are responding to mechanical and chemical stimuli via up- or down-regulation of SMC-related, apoptotic-related, and ECM-related gene expression.

Western blotting and subsequent protein expression would allow for more quantitative protein analysis, while also confirming findings from SMC gene expression. This would also allow for the detection of proteins not seen using immunohistochemistry.

Finally, future work will need to assess functionality of differentiated BMMSCs via the addition of exogenous contractile agents. This is the true test of a fully differentiated and functional SMC, and is a distinguishing characteristic that often goes under-emphasized in much of the related work in tissue engineering and regenerative medicine applications.

7.0 CONCLUSIONS

Previously published work has demonstrated that BMMSCs are capable of differentiating into several different lineages. This has motivated us to explore whether BMMSCs subjected to the appropriate milieu of mechanical stimuli and growth factors will differentiate toward an SMC phenotype. Here, we investigated the effect of mechanical and chemical stimuli on BMMSCs suspended in a 3D fibrin matrix to determine the capacity in which these cells are capable of differentiation. Overall, the purpose of this project was to further investigate the effects of both mechanical and chemical stimulation, and better understand how these stimuli may act synergistically to promote a SMC phenotype relevant to regenerative medicine applications.

The work presented in this thesis suggests that BMMSCs are capable of differentiating into an SMC phenotype, however there is much more work to be done to better elucidate the mechanisms of differentiation, and how mechanical and biochemical stimuli are working together to produce a synergistic effect. As demonstrated through qualitative protein analysis, BMMSCs respond to cyclic stretch with and without TGF-β, as well as static stress in the presence of TGF-β, as evidenced through calponin expression. MTT and f-actin quantification, when taken together, may indicate an increase in the production of 'contractile machinery' intrinsic to a fully differentiated SMC. Lastly, TGF-β stimulation combined with mechanical strain seems to lead to an increase in collagen production. More work needs to better elucidate

the diffusion of TGF-β into these fibrin constructs in order to optimize its effects on SMC differentiation.

In conclusion, this work has provided significant information on the therapeutic potential of BMMSCs toward small diameter graft applications, as well as all other regenerative medicine applications requiring SMCs as a cellular replacement. The results obtained from this project underscore the usefulness of BMMSCs in the realm of tissue engineering and related fields. This work continues to move forward in Dr. Vorp's laboratory as researchers are trying to better understand how various cell types respond to mechanical strain in 2D and 3D models. Other work is moving toward *in vivo* models where we can better understand how this cell type integrates into the host tissue, and how the local environment influences the cell phenotype.

While the 'holy grail' of tissue engineering is still widely sought after, we are perhaps one step further in understanding how the mechanical and chemical environment may work together to influence cell phenotype toward regenerative medicine therapies.

APPENDIX A

PREPARATION OF FIBRIN GEL TISSUE TRAIN CONSTRUCTS

Tissue train constructs for all experimental groups were prepared in accordance with the following protocol:

Each 'batch' of fibrin solution was prepared so as to create 3 ml of working solution, which was sufficient to fabricate 12 tissue train constructs. Because there is a limited amount of time to work with the fibrinogen/thrombin suspension as an enzymatic reaction is taking place (i.e. the clotting cascade), a small volume was chosen for ease of handling. To make 3 ml of final solution, 2 ml of fibrinogen with εACA solution (5 mg/ml of fibrinogen + 1 mg/ml εACA in serum-free a-MEM) was combined with a cell suspension of 6 x 10^6 cells/ml in 0.5 ml, to yield a final concentration of 1 x 10^6 cells/ml. The fibrinogen solution was prepared first and set aside on ice, while cell trypsinization and counting was taking place. Once the appropriate concentration of cells was achieved, 0.5 ml of the cell suspension was added to the fibrinogen solution as described above. The thrombin solution was prepared separately by combining 0.5 ml of serum-free α–MEM and 1 UI of thrombin (10 μl) in a sterile eppendorf tube. For samples receiving TGF-β supplementation, 3 μl of 10 μg/ml TGF-β solution was added to achieve a final

concentration of 10 ng/ml in the constructs. Once all solutions were prepared, they were kept on ice while during device setup.

Tissue train posts, seen below in **Figure A-1** were attached to the baseplate. Tissue train plates were then placed on top of the tissue train posts, while maintaining a tight seal so as to not cause a pressure leak in the system. A vacuum line was then connected from the housevac to the baseplate with tubing. The vacuum was then turned on, allowing the flexible membrane substrate to be pulled into the tissue train troughs of the posts, thereby creating a 3D depression in which to add the fibrinogen/thrombin solution for fibrin gel fabrication.

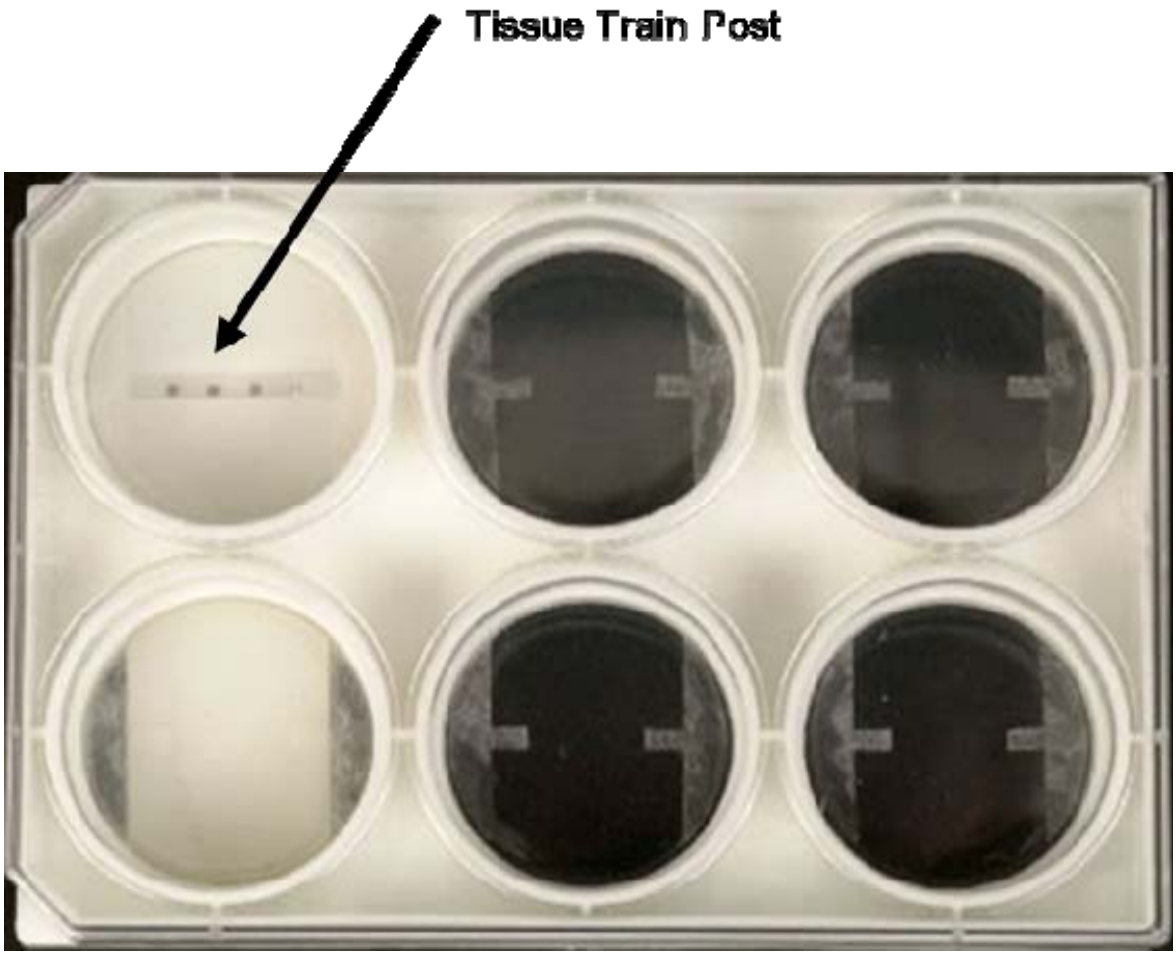

Figure A-1: Tissue train post sitting below tissue train plates. Figure adapted from www.fleccellint.com.

Once the device setup was finalized, the thrombin solution was combined with the fibrinogen/cell suspension and the conical tubes were inverted several times for mixing to ensure homogeneous distribution of cells in the solution. The solution then had to be pipetted quickly as the gel would begin to form within approximately 30 seconds. 180 µl of the fibrin solution was added to the tissue train troughs until 1 batch was completely used. Once this process was completed, the baseplates were transferred to an incubator during the gelation process. After 30 minutes of gelation, 5 ml of media were added to tissue train plates (i.e. CS and SS groups) and 2 ml of media were added to 12-well plates (FF groups). For samples receiving TGF-β, a separate solution of media was prepared with TGF-β to achieve a final concentration of 10 ng/ml of TGF-β in the media, and media was added as described above.

APPENDIX B

OPTIMIZATION OF FIBRIN DEGRADATION FOR FACS

Fluorescence activated cell sorting (FACS) was considered for this work in an effort to quantify SMC protein expression. However, this raised 2 significant questions: 1. How can the cells be recovered from the fibrin matrix following the experiment? 2. Once the cells have been recovered, how can antibodies for FACS work on intracellular SMC proteins of interest? To answer the first question, a fibrin digestion protocol obtained from the laboratory of Kristen Billiar was manipulated and tested to enzymatically digest the fibrin to obtain the greatest percentage of the original cell number.

To digest fibrin gels, media was removed from the wells, and constructs were transferred to 15 ml conical tubes. 10 ml of 50 mM Tris/Calcium Acetate (Sigma-Aldrich, St. Louis, MO) buffer was added to the 15 ml conical tube, followed by the addition of trypsin (Invitrogen, without EDTA) to create a final concentration of 0.05%. 0.02 g of collagenase type II (Washington Biotech) was added to this solution to create a 2 mg/ml concentration. Conical tubes were then placed in heat blocks at 37 C, and were shaken vigorously every 1 – 2 minutes. The fibrin gels were dissolved within 30 – 45 minutes. The remaining digest solution was

centrifuged, resuspended in complete α-MEM, and replated on T25 flasks. 24 hours following the digestion, cells were viewed under a bright field microscope. See **Figure B-1** below.

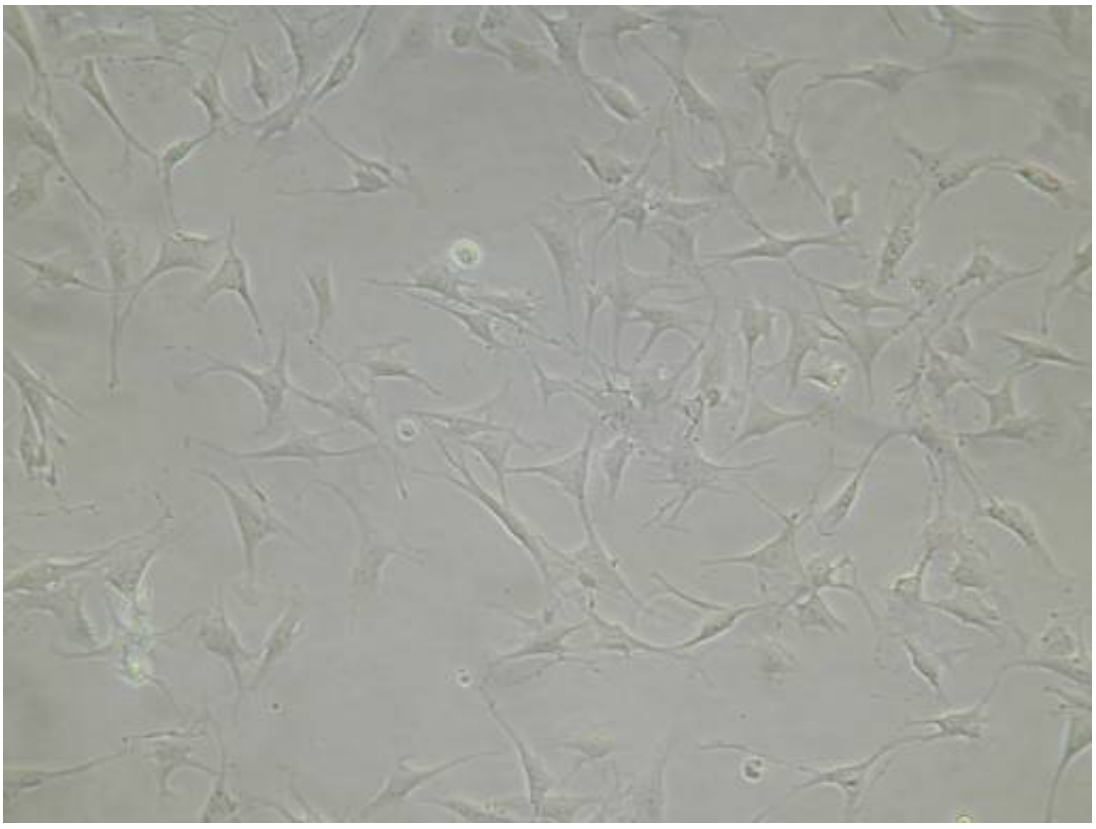

Figure B-1: Recovered BMMSCs from fibrin digestion following replating after 24 hours. Image taken at 20x.

APPENDIX C

H&E STAINING

H&E staining seen in **Figures C-1 – C-5** are images from experiments 1 – 5, respectively.

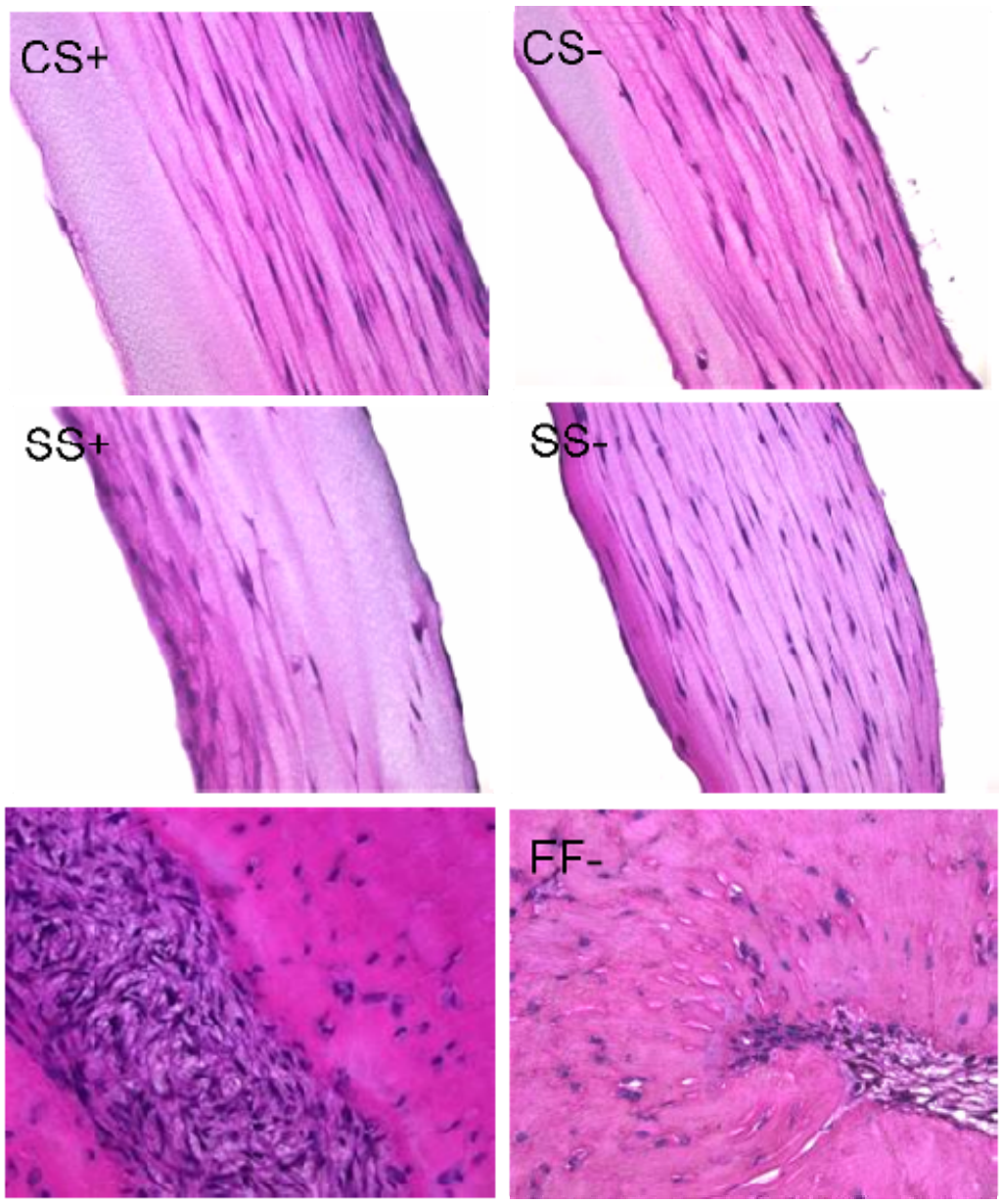

Figure C-1: H&E staining for Experiment 1. Nuclei = purple; Fibrin = pink. All images taken at 40x.

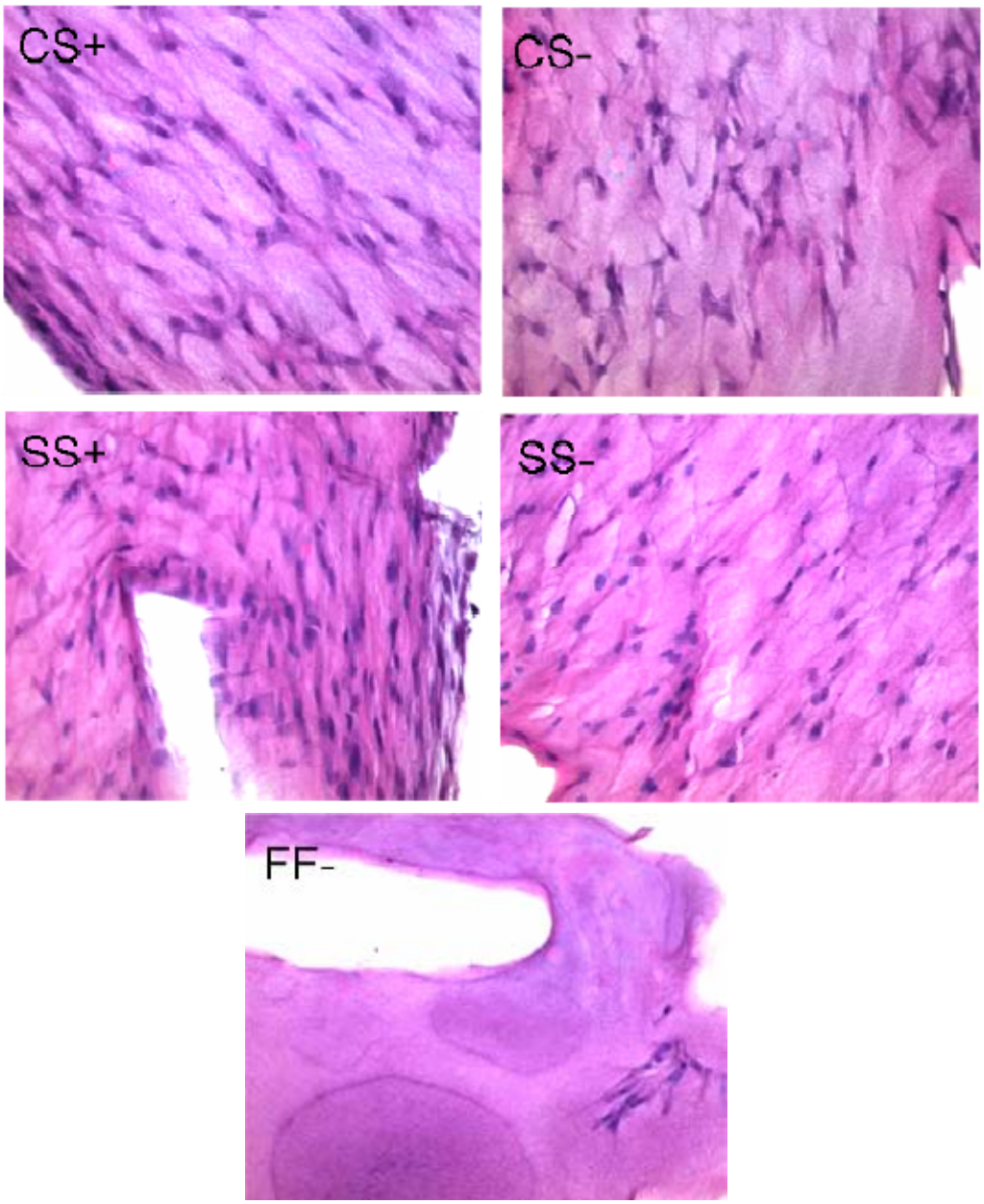

Figure C-2: H&E staining for experiment 2. Nuclei = purple; Fibrin = pink. FF+ group lost during experiment. All images taken at 40x.

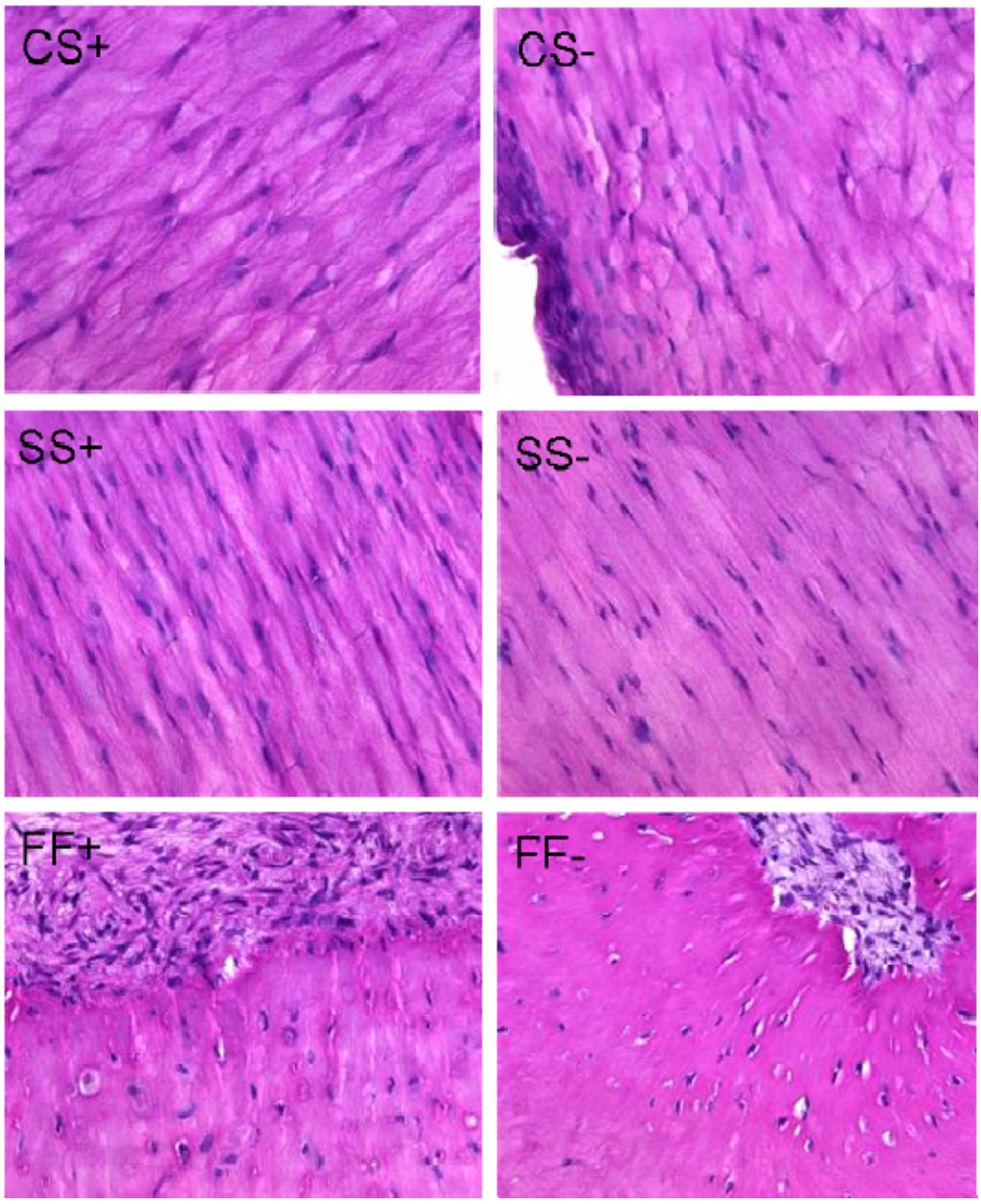

Figure C-3: H&E staining for Experiment 3. Nuclei = purple; Fibrin = pink. All images taken at 40x.

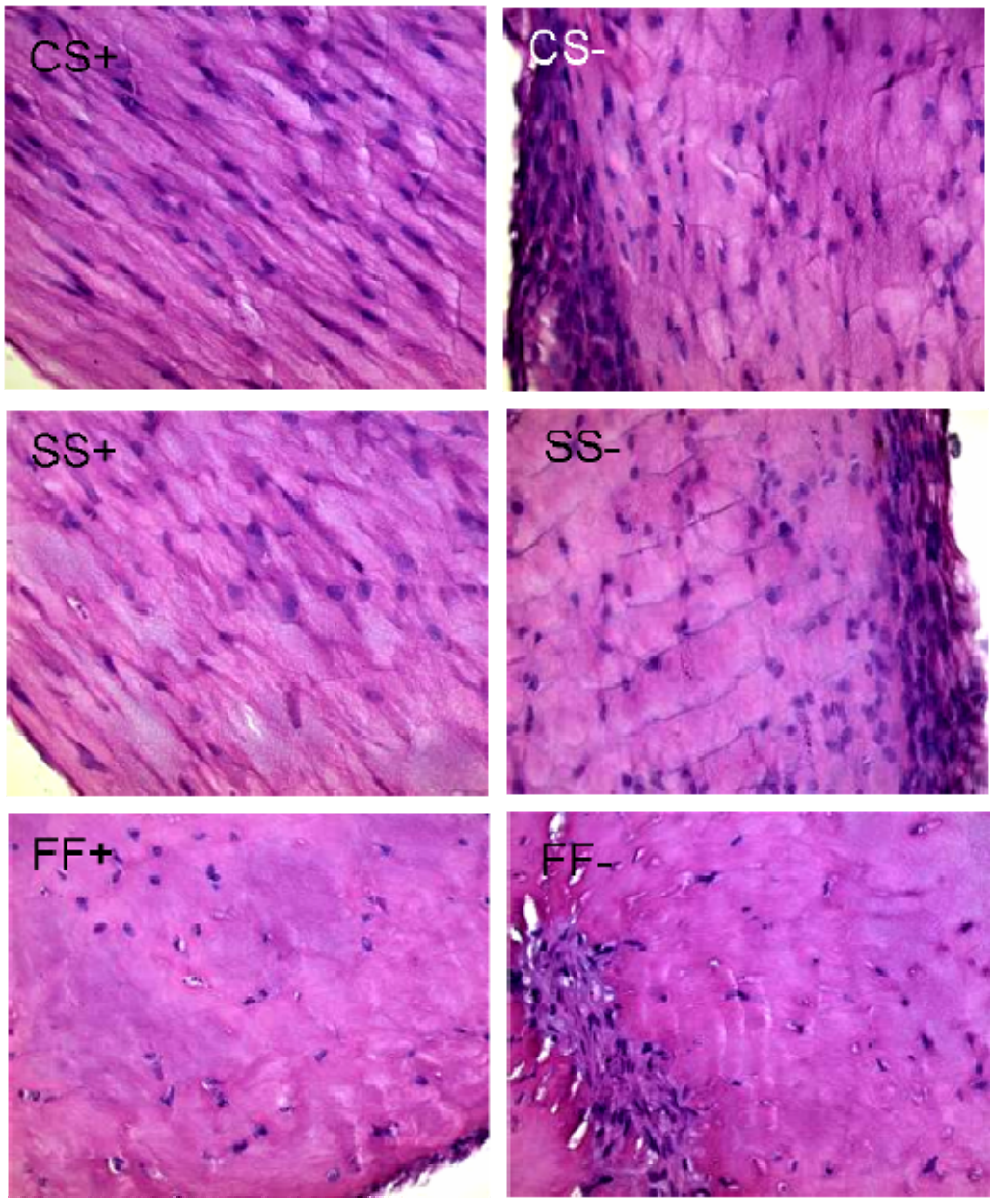

Figure C-4: H&E staining for Experiment 4. Nuclei = purple; Fibrin = pink. All images taken at 40x.

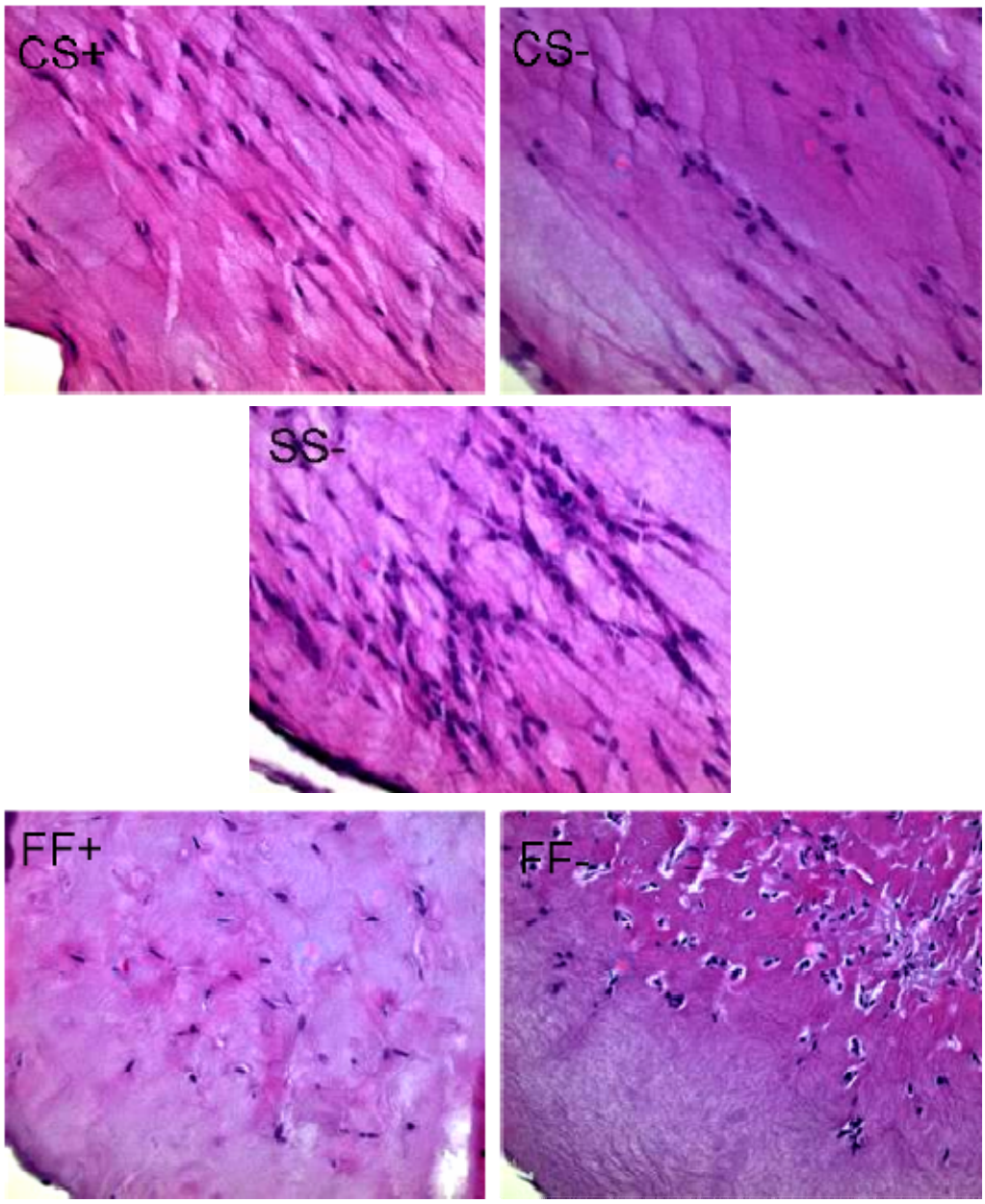

Figure C-5: H&E staining for Experiment 5. Nuclei = purple; Fibrin = pink. SS+ group was lost during the experiment. All images taken at 40x.

APPENDIX D

F-ACTIN

Phalloidin staining seen in **Figures D-1 – D-5** are resulting images from experiments 1 – 5, respectively.

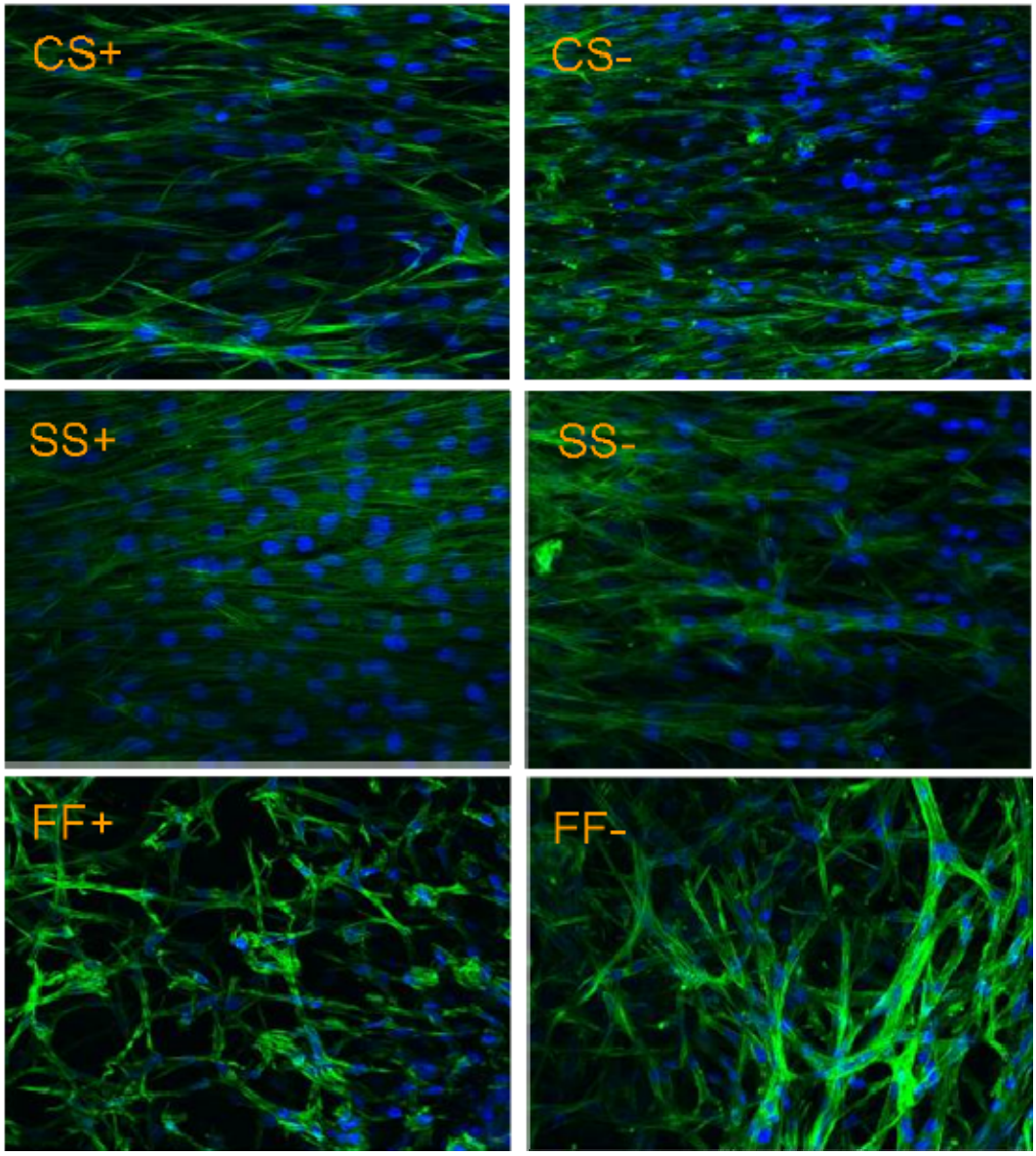

Figure D-1: Phalloidin staining for Experiment 1. Nuclei = blue; F-actin fibers= green. All images taken at 40x.

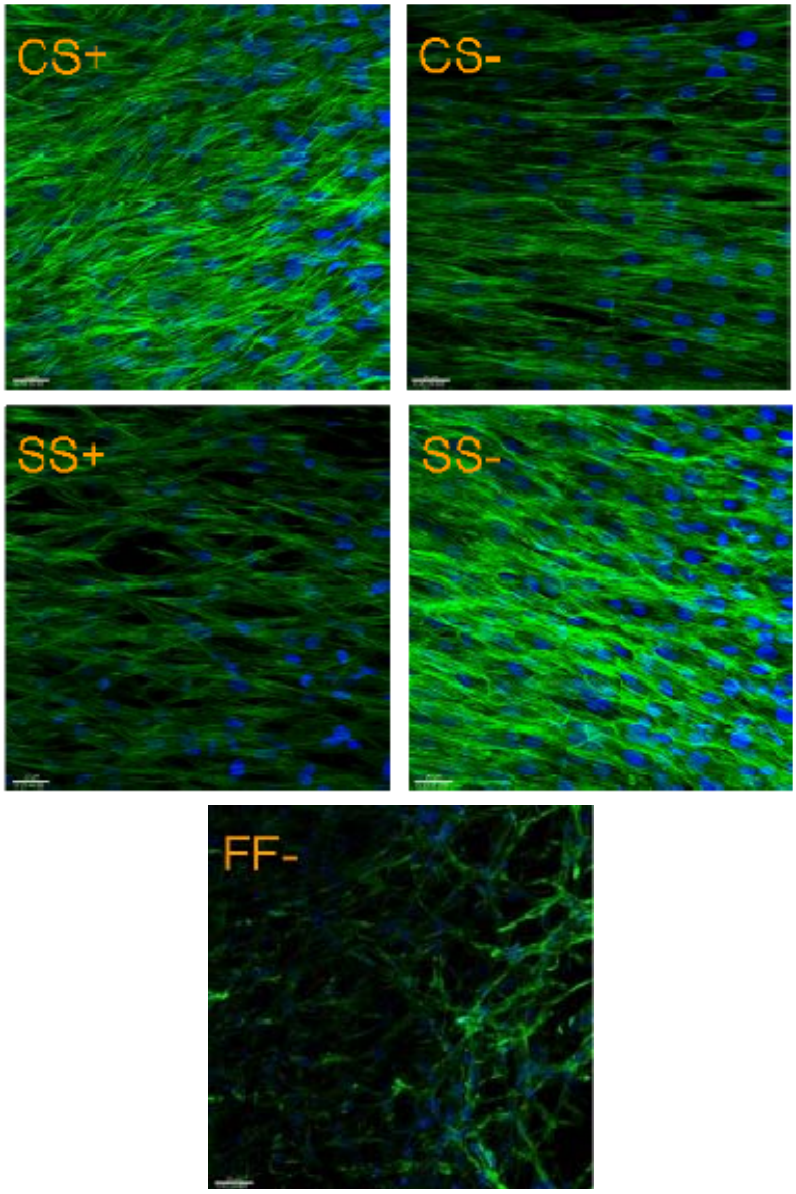

Figure D-2: Phalloidin staining for Experiment 2. Nuclei = blue; F-actin fibers= green. FF+ group lost during the experiment. All images taken at 40x.

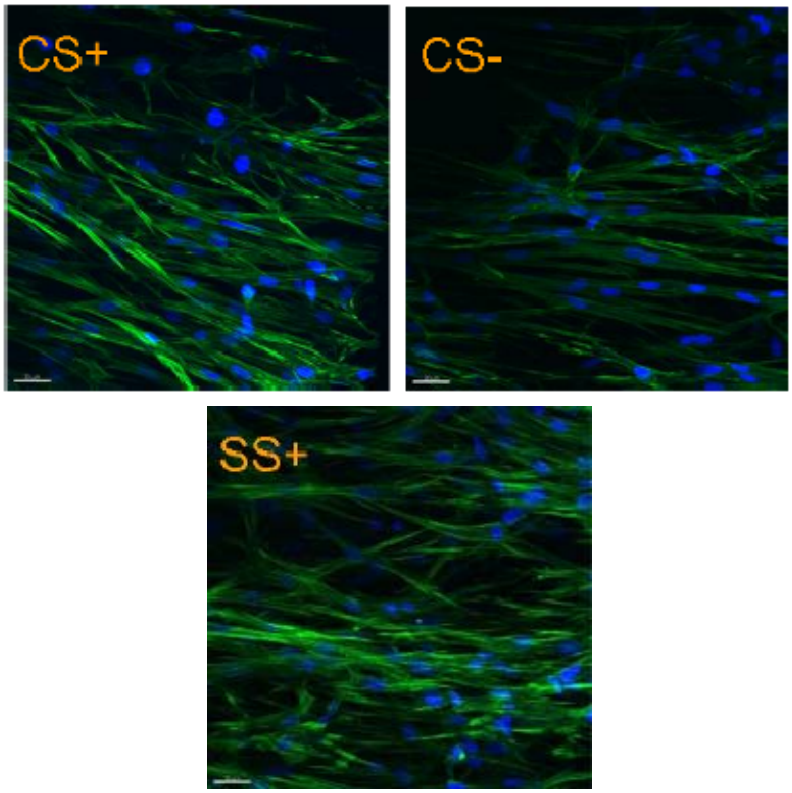

Figure D-3: Phalloidin staining for Experiment 3. Nuclei = blue; F-actin fibers= green. SS-, FF+ and FF- files became corrupt during the image acquisition process. All images taken at 40x.

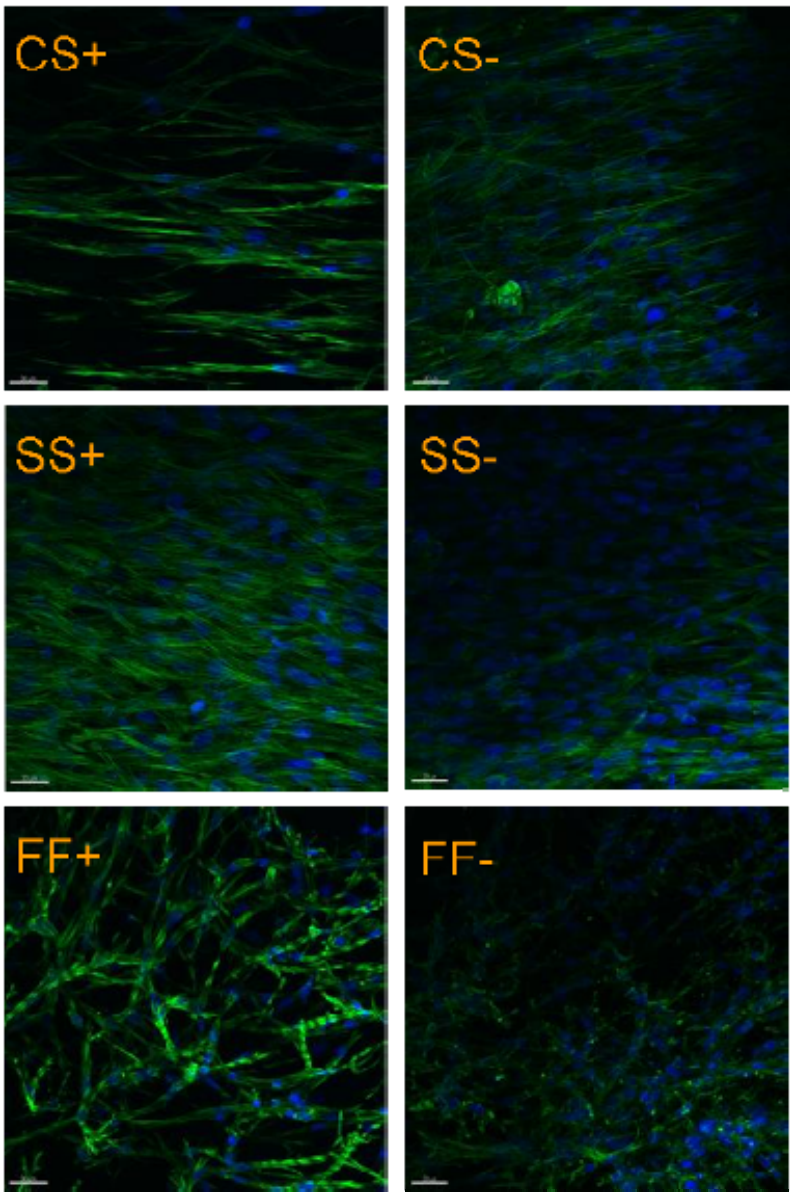

Figure D-4: Phalloidin staining for Experiment 4. Nuclei = blue; F-actin fibers= green. All images taken at 40x.

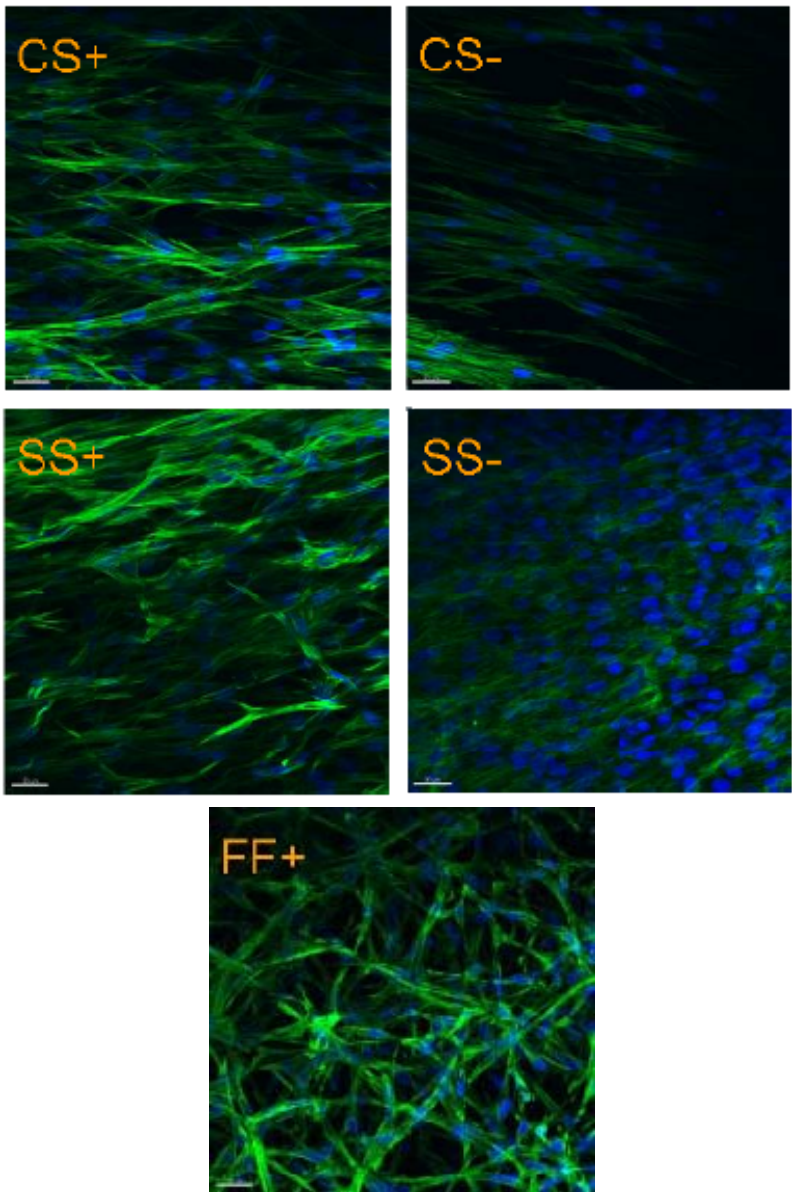

Figure D-5: Phalloidin staining for Experiment 5. Nuclei = blue; F-actin fibers= green. FF- group lost during the experiment. All images taken at 40x.

APPENDIX E

A-SMA

α-SMA staining seen in **Figures E-1 and E-2** are images from experiments 1 and 5, respectively. Data for experiment 2 is seen in Section 4.4.1. For experiments 1,2 and 5, the α-SMA antibody from Sigma was utilized, while for experiments 3 and 4, the Chemicon α-SMA antibody was used (see **Table 3-1**). Experiments 3 and 4 were all negative for α-SMA upon inspection, and therefore were not imaged.

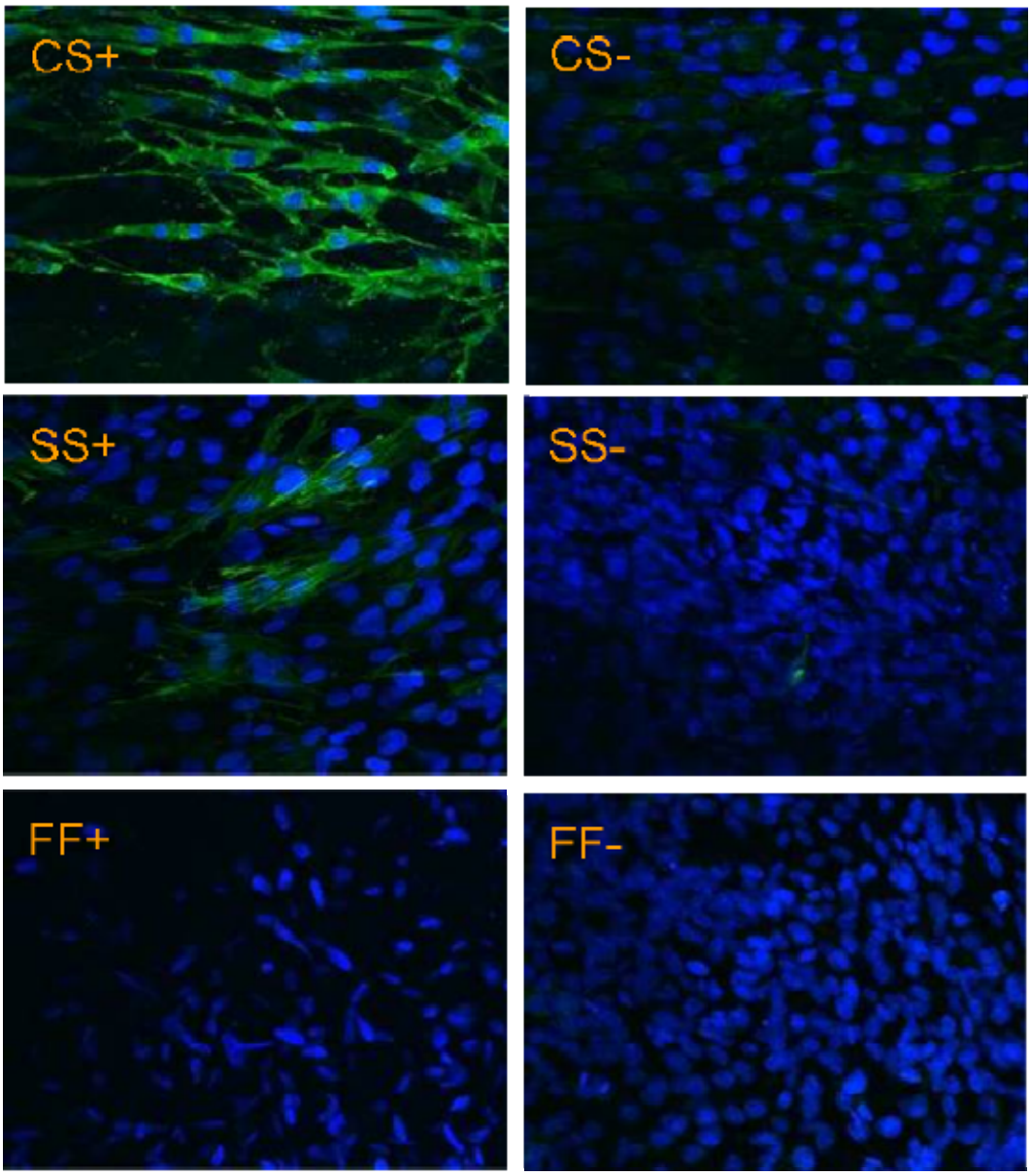

Figure E-1: α-SMA staining for Experiment 1. Nuclei = blue; α-SMA = green. All images taken at 40x.

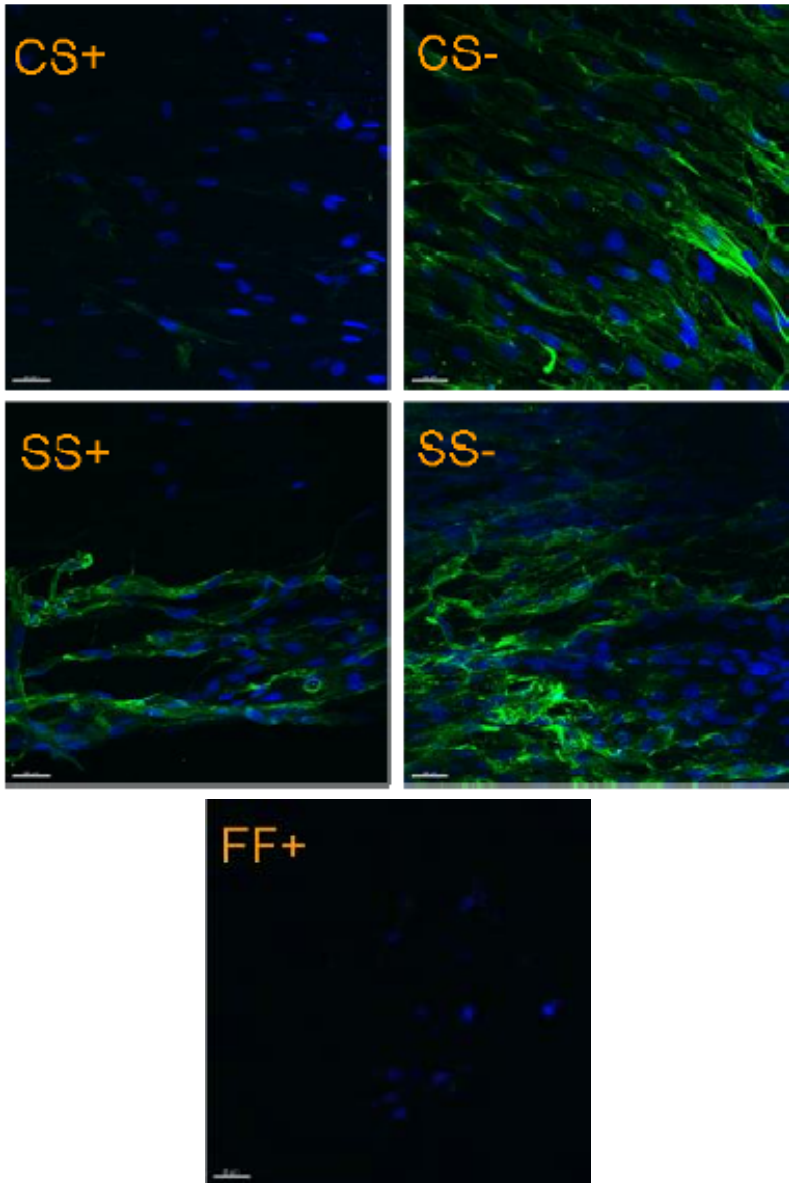

Figure E-2: α-SMA staining for Experiment 5. Nuclei = blue; α-SMA = green. FF- group lost during the experiment. All images taken at 40x.

APPENDIX F

CALPONIN

Calponin staining seen in **Figures F-1 – F-5** are images from experiments 1 – 5, respectively.

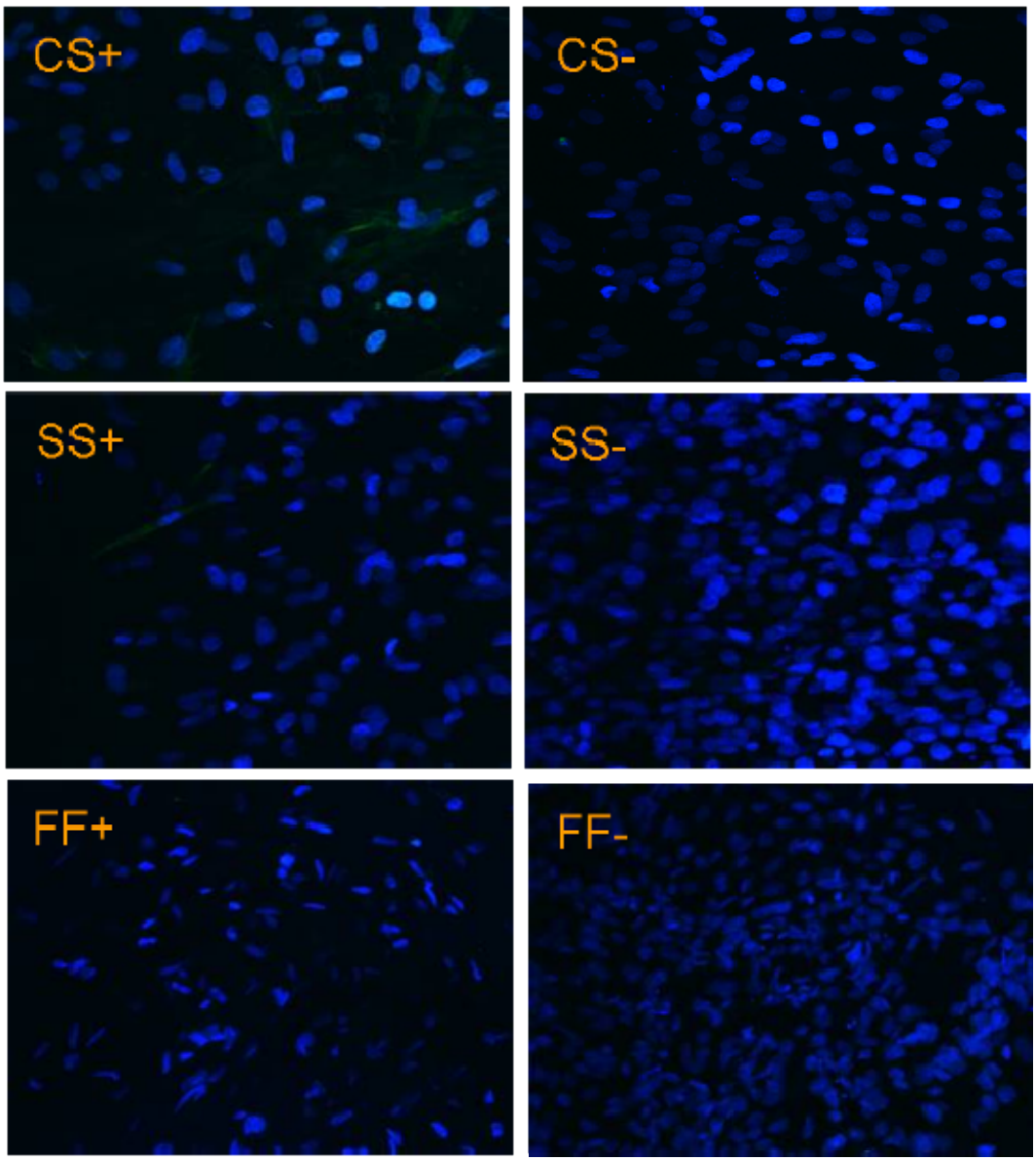

Figure F-1: Calponin staining for Experiment 1. Nuclei = blue; calponin = green. All images taken at 40x.

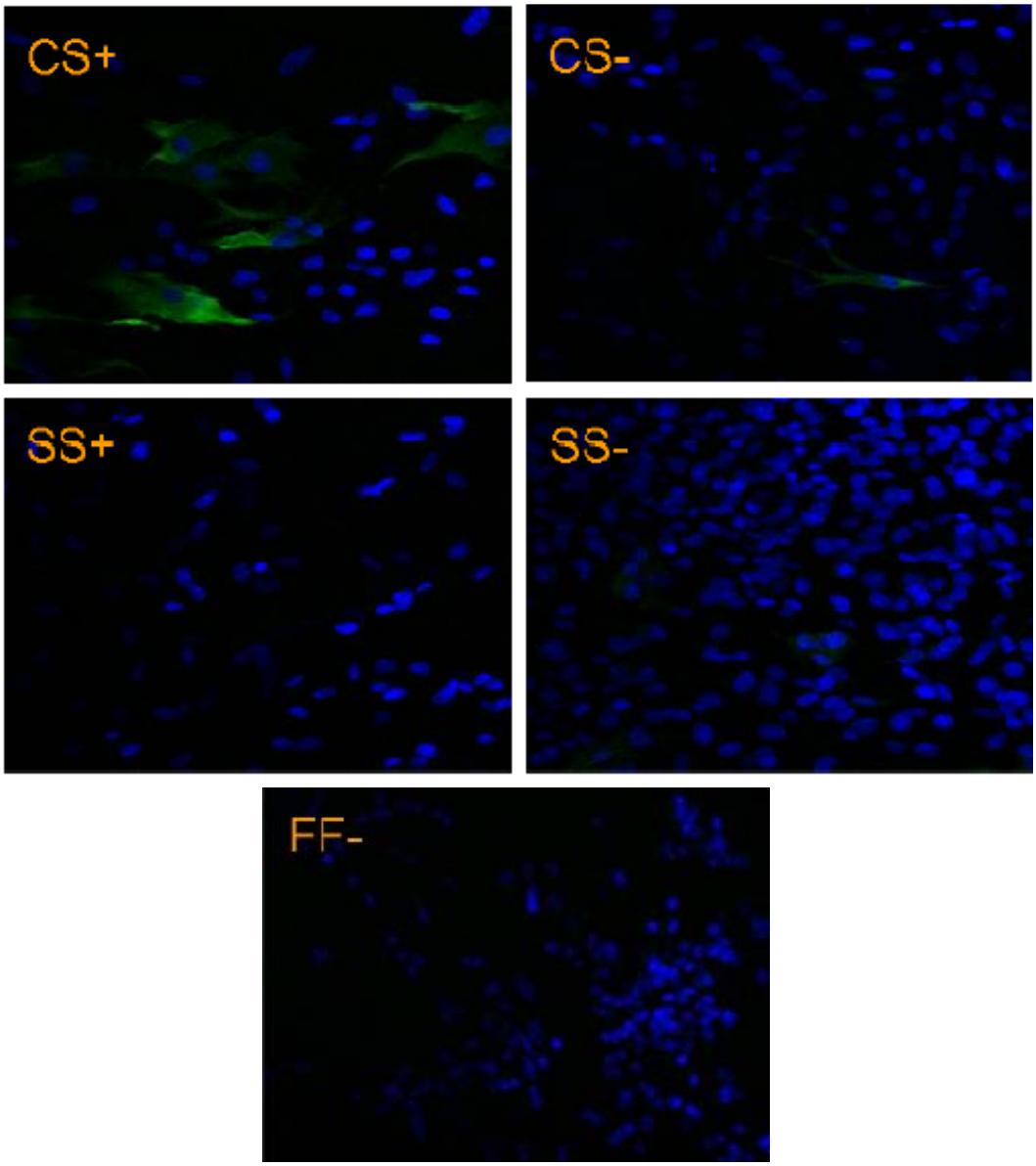

Figure F-2: Calponin staining for Experiment 2. Nuclei = blue; calponin = green. FF+ group lost during the experiment. All images taken at 40x.

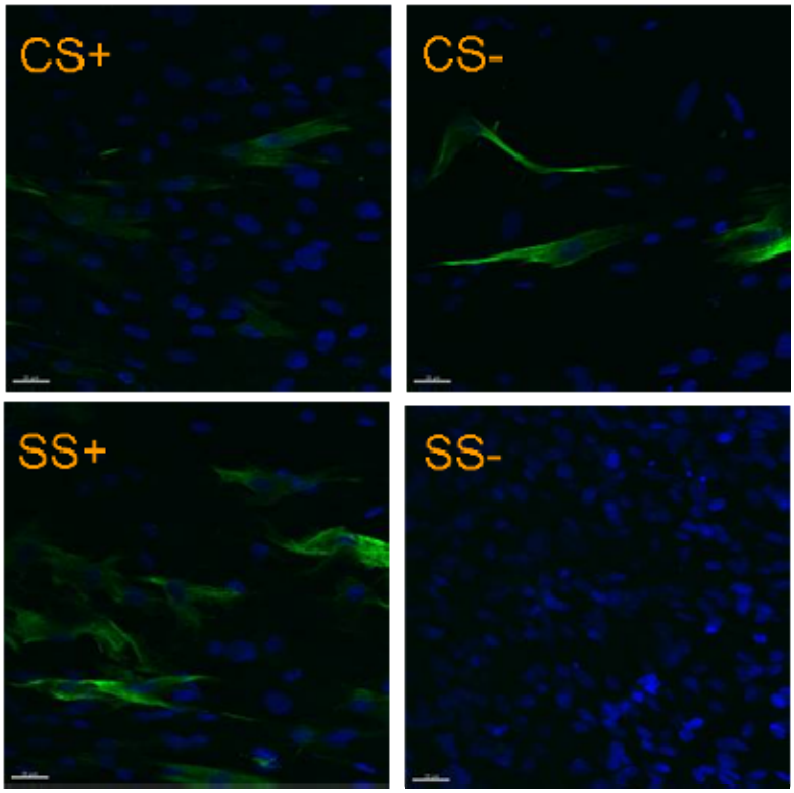

Figure F-3: Calponin staining for Experiment 3. Nuclei = blue; calponin = green. FF+/- groups were negative for calponin and were not imaged in the interest of time. All images taken at 40x.

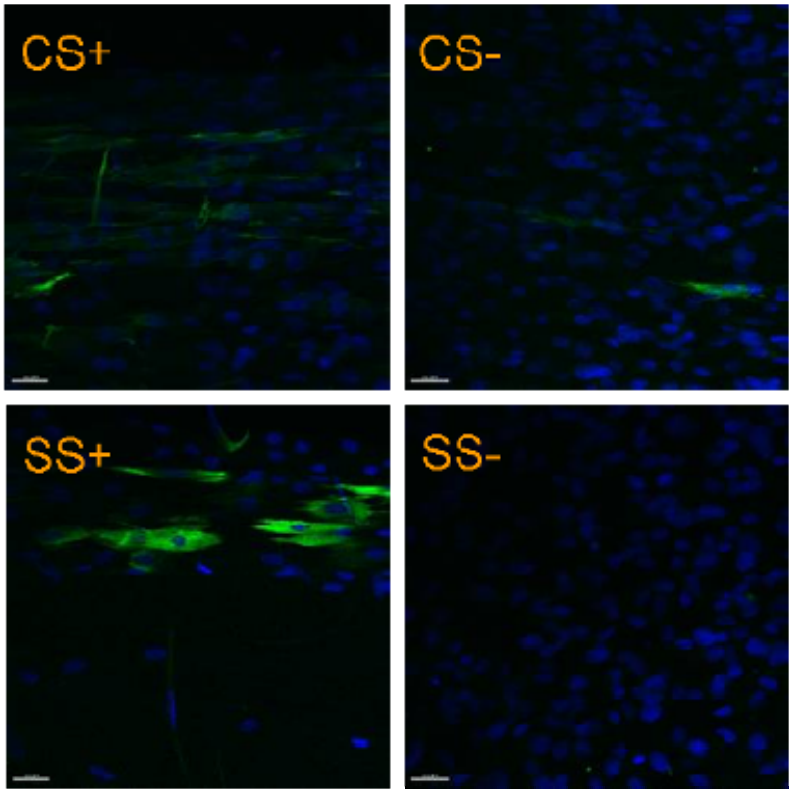

Figure F-4: Calponin staining for Experiment 4. Nuclei = blue; calponin = green. FF+/- groups were negative for calponin and were not imaged in the interest of time. All images taken at 40x.

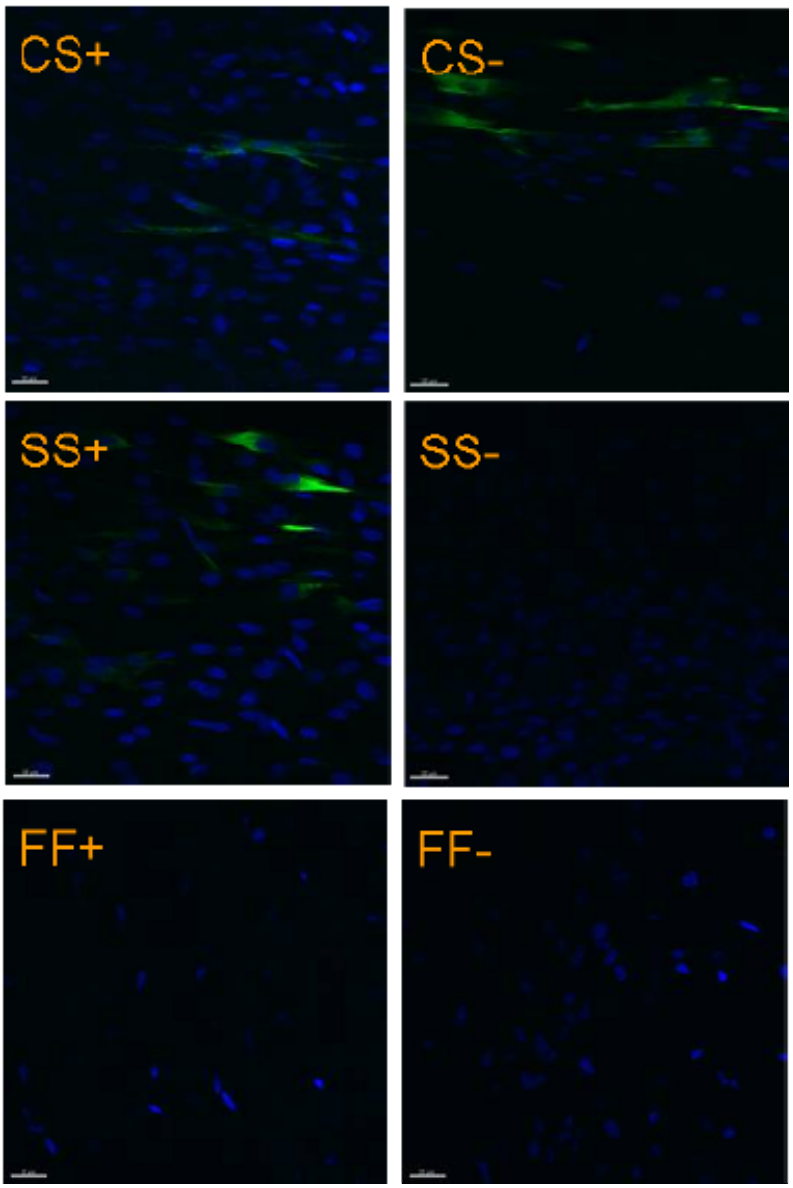

Figure F-5: Calponin staining for Experiment 5. Nuclei = blue; calponin = green. All images taken at 40x.

APPENDIX G

MHC

MHC staining seen in **Figures G-1 – G-5** are images from experiments 1 – 5, respectively.

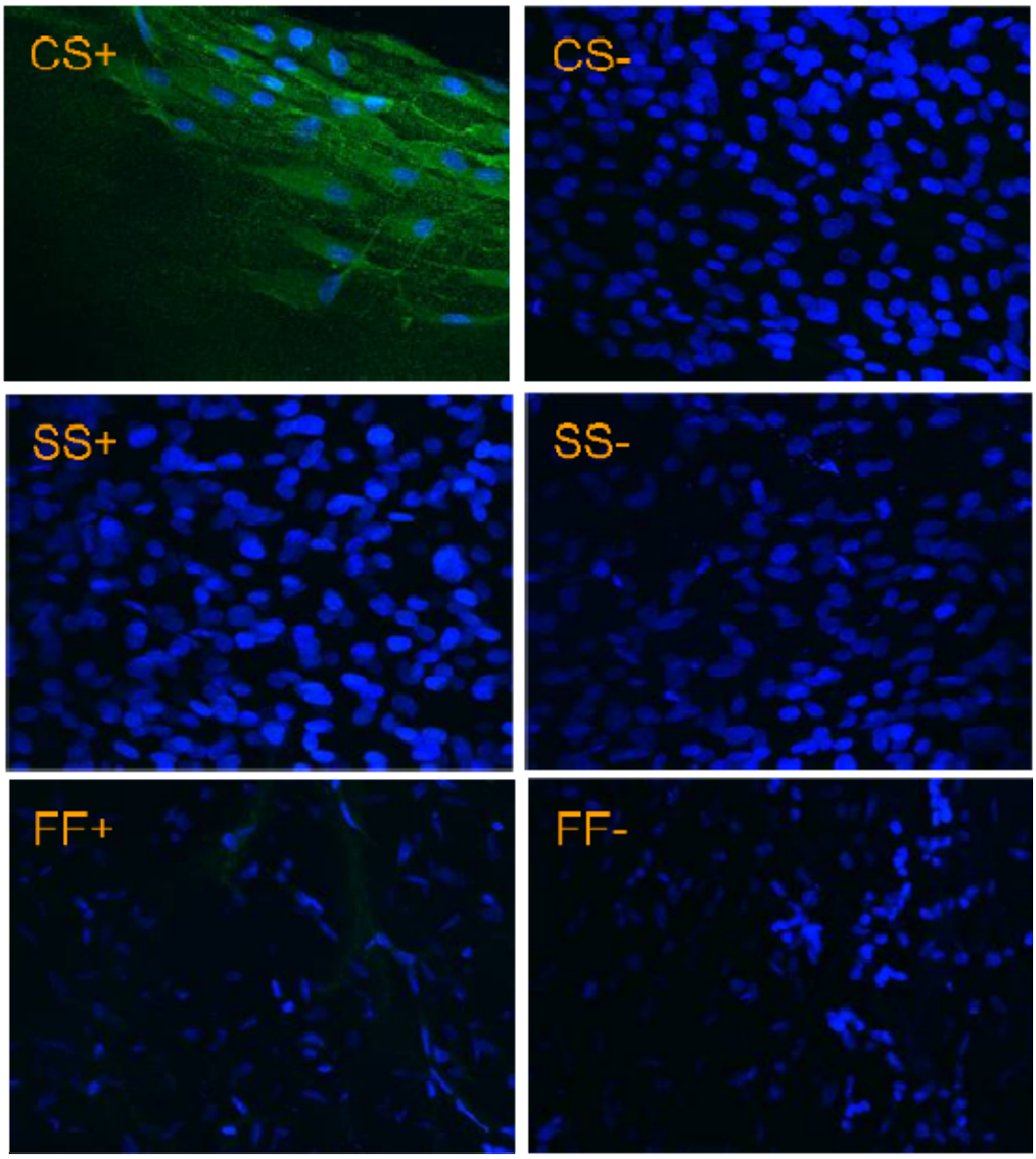

Figure G-1: MHC staining for Experiment 1. Nuclei = blue; MHC = green. Images taken at 40x.

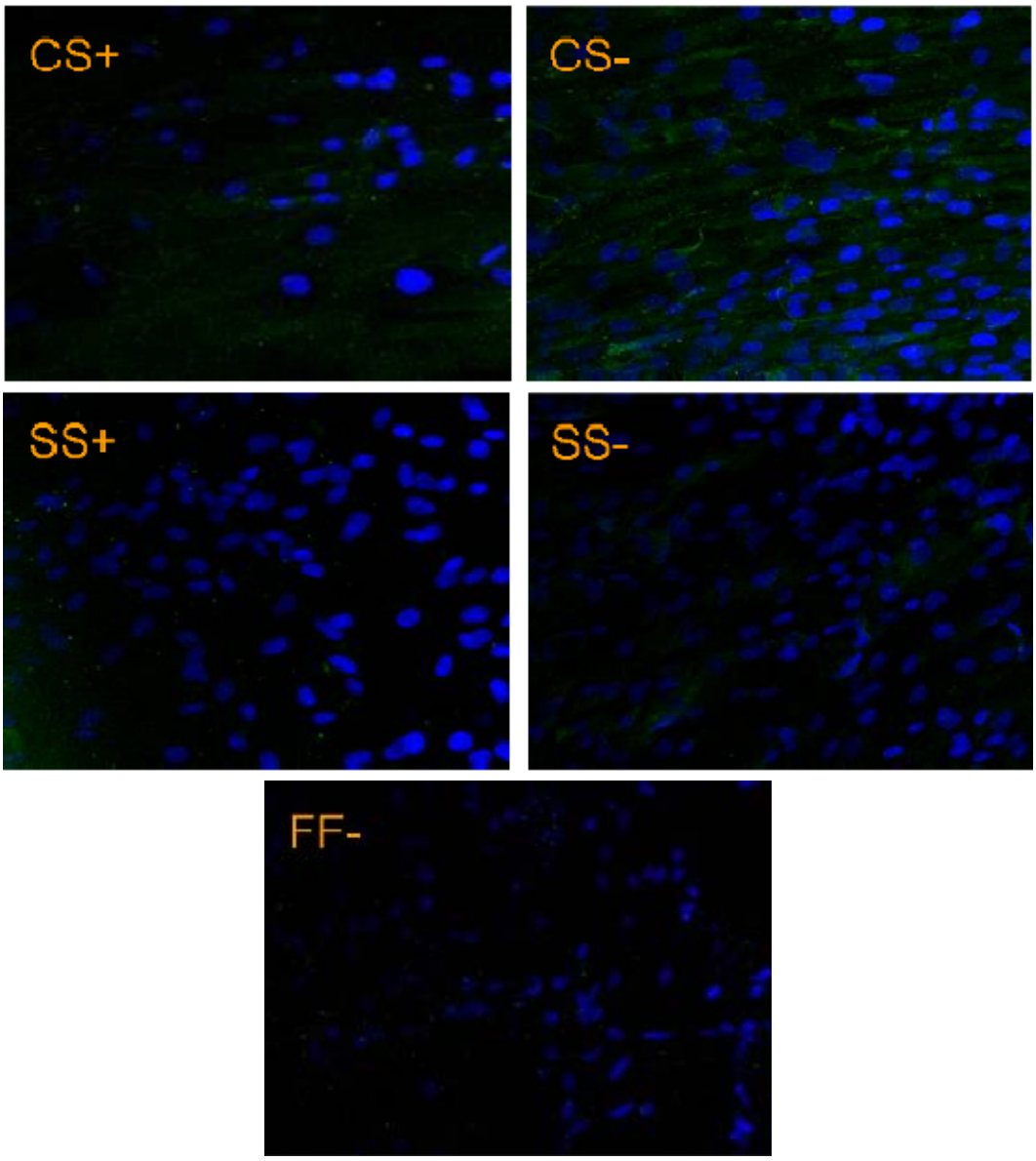

Figure G-2: MHC staining for Experiment 2. Nuclei = blue; MHC = green. FF+ group lost during the experiment. All images taken at 40x.

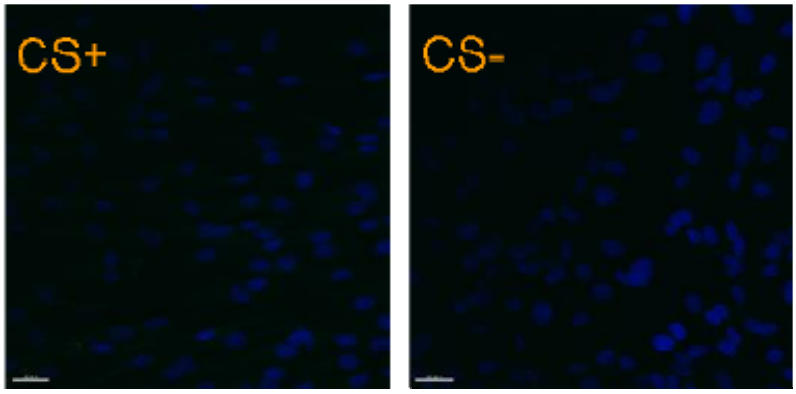

Figure G-3: MHC staining for Experiment 3. Nuclei = blue; MHC = green. SS+/- and FF+/- groups were negative for MHC and were not imaged in the interest of time. All images taken at 40x.

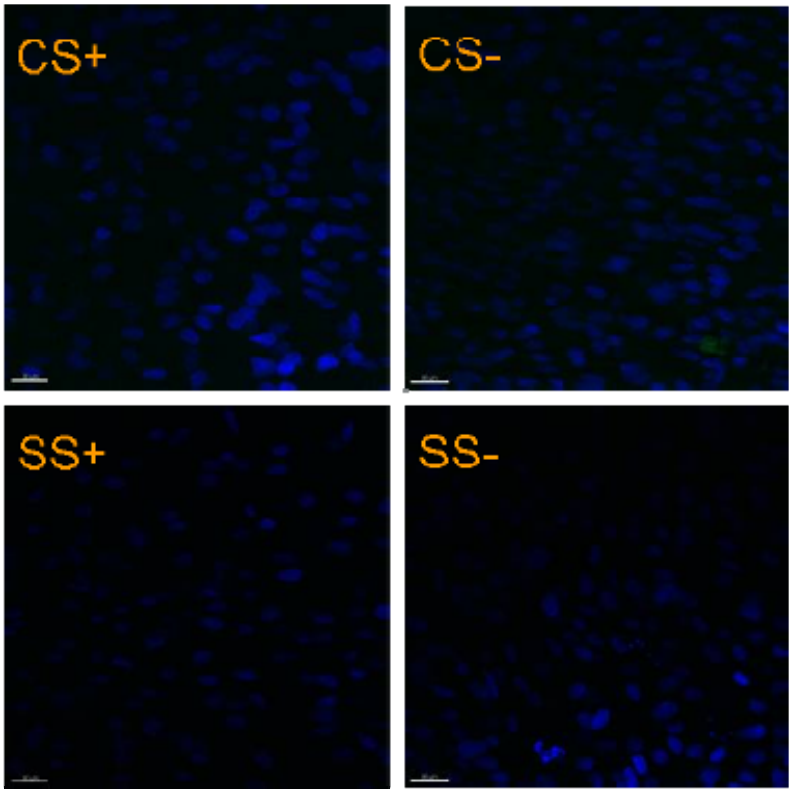

Figure G-4: MHC staining for Experiment 4. Nuclei = blue; MHC = green. FF+/- groups were negative for MHC and were not imaged in the interest of time. All images taken at 40x.

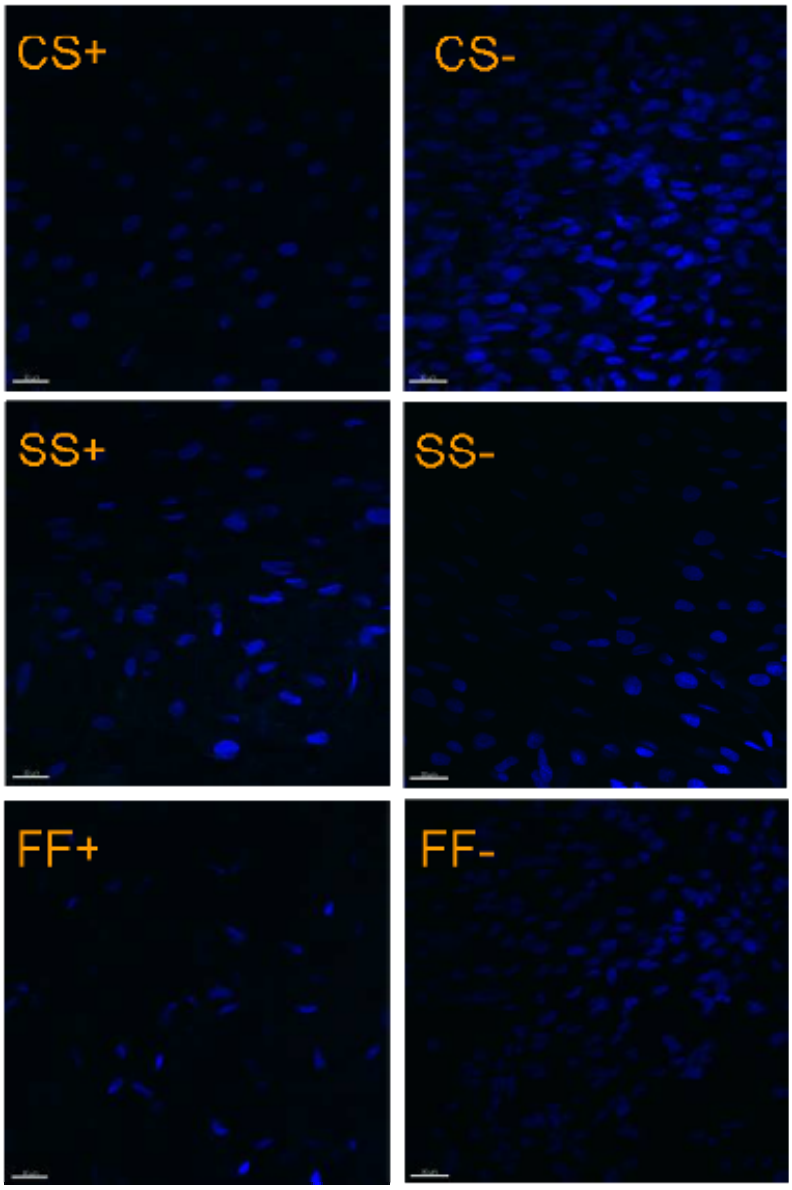

Figure G-5: MHC staining for Experiment 5. Nuclei = blue; MHC = green. All images taken at 40x.

APPENDIX H

MASSON'S TRICHROME

Masson's Trichrome staining seen in **Figures H-1 – H-5** are images from experiments 1 – 5, respectively.

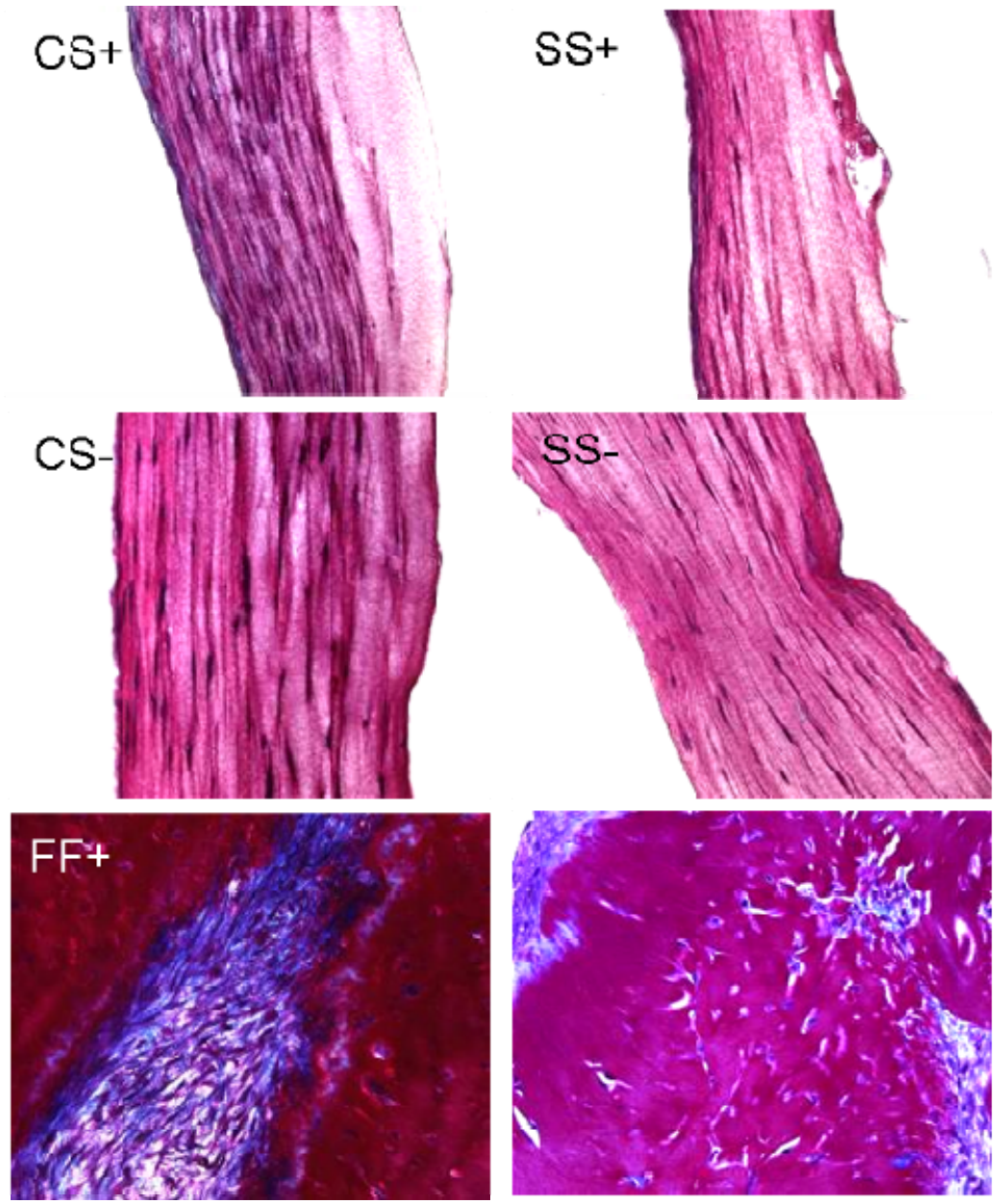

Figure H-1: MT staining for experiment 1. Nuclei = purple; fibrin = pink/purple; collagen = blue. All images taken at 40x.

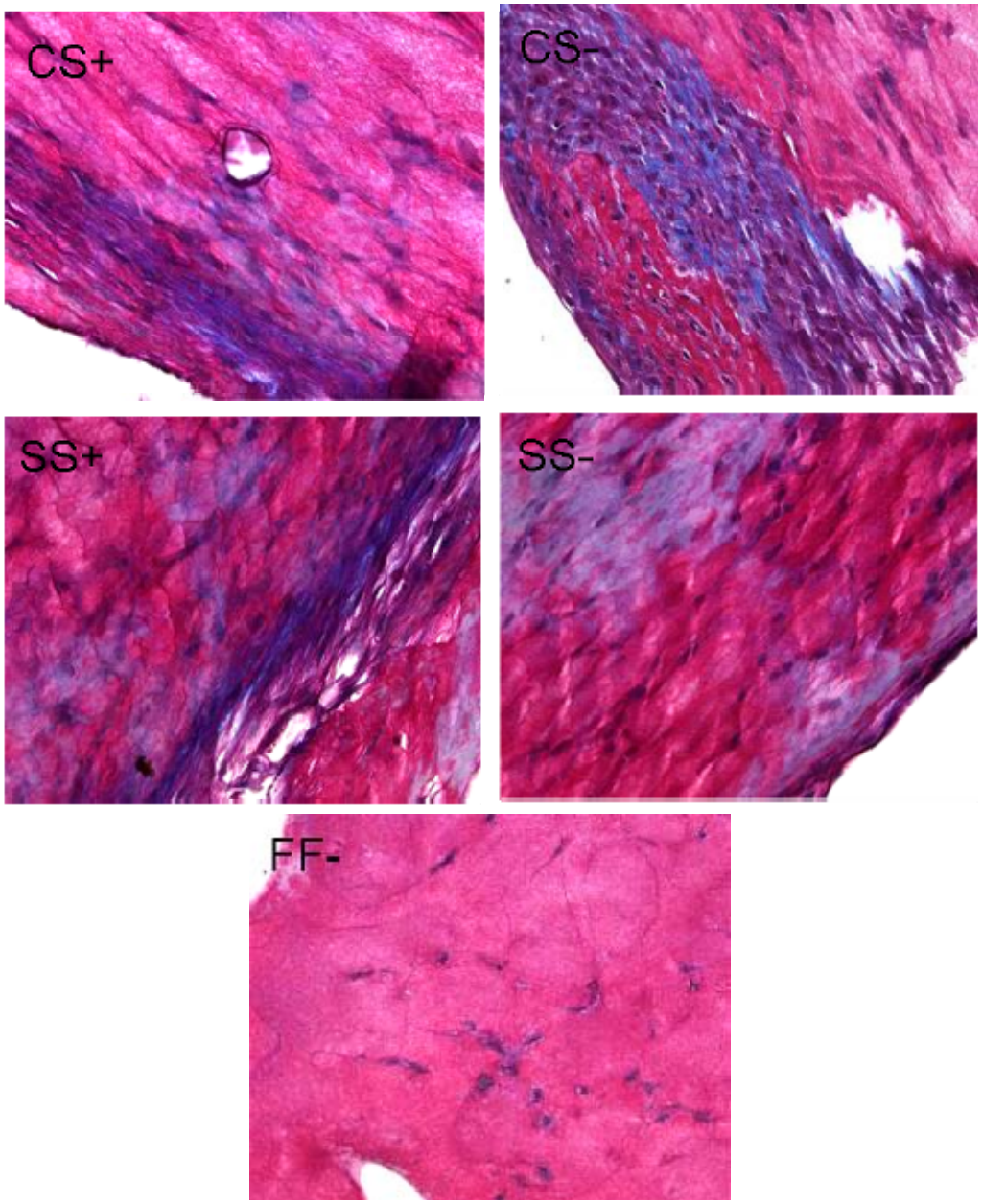

Figure H-2: MT staining for experiment 1. Nuclei = purple; fibrin = pink/purple; collagen = blue. FF- group lost during the experiment. All images taken at 40x.

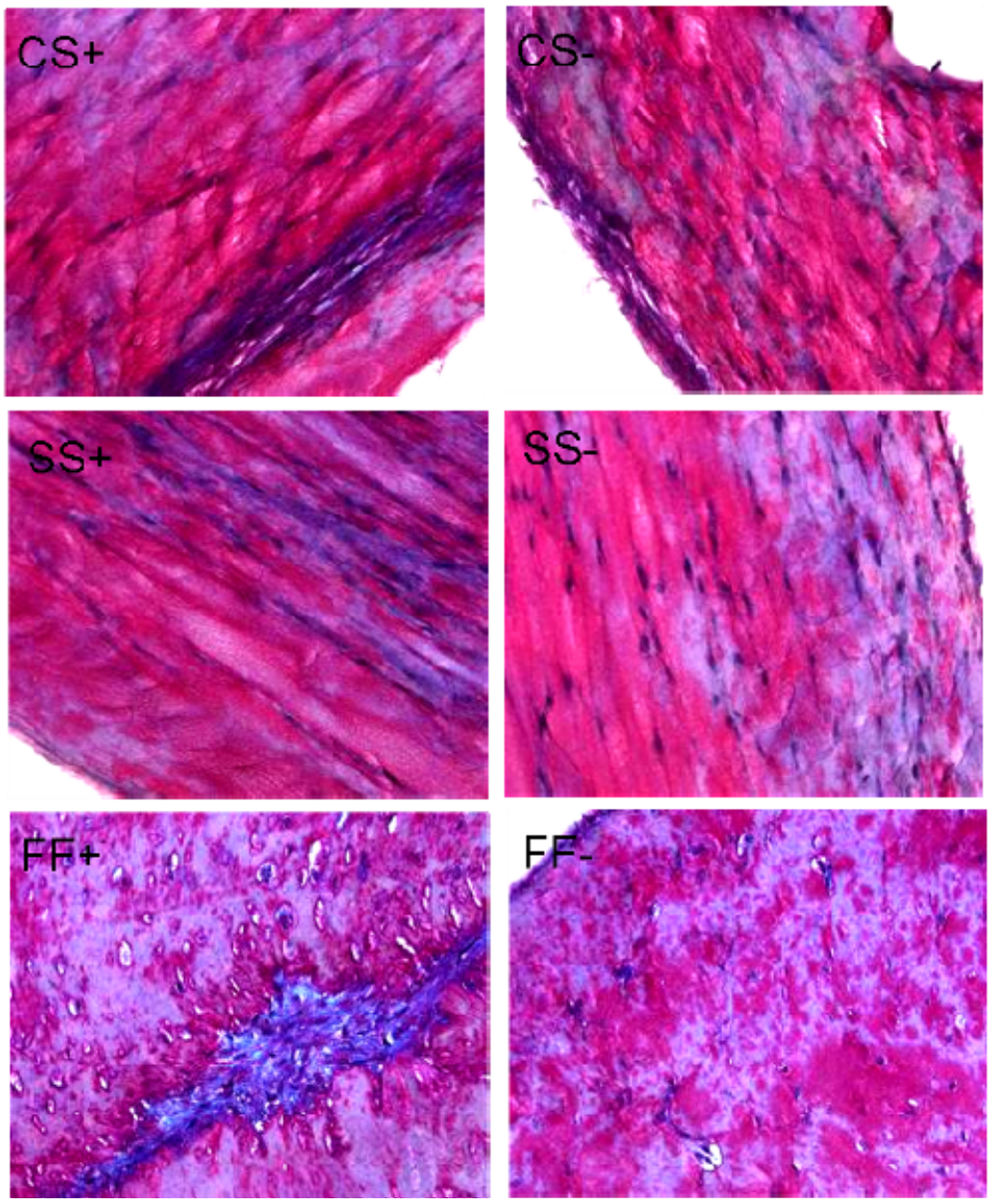

Figure H-3: MT staining for experiment 3. Nuclei = purple; fibrin = pink/purple; collagen = blue. All images taken at 40x.

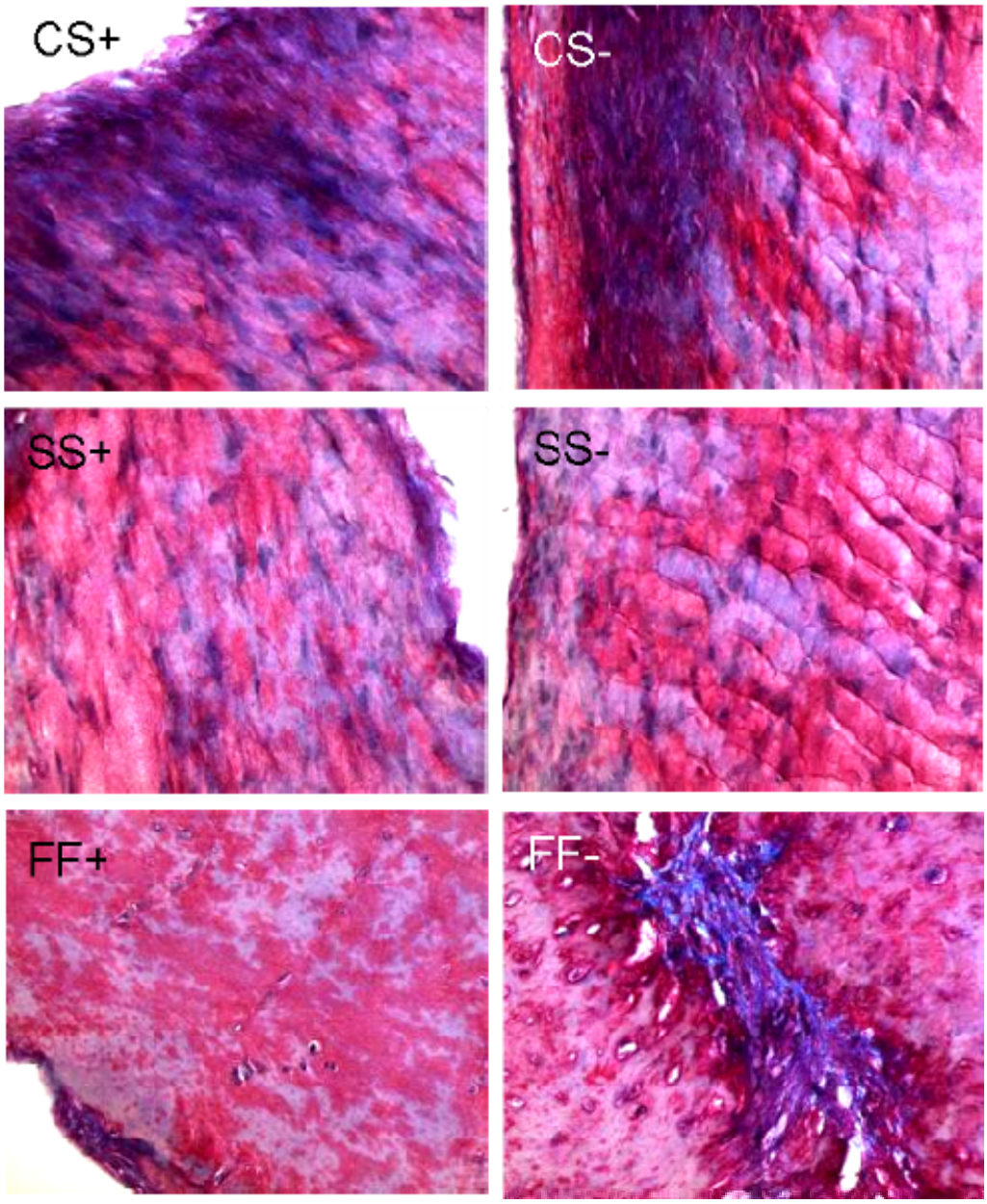

Figure H-4: MT staining for experiment 4. Nuclei = purple; fibrin = pink/purple; collagen = blue. FF- group imaged at 60x. All other images taken at 40x.

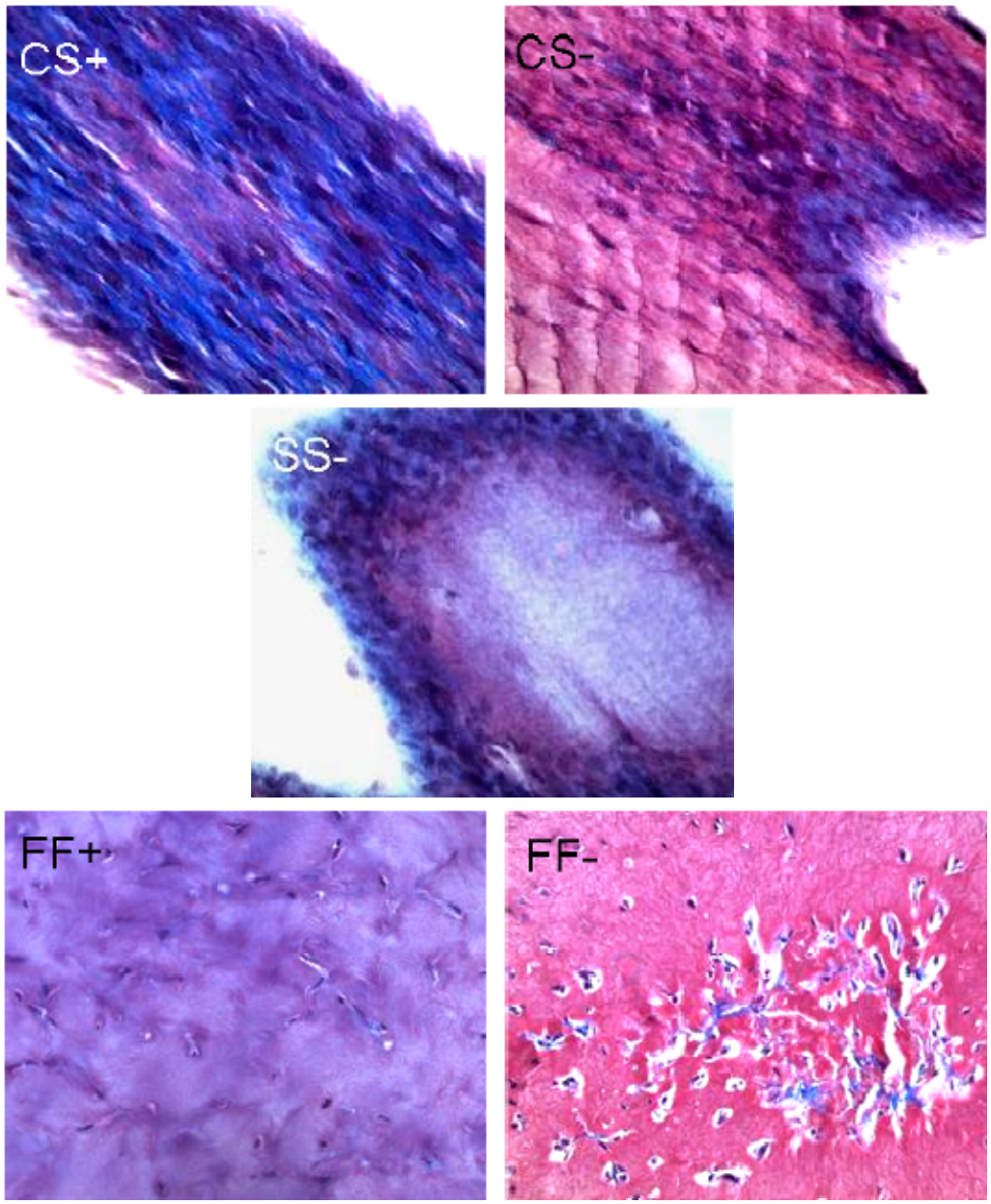

Figure H-5: MT staining for experiment 5. Nuclei = purple; fibrin = pink/purple; collagen = blue. SS+ group lost during the experiment. CS+ group imaged at 60x. All other images taken at 40x.

APPENDIX I

PICROSIRIUS RED

PSR staining seen in **Figures I-1 – I-5** are images from experiments 1 – 5, respectively.

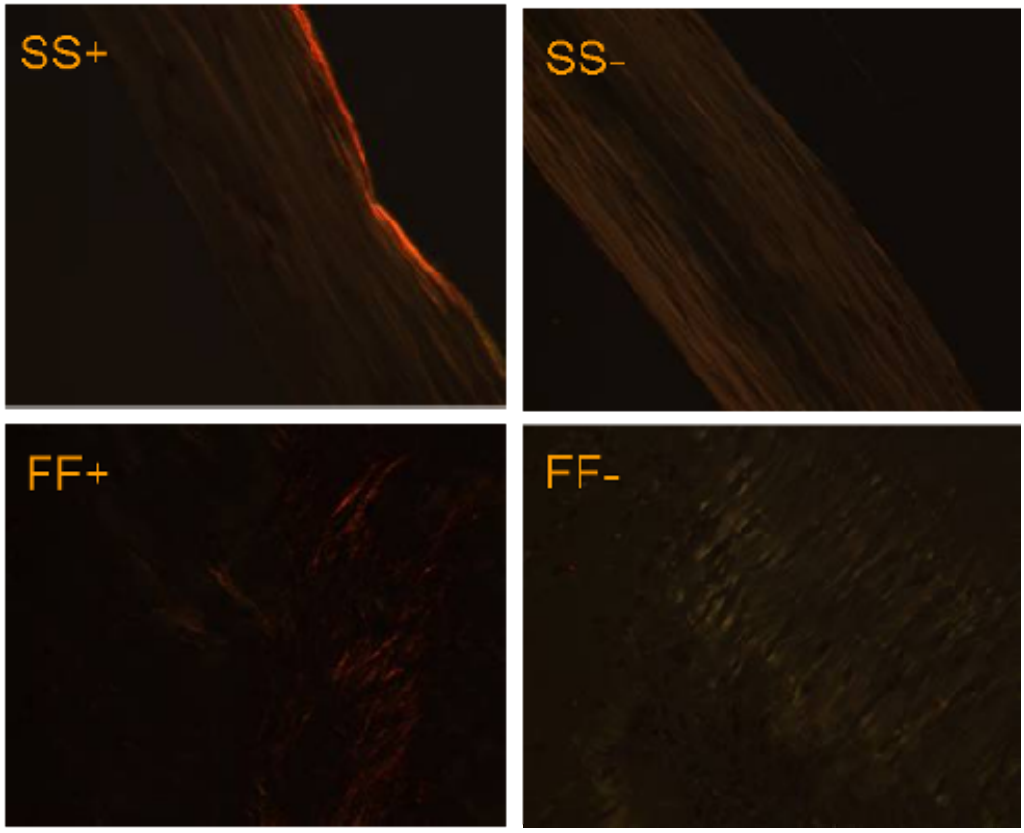

Figure I-1: PSR staining for experiment 1. Green/yellow fibers indicate more immature collagen; orange/red fibers indicate more mature collagen. CS+/- groups were not used for imaging due to artifacts from the sectioning process. All images taken at 40x.

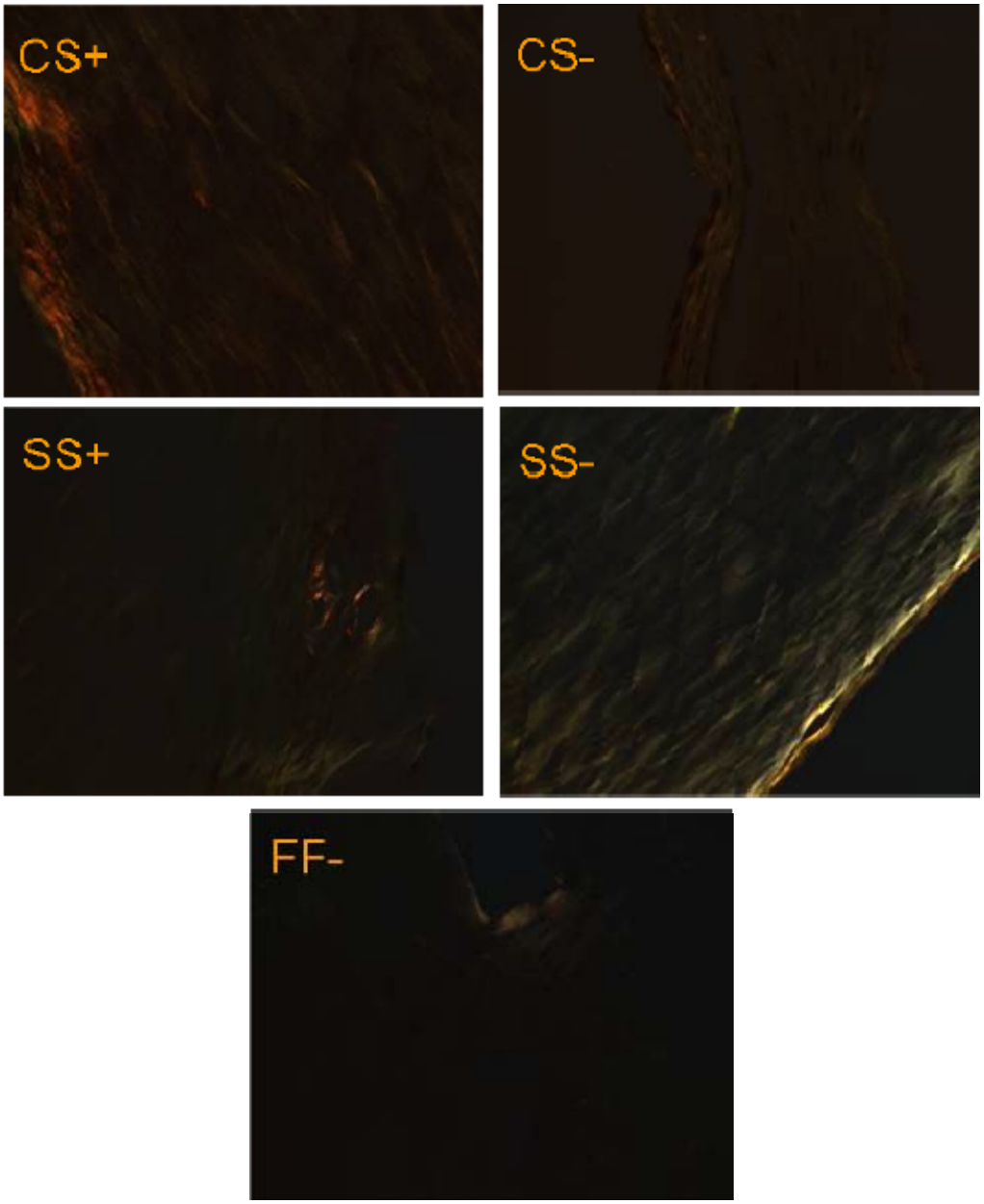

Figure I-2: PSR staining for experiment 2. Green/yellow fibers indicate more immature collagen; orange/red fibers indicate more mature collagen. FF+ group lost during the experiment. All images taken at 40x.

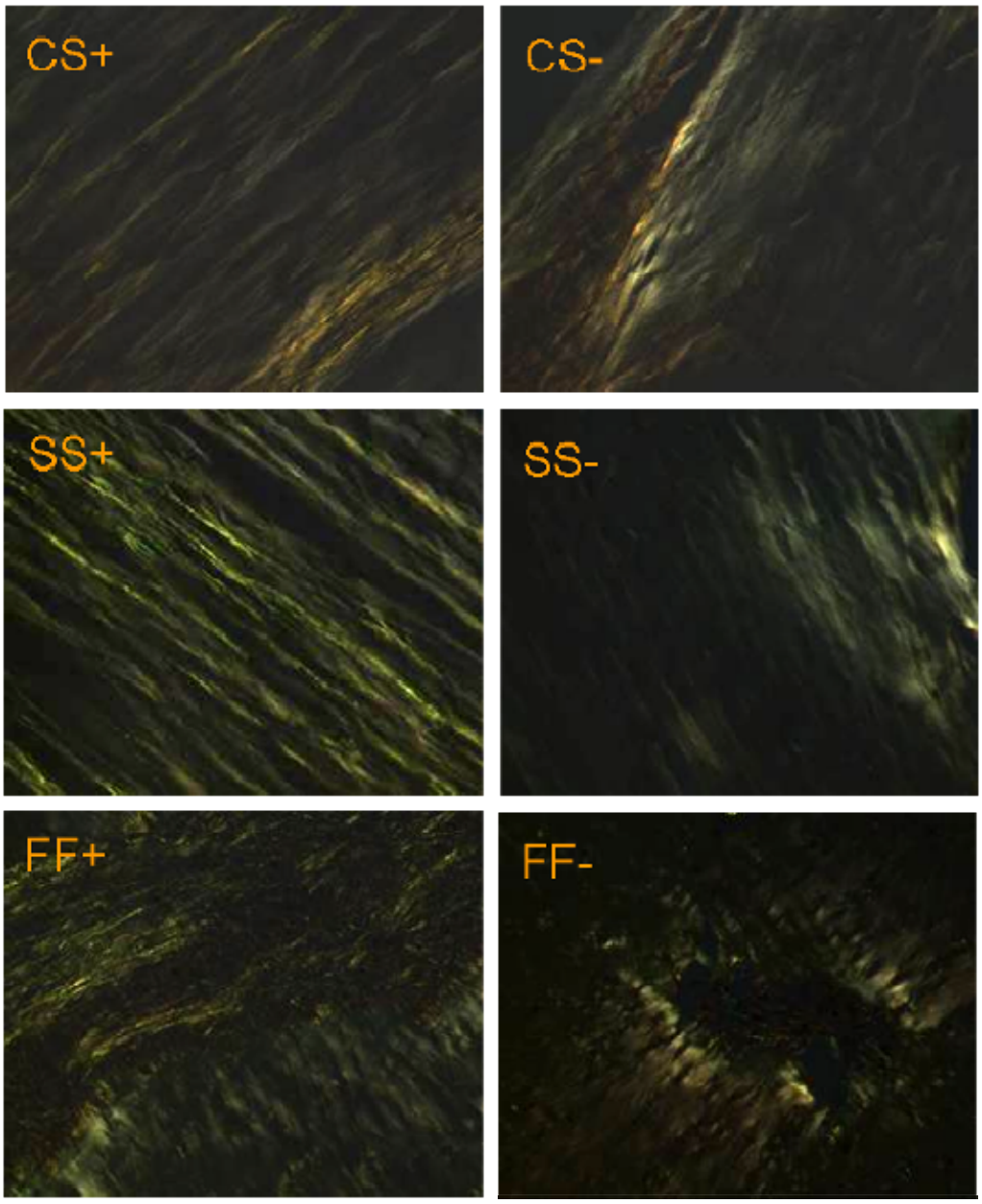

Figure I-3: PSR staining for experiment 3. Green/yellow fibers indicate more immature collagen; orange/red fibers indicate more mature collagen. All images taken at 40x.

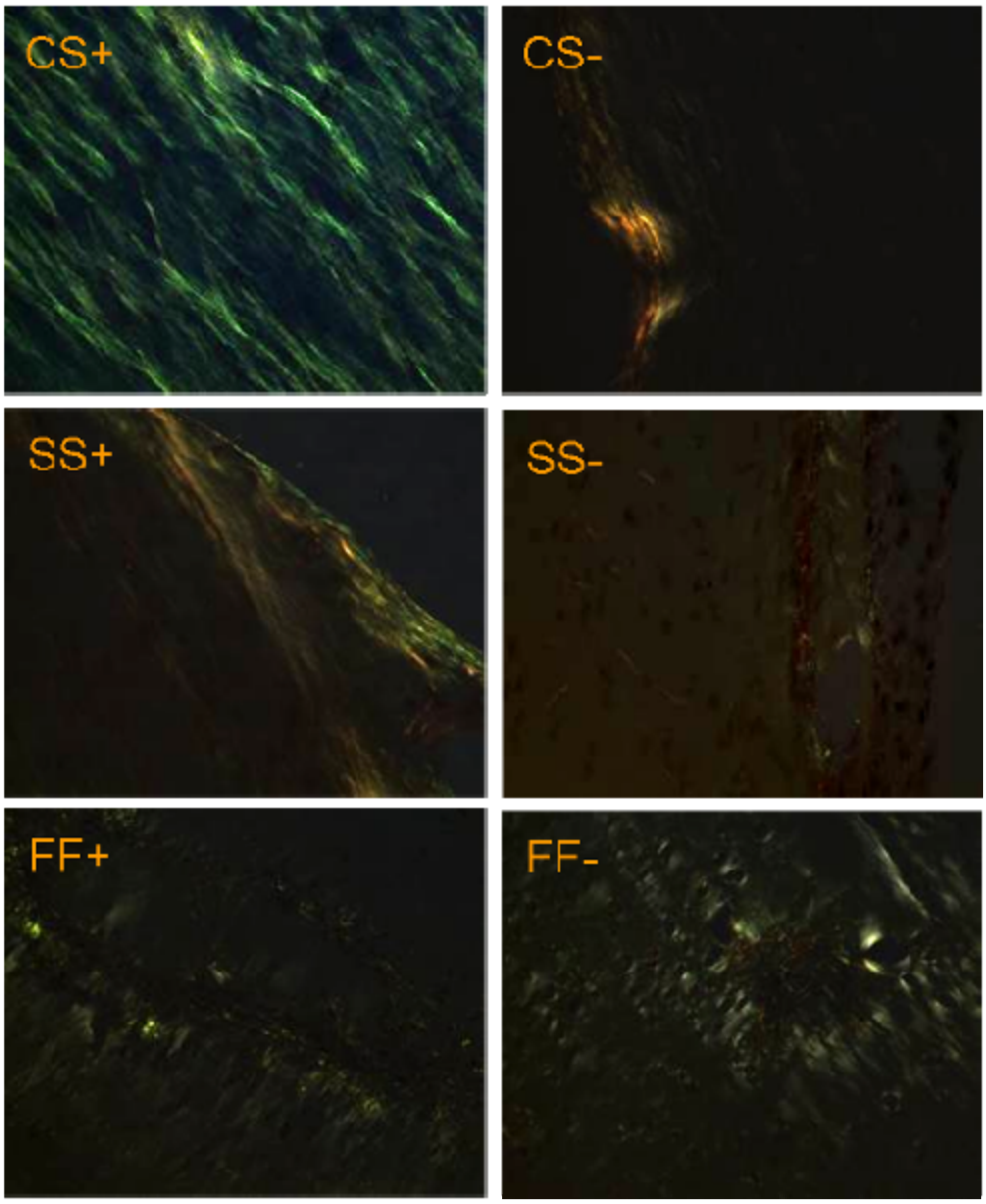

Figure I-4: PSR staining for experiment 4. Green/yellow fibers indicate more immature collagen; orange/red fibers indicate more mature collagen. All images taken at 40x.

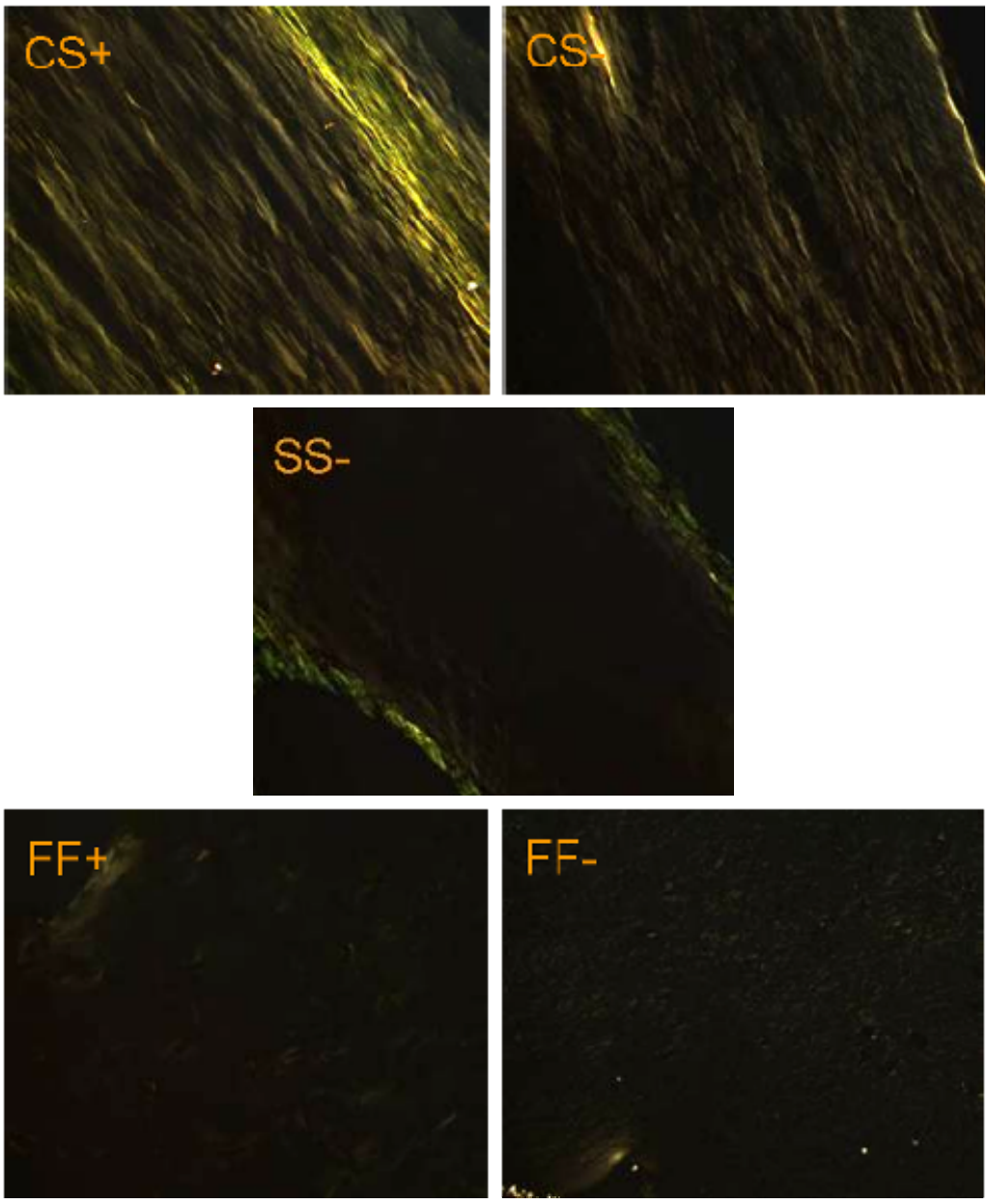

Figure I-5: PSR staining for experiment 5. Green/yellow fibers indicate more immature collagen; orange/red fibers indicate more mature collagen. SS+ group lost during the experiment. All images taken at 40x.

BIBLIOGRAPHY

1. Collins, K. and J.R. Mitchell, *Telomerase in the human organism.* Oncogene, 2002. **21**(4): p. 564-79.

2. McKee, J.A., et al., *Human arteries engineered in vitro.* EMBO Rep, 2003. **4**(6): p. 633-8.

3. Atala, A., et al., *Formation of urothelial structures in vivo from dissociated cells attached to biodegradable polymer scaffolds in vitro.* J Urol, 1992. **148**(2 Pt 2): p. 658-62.

4. Chen, F., J.J. Yoo, and A. Atala, *Acellular collagen matrix as a possible "off the shelf" biomaterial for urethral repair.* Urology, 1999. **54**(3): p. 407-10.

5. De Filippo, R.E., J.J. Yoo, and A. Atala, *Urethral replacement using cell seeded tubularized collagen matrices.* J Urol, 2002. **168**(4 Pt 2): p. 1789-92; discussion 1792-3.

6. Oberpenning, F., et al., *De novo reconstitution of a functional mammalian urinary bladder by tissue engineering.* Nat Biotechnol, 1999. **17**(2): p. 149-55.

7. Atala, A., et al., *Tissue-engineered autologous bladders for patients needing cystoplasty.* Lancet, 2006. **367**(9518): p. 1241-6.

8. Kanematsu, A., et al., *Induction of smooth muscle cell-like phenotype in marrow-derived cells among regenerating urinary bladder smooth muscle cells.* Am J Pathol, 2005. **166**(2): p. 565-73.

9. Walles, T., et al., *Experimental generation of a tissue-engineered functional and vascularized trachea.* J Thorac Cardiovasc Surg, 2004. **128**(6): p. 900-6.

10. Rosamond, W., et al., *Heart disease and stroke statistics--2008 update: a report from the American Heart Association Statistics Committee and Stroke Statistics Subcommittee.* Circulation, 2008. **117**(4): p. e25-146.

11. *Fast Stats: Inpatient Surgery.* Centers for Disease Control, 2003. **Volume 2003**.

12. Gray, J.L., et al., *FGF-1 affixation stimulates ePTFE endothelialization without intimal hyperplasia.* J Surg Res, 1994. **57**(5): p. 596-612.

13. Xue, L. and H.P. Greisler, *Biomaterials in the development and future of vascular grafts.* J Vasc Surg, 2003. **37**(2): p. 472-80.

14. Germain, L., M. Remy-Zolghadri, and F. Auger, *Tissue engineering of the vascular system: from capillaries to larger blood vessels.* Med Biol Eng Comput, 2000. **38**(2): p. 232-40.

15. Teebken, O.E. and A. Haverich, *Tissue engineering of small diameter vascular grafts.* Eur J Vasc Endovasc Surg, 2002. **23**(6): p. 475-85.

16. Ziegler, T. and R.M. Nerem, *Tissue engineering a blood vessel: regulation of vascular biology by mechanical stresses.* J Cell Biochem, 1994. **56**(2): p. 204-9.

17. Vorp, D.A., T. Maul, and A. Nieponice, *Molecular aspects of vascular tissue engineering.* Front Biosci, 2005. **10**: p. 768-89.

18. Conte, M.S., *The ideal small arterial substitute: a search for the Holy Grail?* Faseb J, 1998. **12**(1): p. 43-5.

19. Williams, B., *Mechanical influences on vascular smooth muscle cell function.* J Hypertens, 1998. **16**(12 Pt 2): p. 1921-9.

20. Weston, M.W., K. Rhee, and J.M. Tarbell, *Compliance and diameter mismatch affect the wall shear rate distribution near an end-to-end anastomosis.* J Biomech, 1996. **29**(2): p. 187-98.

21. [cited 2008; Blood vessel anatomy]. Available from: http://ljk.imag.fr/membres/Christophe.Prudhomme/images/artery.jpg.

22. Nerem, R.M. and D. Seliktar, *Vascular tissue engineering.* Annu Rev Biomed Eng, 2001. **3**: p. 225-43.

23. Caplan, A.I., *Mesenchymal stem cells.* J Orthop Res, 1991. **9**(5): p. 641-50.

24. Deasy, B.M. and J. Huard, *Gene therapy and tissue engineering based on muscle-derived stem cells.* Curr Opin Mol Ther, 2002. **4**(4): p. 382-9.

25. Qu-Petersen, Z., et al., *Identification of a novel population of muscle stem cells in mice: potential for muscle regeneration.* J Cell Biol, 2002. **157**(5): p. 851-64.

26. Cao, Y., et al., *Human adipose tissue-derived stem cells differentiate into endothelial cells in vitro and improve postnatal neovascularization in vivo.* Biochem Biophys Res Commun, 2005. **332**(2): p. 370-9.

27. Martinez-Estrada, O.M., et al., *Human adipose tissue as a source of Flk-1+ cells: new method of differentiation and expansion.* Cardiovasc Res, 2005. **65**(2): p. 328-33.

28. Igura, K., et al., *Isolation and characterization of mesenchymal progenitor cells from chorionic villi of human placenta.* Cytotherapy, 2004. **6**(6): p. 543-53.

29. Wulf, G.G., et al., *Mesengenic progenitor cells derived from human placenta.* Tissue Eng, 2004. **10**(7-8): p. 1136-47.

30. Uzan, G., *[Therapeutic potential of circulating endothelial cells].* J Soc Biol, 2005. **199**(2): p. 107-11.

31. Crisan, M., et al., *Purification and long-term culture of multipotent progenitor cells affiliated with the walls of human blood vessels: myoendothelial cells and pericytes.* Methods Cell Biol, 2008. **86**: p. 295-309.

32. Tae, S.K., et al., *Mesenchymal stem cells for tissue engineering and regenerative medicine.* Biomed Mater, 2006. **1**(2): p. 63-71.

33. L'Heureux, N., et al., *A completely biological tissue-engineered human blood vessel.* Faseb J, 1998. **12**(1): p. 47-56.

34. L'Heureux, N. and T. McAllister, *Cytograft Tissue Engineering: a new paradigm in cardiovascular tissue engineering.* Regen Med, 2008. **3**(4): p. 471-5.

35. Asahara, T., et al., *VEGF contributes to postnatal neovascularization by mobilizing bone marrow-derived endothelial progenitor cells.* Embo J, 1999. **18**(14): p. 3964-72.

36. Carmeliet, P., et al., *Targeted deficiency or cytosolic truncation of the VE-cadherin gene in mice impairs VEGF-mediated endothelial survival and angiogenesis.* Cell, 1999. **98**(2): p. 147-57.

37. Stegemann, J.P. and R.M. Nerem, *Phenotype modulation in vascular tissue engineering using biochemical and mechanical stimulation.* Ann Biomed Eng, 2003. **31**(4): p. 391-402.

38. Gronwald, R.G., R.A. Seifert, and D.F. Bowen-Pope, *Differential regulation of expression of two platelet-derived growth factor receptor subunits by transforming growth factor-beta.* J Biol Chem, 1989. **264**(14): p. 8120-5.

39. Sudhir, K., et al., *Mechanical strain stimulates a mitogenic response in coronary vascular smooth muscle cells via release of basic fibroblast growth factor.* Am J Hypertens, 2001. **14**(11 Pt 1): p. 1128-34.

40. Fu, P., et al., *Effects of basic fibroblast growth factor and transforming growth factor-beta on maturation of human pediatric aortic cell culture for tissue engineering of cardiovascular structures.* Asaio J, 2004. **50**(1): p. 9-14.

41. Bajada, S., et al., *Updates on stem cells and their applications in regenerative medicine.* J Tissue Eng Regen Med, 2008. **2**(4): p. 169-83.

42. Becker, A.J., C.E. Mc, and J.E. Till, *Cytological demonstration of the clonal nature of spleen colonies derived from transplanted mouse marrow cells.* Nature, 1963. **197**: p. 452-4.

43. Zuk, P.A., et al., *Multilineage cells from human adipose tissue: implications for cell-based therapies.* Tissue Eng, 2001. **7**(2): p. 211-28.

44. Zuk, P.A., et al., *Human adipose tissue is a source of multipotent stem cells.* Mol Biol Cell, 2002. **13**(12): p. 4279-95.

45. Usas, A. and J. Huard, *Muscle-derived stem cells for tissue engineering and regenerative therapy.* Biomaterials, 2007. **28**(36): p. 5401-6.

46. Halvorsen, Y.D., et al., *Extracellular matrix mineralization and osteoblast gene expression by human adipose tissue-derived stromal cells.* Tissue Eng, 2001. **7**(6): p. 729-41.

47. Erickson, G.R., et al., *Chondrogenic potential of adipose tissue-derived stromal cells in vitro and in vivo.* Biochem Biophys Res Commun, 2002. **290**(2): p. 763-9.

48. Seo, M.J., et al., *Differentiation of human adipose stromal cells into hepatic lineage in vitro and in vivo.* Biochem Biophys Res Commun, 2005. **328**(1): p. 258-64.

49. Safford, K.M., et al., *Neurogenic differentiation of murine and human adipose-derived stromal cells.* Biochem Biophys Res Commun, 2002. **294**(2): p. 371-9.

50. Mizuno, H., et al., *Myogenic differentiation by human processed lipoaspirate cells.* Plast Reconstr Surg, 2002. **109**(1): p. 199-209; discussion 210-1.

51. Rangappa, S., et al., *Transformation of adult mesenchymal stem cells isolated from the fatty tissue into cardiomyocytes.* Ann Thorac Surg, 2003. **75**(3): p. 775-9.

52. De Ugarte, D.A., et al., *Comparison of multi-lineage cells from human adipose tissue and bone marrow.* Cells Tissues Organs, 2003. **174**(3): p. 101-9.

53. Afizah, H., et al., *A comparison between the chondrogenic potential of human bone marrow stem cells (BMSCs) and adipose-derived stem cells (ADSCs) taken from the same donors.* Tissue Eng, 2007. **13**(4): p. 659-66.

54. Lee, W.C., J.P. Rubin, and K.G. Marra, *Regulation of alpha-smooth muscle actin protein expression in adipose-derived stem cells.* Cells Tissues Organs, 2006. **183**(2): p. 80-6.

55. Nieponice, A., et al., *Development of a tissue-engineered vascular graft combining a biodegradable scaffold, muscle-derived stem cells and a rotational vacuum seeding technique.* Biomaterials, 2008. **29**(7): p. 825-33.

56. Friedenstein, A.J., S. Piatetzky, II, and K.V. Petrakova, *Osteogenesis in transplants of bone marrow cells.* J Embryol Exp Morphol, 1966. **16**(3): p. 381-90.

57. Pittenger, M.F., et al., *Multilineage potential of adult human mesenchymal stem cells.* Science, 1999. **284**(5411): p. 143-7.

58. Noth, U., et al., *Multilineage mesenchymal differentiation potential of human trabecular bone-derived cells.* J Orthop Res, 2002. **20**(5): p. 1060-9.

59. Zhao, L.R., et al., *Human bone marrow stem cells exhibit neural phenotypes and ameliorate neurological deficits after grafting into the ischemic brain of rats.* Exp Neurol, 2002. **174**(1): p. 11-20.

60. Jiang, Y., et al., *Pluripotency of mesenchymal stem cells derived from adult marrow.* Nature, 2002. **418**(6893): p. 41-9.

61. Charbord, P., et al., *The cytoskeleton of stromal cells from human bone marrow cultures resembles that of cultured smooth muscle cells.* Exp Hematol, 1990. **18**(4): p. 276-82.

62. Galmiche, M.C., et al., *Stromal cells from human long-term marrow cultures are mesenchymal cells that differentiate following a vascular smooth muscle differentiation pathway.* Blood, 1993. **82**(1): p. 66-76.

63. Goodell, M.A., et al., *Stem cell plasticity in muscle and bone marrow.* Ann N Y Acad Sci, 2001. **938**: p. 208-18; discussion 218-20.

64. Grounds, M.D., et al., *The role of stem cells in skeletal and cardiac muscle repair.* J Histochem Cytochem, 2002. **50**(5): p. 589-610.

65. Hirschi, K. and M. Goodell, *Common origins of blood and blood vessels in adults?* Differentiation, 2001. **68**(4-5): p. 186-92.

66. Takahashi, T., et al., *Ischemia- and cytokine-induced mobilization of bone marrow-derived endothelial progenitor cells for neovascularization.* Nat Med, 1999. **5**(4): p. 434-8.

67. Tepper, O.M., et al., *Adult vasculogenesis occurs through in situ recruitment, proliferation, and tubulization of circulating bone marrow-derived cells.* Blood, 2005. **105**(3): p. 1068-77.

68. Shin'oka, T., et al., *Midterm clinical result of tissue-engineered vascular autografts seeded with autologous bone marrow cells.* J Thorac Cardiovasc Surg, 2005. **129**(6): p. 1330-8.

69. Altman, G.H., et al., *Cell differentiation by mechanical stress.* Faseb J, 2002. **16**(2): p. 270-2.

70. Arakawa, E., et al., *A mouse bone marrow stromal cell line, TBR-B, shows inducible expression of smooth muscle-specific genes.* FEBS Lett, 2000. **481**(2): p. 193-6.

71. Blank, R.S., et al., *A retinoic acid-induced clonal cell line derived from multipotential P19 embryonal carcinoma cells expresses smooth muscle characteristics.* Circ Res, 1995. **76**(5): p. 742-9.

72. Cummings, C.L., et al., *Properties of engineered vascular constructs made from collagen, fibrin, and collagen-fibrin mixtures.* Biomaterials, 2004. **25**(17): p. 3699-706.

73. Gong, Z. and L.E. Niklason, *Small-diameter human vessel wall engineered from bone marrow-derived mesenchymal stem cells (hMSCs).* Faseb J, 2008. **22**(6): p. 1635-48.

74. Hamilton, D.W., T.M. Maul, and D.A. Vorp, *Characterization of the response of bone marrow-derived progenitor cells to cyclic strain: implications for vascular tissue-engineering applications.* Tissue Eng, 2004. **10**(3-4): p. 361-9.

75. Kinner, B., J.M. Zaleskas, and M. Spector, *Regulation of smooth muscle actin expression and contraction in adult human mesenchymal stem cells.* Exp Cell Res, 2002. **278**(1): p. 72-83.

76. Kurpinski, K., et al., *Anisotropic mechanosensing by mesenchymal stem cells.* Proc Natl Acad Sci U S A, 2006. **103**(44): p. 16095-100.

77. Narita, Y., et al., *Effects of transforming growth factor-beta 1 and ascorbic acid on differentiation of human bone-marrow-derived mesenchymal stem cells into smooth muscle cell lineage.* Cell Tissue Res, 2008.

78. Nieponice, A., et al., *Mechanical stimulation induces morphological and phenotypic changes in bone marrow-derived progenitor cells within a three-dimensional fibrin matrix.* J Biomed Mater Res A, 2007. **81**(3): p. 523-30.

79. Riha, G.M., et al., *Cyclic strain induces vascular smooth muscle cell differentiation from murine embryonic mesenchymal progenitor cells.* Surgery, 2007. **141**(3): p. 394-402.

80. Simper, D., et al., *Smooth muscle progenitor cells in human blood.* Circulation, 2002. **106**(10): p. 1199-204.

81. Owens, G.K., *Regulation of differentiation of vascular smooth muscle cells.* Physiol Rev, 1995. **75**(3): p. 487-517.

82. Fatigati, V. and R.A. Murphy, *Actin and tropomyosin variants in smooth muscles. Dependence on tissue type.* J Biol Chem, 1984. **259**(23): p. 14383-8.

83. Owens, G.K. and M.M. Thompson, *Developmental changes in isoactin expression in rat aortic smooth muscle cells in vivo. Relationship between growth and cytodifferentiation.* J Biol Chem, 1986. **261**(28): p. 13373-80.

84. Hossain, M.M., et al., *Cytoskeletal tension regulates both expression and degradation of h2-calponin in lung alveolar cells.* Biochemistry, 2006. **45**(51): p. 15670-83.

85. Huang, Q.Q., et al., *Role of h2-calponin in regulating macrophage motility and phagocytosis.* J Biol Chem, 2008.

86. Hossain, M.M., et al., *h2-Calponin is regulated by mechanical tension and modifies the function of actin cytoskeleton.* J Biol Chem, 2005. **280**(51): p. 42442-53.

87. Stegemann, J.P. and R.M. Nerem, *Altered response of vascular smooth muscle cells to exogenous biochemical stimulation in two- and three-dimensional culture.* Exp Cell Res, 2003. **283**(2): p. 146-55.

88. Kanda, K., T. Matsuda, and T. Oka, *Two-dimensional orientational response of smooth muscle cells to cyclic stretching.* Asaio J, 1992. **38**(3): p. M382-5.

89. Asanuma, K., et al., *Uniaxial strain upregulates matrix-degrading enzymes produced by human vascular smooth muscle cells.* Am J Physiol Heart Circ Physiol, 2003. **284**(5): p. H1778-84.

90. O'Callaghan, C.J. and B. Williams, *Mechanical strain-induced extracellular matrix production by human vascular smooth muscle cells: role of TGF-beta(1).* Hypertension, 2000. **36**(3): p. 319-24.

91. Banes, A.J., et al., *A new vacuum-operated stress-providing instrument that applies static or variable duration cyclic tension or compression to cells in vitro.* J Cell Sci, 1985. **75**: p. 35-42.

92. Sotoudeh, M., et al., *A strain device imposing dynamic and uniform equi-biaxial strain to cultured cells.* Ann Biomed Eng, 1998. **26**(2): p. 181-9.

93. Kurpinski, K., et al., *Regulation of vascular smooth muscle cells and mesenchymal stem cells by mechanical strain.* Mol Cell Biomech, 2006. **3**(1): p. 21-34.

94. Birukov, K.G., et al., *Stretch affects phenotype and proliferation of vascular smooth muscle cells.* Mol Cell Biochem, 1995. **144**(2): p. 131-9.

95. Reusch, P., et al., *Mechanical strain increases smooth muscle and decreases nonmuscle myosin expression in rat vascular smooth muscle cells.* Circ Res, 1996. **79**(5): p. 1046-53.

96. Yang, Z., G. Noll, and T.F. Luscher, *Calcium antagonists differently inhibit proliferation of human coronary smooth muscle cells in response to pulsatile stretch and platelet-derived growth factor.* Circulation, 1993. **88**(3): p. 832-6.

97. Kim, B.S., et al., *Cyclic mechanical strain regulates the development of engineered smooth muscle tissue.* Nat Biotechnol, 1999. **17**(10): p. 979-83.

98. Park, J.S., et al., *Differential effects of equiaxial and uniaxial strain on mesenchymal stem cells.* Biotechnol Bioeng, 2004. **88**(3): p. 359-68.

99. Oluwole, B.O., et al., *Gene regulation by mechanical forces.* Endothelium, 1997. **5**(2): p. 85-93.

100. Hultgardh-Nilsson, A., et al., *Expression of phenotype- and proliferation-related genes in rat aortic smooth muscle cells in primary culture.* Cardiovasc Res, 1997. **34**(2): p. 418-30.

101. Kanda, K. and T. Matsuda, *Behavior of arterial wall cells cultured on periodically stretched substrates.* Cell Transplant, 1993. **2**(6): p. 475-84.

102. Stiles, C.D., et al., *Dual control of cell growth by somatomedins and platelet-derived growth factor.* Proc Natl Acad Sci U S A, 1979. **76**(3): p. 1279-83.

103. Bjorkerud, S., *Effects of transforming growth factor-beta 1 on human arterial smooth muscle cells in vitro.* Arterioscler Thromb, 1991. **11**(4): p. 892-902.

104. Hautmann, M.B., C.S. Madsen, and G.K. Owens, *A transforming growth factor beta (TGFbeta) control element drives TGFbeta-induced stimulation of smooth muscle alpha-actin gene expression in concert with two CArG elements.* J Biol Chem, 1997. **272**(16): p. 10948-56.

105. Sinha, S., et al., *Transforming growth factor-beta1 signaling contributes to development of smooth muscle cells from embryonic stem cells.* Am J Physiol Cell Physiol, 2004. **287**(6): p. C1560-8.

106. Bobik, A., *Transforming growth factor-betas and vascular disorders.* Arterioscler Thromb Vasc Biol, 2006. **26**(8): p. 1712-20.

107. Pepper, M.S., *Transforming growth factor-beta: vasculogenesis, angiogenesis, and vessel wall integrity.* Cytokine Growth Factor Rev, 1997. **8**(1): p. 21-43.

108. Battegay, E.J., et al., *TGF-beta induces bimodal proliferation of connective tissue cells via complex control of an autocrine PDGF loop.* Cell, 1990. **63**(3): p. 515-24.

109. Singh, N.N. and D.P. Ramji, *The role of transforming growth factor-beta in atherosclerosis.* Cytokine Growth Factor Rev, 2006. **17**(6): p. 487-99.

110. Yamashita, J., et al., *Flk1-positive cells derived from embryonic stem cells serve as vascular progenitors.* Nature, 2000. **408**(6808): p. 92-6.

111. Chen, S. and R.J. Lechleider, *Transforming growth factor-beta-induced differentiation of smooth muscle from a neural crest stem cell line.* Circ Res, 2004. **94**(9): p. 1195-202.

112. Miano, J.M. and B.C. Berk, *Retinoids: versatile biological response modifiers of vascular smooth muscle phenotype.* Circ Res, 2000. **87**(5): p. 355-62.

113. Yoon, Y.S., et al., *Clonally expanded novel multipotent stem cells from human bone marrow regenerate myocardium after myocardial infarction.* J Clin Invest, 2005. **115**(2): p. 326-38.

114. Suzuki, T., et al., *Preferential differentiation of P19 mouse embryonal carcinoma cells into smooth muscle cells. Use of retinoic acid and antisense against the central nervous system-specific POU transcription factor Brn-2.* Circ Res, 1996. **78**(3): p. 395-404.

115. Barry, F., et al., *Chondrogenic differentiation of mesenchymal stem cells from bone marrow: differentiation-dependent gene expression of matrix components.* Exp Cell Res, 2001. **268**(2): p. 189-200.

116. Bonanno, E., et al., *Homogeneous stromal cell population from normal human adult bone marrow expressing alpha-smooth muscle actin filaments.* Lab Invest, 1994. **71**(2): p. 308-15.

117. Conget, P.A. and J.J. Minguell, *Phenotypical and functional properties of human bone marrow mesenchymal progenitor cells.* J Cell Physiol, 1999. **181**(1): p. 67-73.

118. Jaiswal, N., et al., *Osteogenic differentiation of purified, culture-expanded human mesenchymal stem cells in vitro.* J Cell Biochem, 1997. **64**(2): p. 295-312.

119. Azuma, N., et al., *Endothelial cell response to different mechanical forces.* J Vasc Surg, 2000. **32**(4): p. 789-94.

120. Cowan, D.B. and B.L. Langille, *Cellular and molecular biology of vascular remodeling.* Curr Opin Lipidol, 1996. **7**(2): p. 94-100.

121. Han, C.I., G.R. Campbell, and J.H. Campbell, *Circulating bone marrow cells can contribute to neointimal formation.* J Vasc Res, 2001. **38**(2): p. 113-9.

122. Hirschi, K.K. and M.A. Goodell, *Hematopoietic, vascular and cardiac fates of bone marrow-derived stem cells.* Gene Ther, 2002. **9**(10): p. 648-52.

123. Joe, P., et al., *Effects of mechanical factors on growth and maturation of the lung in fetal sheep.* Am J Physiol, 1997. **272**(1 Pt 1): p. L95-105.

124. Resnick, N. and M.A. Gimbrone, Jr., *Hemodynamic forces are complex regulators of endothelial gene expression.* Faseb J, 1995. **9**(10): p. 874-82.

125. Javazon, E.H., et al., *Rat marrow stromal cells are more sensitive to plating density and expand more rapidly from single-cell-derived colonies than human marrow stromal cells.* Stem Cells, 2001. **19**(3): p. 219-25.

126. Maul, T., *MECHANOBIOLOGY OF STEM CELLS: IMPLICATIONS FOR VASCULAR TISSUE ENGINEERING*, in *Bioengineering*. 2007, University of Pittsburgh: Pittsburgh. p. 381.